Development of Multiscale Electrospun Scaffolds for Promoting Neural Differentiation of Induced Pluripotent Stem Cells

by

Nima Khadem Mohtaram
MSc., Iran Polymer and Petrochemical Institute, 2008
BSc., Tehran Polytechnic, 2002

A Dissertation Submitted in Partial Fulfillment
of the Requirements for the Degree of

Doctor of Philosophy

in the Department of Mechanical Engineering

© Nima Khadem Mohtaram, 2014
University of Victoria

All rights reserved. This thesis may not be reproduced in whole or in part, by photocopy or other means, without the permission of the author.

Supervisory Committee

Development of Multiscale Electrospun Scaffolds for Promoting Neural Differentiation of Induced Pluripotent Stem Cells

by

Nima Khadem Mohtaram
MSc., Iran Polymer and Petrochemical Institute, 2008
BSc., Tehran Polytechnic, 2002

Supervisory Committee

Dr. Stephanie Willerth (Department of Mechanical Engineering and Division of Medical Sciences)
Supervisor

Dr. Martin Byung-Guk Jun (Department of Mechanical Engineering)
Departmental Member

Dr. Bob Chow (Department of Biology)
Outside Member

Dr. Alex Brolo (Department of Chemistry)
Outside Member

Abstract

Supervisory Committee

Dr. Stephanie Willerth (Department of Mechanical Engineering and Division of Medical Sciences)
Supervisor

Dr. Martin Byung-Guk Jun (Department of Mechanical Engineering)
Departmental Member

Dr. Bob Chow (Department of Biology)
Ouside Member

Dr. Alex Brolo (Department of Chemistry)
Outside Member

Electrospun biomaterial scaffolds can be engineered to support the neural differentiation of induced pluripotent stem cells. As electrospinning produces scaffolds consisting of nano or microfibers, these topographical features can be used as cues to direct stem cell differentiation. These nano and microscale scaffolds can also be used to deliver chemical cues, such as small molecules and growth factors, to direct the differentiation of induced pluripotent stem cells into neural phenotypes. Induced pluripotent stem cells can become any cell type found in the body, making them a powerful tool for engineering tissues. Therefore, a combination of an engineered biomaterial scaffold with induced pluripotent stem cells is a promising approach for neural tissue engineering applications. As detailed in this thesis, electrospun scaffolds support the neuronal differentiation of induced pluripotent stem cells through delivering the appropriate chemical cues and also presenting physical cues, specifically topography to enhance neuronal regeneration. This thesis seeks to evaluate the following topics: multifunctional electrospun scaffolds for promoting neuronal differentiation of induced pluripotent stem cells, neuronal differentiation of human induced pluripotent stem cells seeded on electrospun scaffolds with varied topographies, and controlled release of glial cell-derived neurotrophic factor from random and aligned electrospun nanofibers.

Acknowledgments

First and foremost I want to thank my advisor Dr. Stephanie Willerth. It has been an honor to be her first Ph.D. student. I appreciate all her contributions of time, ideas, and funding to make my Ph.D. experience productive and stimulating. The joy and enthusiasm she has for her research was contagious and motivational for me, even during tough times in the Ph.D. pursuit. I would like to extend my best words of thanks to the committee members, Dr. Martin Byung-Guk Jun, Dr. Bob Chow, Dr. Alex Brolo, and Dr. Rizhi Wang.

The members of the Willerth lab have contributed immensely to my personal and professional time at the University of Victoria (UVic). The group has been a source of friendships as well as good advice and collaboration. I would like to acknowledge Mrs. Amy Montgomery, Mrs. Lin Sun, and Mrs. Meghan Robinson. We worked together on the stem cells culture experiments, and I very much appreciated their enthusiasm, intensity, willingness to help me, and their amazing ability to do stem cell cultures. I am especially grateful for the Dr. Jun group member as well: Junghuyk Ko. Other past and present group members that I have had the pleasure to work with or alongside of are Jose Gomez, Andrew Agbay, David Rattray, Nathan Muller, Paul O'Neil, Craig King, Michael Carlson, Alix Wong, and Kathleen Kolehmainen; and the numerous summer and Co-Op students who have come through the lab.

I gratefully acknowledge the funding sources that made my Ph.D. work possible. I was funded by the Natural Sciences and Engineering Research Council of Canada (NSERC) fund.

Lastly, I would like to thank my family for all their love and encouragement. For the presence of my parents here in Victoria for my last semester at UVic. And most of all for my loving, supportive, encouraging friends, whose faithful support during the final stages of this Ph.D. is so appreciated. Thank you.

Nima Khadem Mohtaram
University of Victoria
December 2014

Table of Contents

List of Tables

List of Figures

Abbreviations

bovine serum albumin (BSA)
brain-derived neurotrophic factor (BDNF)
cell line-derived neurotrophic factor (GDNF)
central nervous system (CNS)
cycle threshold (C_t)
dichloromethane (DCM)
diclofenac sodium (DS)
dorsal root ganglion (DRG)
embryoid bodies (EBs)
embryonic stem cells (ESCs)
enzyme-linked immunosorbent assay (ELISA)
fetal bovine serum (FBS)
food and drug administration (FDA)
human serum albumin (HAS)
induced Pluripotent stem cells (iPSCs)
leukemia inhibitory factor (LIF)
methanol (MeOH)
nerve growth factor (NGF)
neural induction medium (NIM)
neural progenitor cells (NPCs)
neural stem cells (NSCs)
neurotrophin-3 (NT-3)
peripheral nervous system (PNS)
phosphate buffer saline (PBS)
pluripotent stem cells (PSCs)
poly (Ɛ-caprolactone) (PCL)
poly (ethylene oxide) (PEO)
poly(ε-caprolactone)-co-(ethyl ethylene phosphate) (PCLEEP)
poly-L-ornithine (PLO)
quantitative real-time polymerase chain reaction (qPCR)
scanning electron microscope (SEM)
spinal cord injury (SCI)
β-III-tubulin (TUJ1)

Chapter 1 Introduction

Pluripotent stem cells[1]

Pluripotent stem cells (PSCs) are characterised by immortality–the ability to continuously self-renew–and pluripotency–the ability to differentiate into all somatic cell types. PSCs include both embryonic stem cells (ESCs) and induced PSCs (iPSCs). ESCs originate from the inner cell mass of an early stage embryo and were first derived from mice by Evans and Kaufman in 1981 and from humans by Thomson et al. in 1998 [1, 2]. Nearly a decade later in 2006 and 2007, Takahashi et al. generated the first iPSCs showing that murine and human somatic cells could be reprogrammed to behave like ESCs by introducing four defined transcription factors via viral transduction [3, 4]. These factors, Oct3/4, Sox2, c-Myc and Klf4, were termed the Yamanaka factors. The development of iPSCs has tremendous implications for regenerative medicine due to the possibility of generating patient-specific cell therapies and the ability to generate PSC lines without the use of embryos.

Multipotent stem cells can give rise to multiple mature phenotypes and exist within specialised niches in many adult tissues. Temple first described neural stem cells (NSCs) isolated from the rat forebrain and characterised them by their ability to develop into the primary cells of the central nervous system (CNS)[5]. In 1992, Reynolds and Weiss successfully demonstrated that isolated cells from adult mouse striatum could be[2] induced to differentiate into neurons and

[1] The following section contains excerpts from: **Combining protein-based biomaterials with stem cells for spinal cord injury repair,** Montgomery et al., 2014 OA Stem Cells Review, Jan 18;2(1):1. Copyright Permission Pending.

astrocytes using epidermal growth factor [6]. Unlike PSCs, NSCs possess a fixed capacity only to differentiate into the cells of the nervous system.

Both pluripotent and multipotent stem cells can generate the necessary quantities of cells required for transplantation due to their ability to continuously divide. These cells can then be differentiated into desired phenotypes for therapeutic applications. For spinal cord injury (SCI) treatment, stem cells are differentiated into neural cells to overcome the inhibitory glial scarring which seals off the injury site and replaces the functional cells lost during injury. Stem cell-derived neural progenitor cells (NPCs) transplanted in a non-inhibitory environment survive and differentiate into neurons and oligodendrocytes leading to regeneration while the environment of an injured spinal cord inhibits NPC survival and promotes differentiation into astrocytes contributing to glial scarring [7, 8]. Therefore, many stem cell-based therapies seek to promote the generation of neurons and oligodendrocytes while reducing the differentiation of astrocytes. Another therapeutic approach utilises the protective function of astrocytes to improve the conditions after SCI [9].

iPSCs serve as a fascinating alternative for cell sourcing compared to ESCs. Not only do iPSCs circumvent the need for embryos when deriving pluripotent stem cell, there is the potential to generate patient specific iPSCs lines and therefore patient specific engineered tissues. Many studies have reported the differentiation human iPSCs into neural phenotypes for a variety of applications[10-16]. For instance, one study showed that transplanted neural crest cells derived from human iPSCs supported accelerated regeneration of the sciatic nerve in a rat injury model and no tumor formation was reported[17]. Another study differentiated human iPSCs into neural crest cells *in vitro* and then transplanted these cells into a fetal lamb model of spinal cord injury[18]. These cells survived and differentiated into neurons after transplantation and no

tumor formation was observed. This body of work illustrates the potential of iPSC-derived neural cells as a treatment for SCI.

Biomaterial scaffolds for spinal cord injury[3]

The spinal cord, the brain, and the blood-brain barrier are three major components of the CNS [19]. Two cell types, neuronal and glial cells, are found in the CNS. Neurons are responsible for the information transmission, while glial cells including astrocytes and oligodendrocytes provide nutrients to the nervous tissue, and support and insulate the axons respectively. The death of neurons and the formation of scar tissue that inhibits regeneration, contribute to loss of function of spinal cord. For stem cell treatment applied at the injury site of spinal cord, it is important that the cells be directed to become neurons or oligodendrocytes which will promote regeneration rather than other cell types such as astrocytes that will contribute to the scar tissue. Thus, a tissue engineered scaffold must be used as a replacement for the tissue which both promote neuronal differentiation and deliver the appropriate chemical cues in order to enhance neuronal regeneration.

Biomaterials are materials used with biological systems and can be derived from natural sources or synthetically produced. As a promising alternative to natural polymers, synthetic polymers play an important role in neural tissue engineering applications. Synthetic polymers offer a number of advantages over natural polymers. Virtues include reproducibility of composition, the ability to alter their biodegradability and biocompatibility, the ability to tailor their mechanical properties and the capability for chemical and physical surface modification.

[2] The following section contains excerpts from: **Neural tissue engineering applications.** Mohtaram, N.K., Montgomery, A.L., Gomez, J.C., Agbay, A. and Willerth, S.M. CRC Press (2014). Copyright Permission Pending.

Various combinations of biomaterials with stem cells can be used to replace lost or damaged tissue following SCI. Synthetic biomaterials can be combined with stem cells to develop therapies that aid in the regeneration of injured spinal cords. These approaches use various scaffolds to support the survival and differentiation of implanted stem cell-derived populations into functional neurons and glial cells with the aim of overcoming the inhibitory scarring that restricts cell regrowth after spinal cord injury. Neural tissue engineering uses biomaterial scaffolds that mimic the microenvironment present in healthy tissue to direct stem cell differentiation into neural phenotypes.

Solution and melt electrospinning techniques [4,5]

Nano and microfabrication techniques can be used to produce various biomaterial scaffolds that can mimic the microenvironment present in healthy tissue while reconstructing the damaged tissue through tissue engineering approaches. Using solution electrospinning technique, one can develop nanostructured biomaterial scaffolds to mimic the extracellular matrix of the neural tissue found in the spinal cord. In recent decades, the process of electrospinning has received remarkable attention due to its ability to fabricate polymer fibers ranging in size from nanometer to micrometer scale in diameter [20]. The introduction of the electric field was able to change the hemispherical liquid drop suspended in equilibrium at the end of needle into Taylor cone. By introducing the electric field, the electric potential balance against the surface tension and viscosity of the polymer solution and polymer melts. Electrospun scaffolds have been

[4] The following section contains excerpts from: **Nanofabrication of Electrospun Fibers for Controlled Release of Retinoic Acid**. Nima Khadem Mohtaram, Junghuyk Ko, Michael Carlson, Martin Byung-Guk Jun, Stephanie M Willerth. 9th International Conference on MicroManufacturing (ICOMM 2013).

[5] The following section contains excerpts from: Junghyuk Ko, Nima Khadem Mohtaram, Farid Ahmed, Am Montgomery, Michael Carlson, Patrick CD Lee, Stephanie M Willerth, Martin BG Jun **Fabrication of poly (ϵ caprolactone) microfiber scaffolds with varying topography and mechanical properties for stem cell-based tissue engineering applications**. Journal of Biomaterials Science, Polymer Edition 25;(1); 1-17. Copyright Permission Pending.

extensively evaluated for use in neural tissue engineering applications [21-23]. In terms of delivering chemical cues, emulsion electrospinning involves dissolving specific chemical cues into the desired polymer solution, which is then electrospun [24]. For presentation of physical cues, using different collection methods of the electrospun fibers results in different types of nanoscale topography [25]. Yet, for presentation of chemical cues, challenges still remain including obtaining bead-free morphology, while an agent needs to be encapsulated inside the nanofibers. Both of these properties can be achieved by tuning operational parameters, such as applied voltage and collecting distance, for the desired polymer solution with known concentration.

Electrospinning without solvents via the melt may be attractive for biomedical applications such as the tissue engineering of cell constructs where solvent accumulation or toxicity is a worry. Moreover, melt electrospinning is relatively under-studied compared to solution electrospinning and fiber diameter from melt electrospinning process was reported approximately 100μm [26-33]. In order to reduce fiber size, some researchers have used copolymerization to make lower molecular weight polymer and used a hybrid process that combines two different processes. For example, using polymer melt deposition and solution electrospinning together has been used to fabricate different fibers, [26, 31-34].

The process of melt electrospinning involves heating up the desired polymer with the resulting melt being extruded into fibers, resulting in better reproducibility than solution electrospinning [26, 27, 32-34]. The melt electrospinning process does not require the use of undesirable toxic solvents for dissolving polymers like solution electrospinning does [26]. More importantly, melt electrospinning enables better control of topography compared to solution electrospinning. Pioneering works by Larrondo and Manley in the early 1980s characterized

dependences of fiber diameter on the applied electrical field as well as temperature and viscosity of the polymer melt[29]. Additionally, other researchers characterized the mechanical and structural properties of melt electrospun fibers compared to the bulk properties of the polymer and they observed that fiber orientation influenced the bulk properties of the scaffold [29, 35].

Recent tissue engineering approaches have combined ESCs with biomaterial scaffolds to direct differentiation into functional tissue replacements[36]. For instance, neural tissue engineering can be used to develop therapies for reconstructing damaged nerves through the use of biomaterial scaffolds and stem cells that can mimic the microenvironment present in healthy tissue [36, 37]. Many studies have successfully shown that chemical cues presented by biomaterial scaffolds can promote ESC differentiation [19, 38-40]. A similar body of work demonstrates the role of physical cues presented by scaffolds such as elasticity, micro and nanostructures of these structures can influence stem cell differentiation as well [25, 41, 42]. For example, aligned nanoscale topography significantly enhanced the neuronal differentiation of ESCs [25, 43]. For electrospun fibers, these physical and mechanical factors include morphological and mechanical properties of such scaffolds, which are highly influenced by altering fiber diameter.

Synthetic polymers for neural tissue engineering applications[6]

Synthetic polymers are commonly used for biomedical applications. One synthetic polymer, Poly (Ɛ-caprolactone) (PCL), is promising for fabricate scaffolds. PCL is biodegradable, saturated polyester with tunable mechanical properties, rate of surface and bulk biodegradation,

[6] The following section contains excerpts from: **Neural tissue engineering applications.** Mohtaram, N.K., Montgomery, A.L., Gomez, J.C., Agbay, A. and Willerth, S.M. CRC Press (2014). Copyright Permission Pending. 2014.

solubility and crystallinity, and structural topography. PCL has a very low melting point (55 ~ 60^{o}C) and glass transition temperature (-54^{o}C) [44]. PCL has been applied in diverse settings nerve, cartilage, heart and bone tissue engineering [25, 30, 45-54]. An up-to-date review on PCL based formulations for drug delivery, along their purpose and brief conclusions is given by Dash and Konkimalla [20]. Moreover, PCL has been fabricated into various micro and nano-scale structures, depending on the desired biomedical applications. These diverse structures include microspheres, microfibers, micelles, films, nanoparticles, nanofibers and nanowires. For instance, Bechara *et al.* used PCL nanowires to investigate their ability to enhance the neuronal behavior of PC12 cells [45]. They have shown that cells adhered to the PCL nanowires could form a neuronal network after 7 days of culture. Interestingly, PCL nanofiber scaffolds have also supported the neurite extension of explant dorsal root ganglion (DRG)[55]. In addition to pure PCL nanofibers, functional immobilization of brain-derived neurotrophic factor (BDNF) on the surface PCL nanofibers can promote NSC proliferation [49]. BDNF is a neurotrophic factor which promotes the development, survival, and regeneration of neurons. Xie and his colleagues showed that the differentiation of ESCs into neural phenotypes is highly influenced by the topography of PCL scaffolds [25].

PCL can serve as a reservoir for drug encapsulation with the aim of the long term controlled release of up to several months. The controlled release of nerve growth factor (NGF) from PCL nanofibers was demonstrated by Valmikinathan and his colleagues [53]. Jiang *et al.* showed that the controlled release of retinoic acid (RA), a hydrophobic small molecule (molar mass ~ 300 g/mol) involved in neural patterning, can be achieved using electrospun PCL nanofibers [56]. Wang *et al.* functionalized electrospun PCL nanofibers with glial cell line-derived neurotrophic factor (GDNF) to promote the integration of NSCs into the parenchyma of

the mouse brain [57]. All of these studies demonstrate how PCL can be used to deliver neurotrophic factors and such strategies can be translated for clinical applications. In spite of its advantages, the hydrophobicity of PCL prevents the efficient encapsulation of growth factors and other small hydrophilic molecules [58]. Using toxic solvents in order to improve the encapsulation efficiency of loaded drug remains one of the most important biological concerns when designing PCL based delivery systems. Addressing these challenges will enable more widespread acceptable of PCL scaffolds for neural tissue engineering applications.

Controlled release of neurotrophic factors [7]

Drug delivery of neurotrophic factors serves as a promising approach for the treatment of nervous system diseases and disorders[59-62]. Neurotrophic factors are proteins that promote the development, survival, and regeneration of neurons. Examples include NGF, GDNF, BDNF and neurotrophin-3 (NT-3) and each factor targets specific populations of neural cells. NGF plays a prominent role in sensory neurons by stimulating neurite outgrowth and increasing the survival of sympathetic neurons during inflammation [61]. It also promotes axonal regeneration in central and peripheral nervous system after injuries [59]. GDNF enhances nerve regeneration in a rat nerve injury models and promotes survival of motor neurons[63]. It has exhibited both neurorestorative and neuroprotective effects for the dopaminergic neurons present in Parkinsonian animal models [37]. NT-3 promotes the differentiation of new neurons and enhances corticospinal tract formation during development [37].

[7] The following section contains excerpts from: **Biomaterial based drug delivery systems for controlled release of neurotrophic factors.** Mohtaram, N.K., Montgomery, and Willerth, Biomed Mater. 2013 Apr;8(2):022001. doi: 10.1088/1748-6041/8/2/022001. Epub 2013 Feb 5. Copyright Permission Approved 2014.

Controlled release drug delivery systems are a promising approach to modulate the release duration and localization of therapeutic agents. The main goal of drug delivery systems is to transport biological active agents such as growth factors and genetic materials into the desired location in order to prompt therapeutic healing of disease [37, 64, 65]. A delivery system is produced usually by combining the active agent with a delivery system.

Reservoir-based delivery systems are defined as porous devices where diffusion mechanisms control the rate of drug release[66]. In these systems, the drug is suspended or dissolved within a polymer reservoir. Drug delivery is initially controlled by penetration of the drug through the biodegradable polymer structure, followed by release of the drug due to surface and bulk erosion of the reservoir. The reservoir can be broadly classified into: nanogels, nanoparticles, micelles, hydrogels, microspheres, electrospun nanofibers and combined systems.

These nanofiber scaffolds are commonly used as reservoir-based drug delivery systems as electrospinning enables the incorporation of bioactive agents, making it a versatile technique [21]. In particular, electrospinning has many benefits, including flexibility in surface functionalization, reduced initial burst release, and the ability to fabricate scaffolds into a variety of shapes [67-69]. Electrospun nanofibers possess a 3D, interconnected porous structure with high surface area-to-volume ratio, and thus have great potential for drug delivery applications [50, 56, 70, 71].

Often, the first step in incorporating bioactive neurotrophic factors into electrospun nanofibers is to characterize the release properties by using model proteins such as bovine serum albumin (BSA), human serum albumin (HSA), or lysozyme before using bioactive neurotrophic factors, which can be more costly. Encapsulation of drugs inside electrospun nanofibers can be carried out by emulsion electrospinning where the target drug is dissolved in the desired polymer

solution[72]. Using this method, Piras *et al.* produced polymeric nanofibers containing diclofenac sodium (DS) and HSA by electrospinning[73]. A different method, core-shell electrospinning, can lead to enhanced protection of bioactive factors as a coaxial syringe is used to form a core-shell structure from two separate polymer solutions. Jiang *et al*. implemented a method of two coaxial capillaries to incorporate two model proteins, BSA and lysozyme into PCL nanofibers [50]. A slight burst release of BSA was observed during the first day and the released lysozyme retained enzymatic function. In another study, Liao *et al.* successfully demonstrated the encapsulation of platelet derived growth factor-BB into aligned PCL core-shell nanofibers [74, 75]. The use of coaxial electrospinning did not have a negative effect on the stability of the released lysozyme. Kim *et al.* showed that by varying the concentration of poly (ethylene oxide) (PEO) used in electrospinning fibers containing lysozyme that the encapsulation efficiency of the process could be increased[70]. Furthermore, the released lysozyme showed the enzymatic activity as a proof of its bioactivity stability during the electrospinning process and after controlled release. These release studies using model proteins provide a useful starting point for incorporating neurotrophic factors into electrospun nanofibers.

Many groups have encapsulated neurotrophic factors inside of electrospun nanofibers for neural tissue engineering applications[24]. For instance, Jiang *et al.* showed that nanofiber morphology along with controlled release of RA, a small molecule that regulates neural development, enhances the differentiation of mesenchymal stem cells into neural lineages[56]. They demonstrated that ~60% of the encapsulated RA from aligned PCL nanofibers was released after 14 days. When the mesenchymal stem cells were seeded on these scaffolds, they showed increased expression of neuronal markers, Tuj-1 and MAP2, compared to untreated cells. A study by Chew *et al.* showed sustained release of NGF from aligned ε-caprolactone and ethyl

ethylene phosphate (PCLEEP) nanofibers[67]. They reported the controlled release of NGF. However, the encapsulation efficiency of NGF inside the fibers was very low and may be due to the immiscibility of NGF in the protein aqueous phase with PCLEEP solution phase. Valmikinathan *et al.* used a mixture of BSA and NGF to enhance encapsulation efficiency[53]. Sustained release of NGF was detected through ELISA for 28 days and an *in vitro* bioactivity assay was performed using the PC12 cells seeded on NGF releasing electrospun nanofibers. Results from this study showed that the NGF released from the electrospun scaffolds induced neurite outgrowth, indicating that BSA serves as a carrier protein that can preserve growth factor activity. Furthermore, the efficiency of encapsulation of the NGF was reported to be 26.4 % for PCL-NGF alone, while a higher efficiency of 88.6 % was found when using BSA in the encapsulation process.

In addition to the aforementioned benefits of electrospinning, such as flexibility in surface functionalization and reduced initial burst release, electrospun nanofibers have a few disadvantages as well. The main drawback is the formation of drug aggregates along non-smooth fibers. A set of parametric studies has to be designed to find out the optimum condition of perfect drug encapsulation inside the fibers [40]. Moreover, controlling the uniform distribution of fiber size is very challenging. Wider range of fiber size distribution may lead to poorer control on the drug release. Furthermore, using toxic solvents to make polymer-drug emulsion is the most important biological concern of drug delivery from nanofibers. In order to enhance the protection of bioactive factors, using a coaxial syringe is highly recommended. All of these studies demonstrate the potential of electrospun nanofibers as reservoir-based delivery systems for the delivery of neurotrophic factors.

In summary, many drugs are commonly used in the field of neural tissue engineering, but among them, RA and GDNF both play a key role in promotingneuronal differentiation of iPSCs. RA is a small hydrophobic molecule (molar mass ~ 300 g/mol) derived from vitamin A. During early embryonic development, RA, regulates germ layer formation, and it also plays important roles in neural cell growth and reagulates the neural differentiation of iPSCs. Growth factors also have a promising effect on stimulation the differentiation of iPSCs toward neural phenoytpes as well. GDNF is a protein that enhances the survival of neurons. GDNF, a hydrophilic macromolecule (molecular weight ~30 kDa), has different chemical and physical properties which make it more challenging to encapsulate inside hydrophobic polymers such as PCL for drug delivery applications. It supports the survival and differentiation of neurons and has the potential to treat neurodegenerative diseases such as Parkinson's disease. GDNF promotes the survival of motor and dopaminergic neurons, making it a promising therapeutic for the treatment of neurodegenerative diseases and it can also be used to enhance cell survival after transplantation in the damaged CNS [59,63].

Research aims

As dicussed in this introduction, there are many approaches that combine pluripotent stem cells with electrospun scaffolds for promoting the differentiation of such cells into desired phenotypes. However, these studies have not yet combined physical and chemical cues together to enhance the efficacy of electrospun scaffolds to induce neuronal differentiation of iPSCs. Therefore, it is hypothesized that multiscale and multifunctional electrospun PCL fiber scaffolds are capable of enhancing the differentiation of mouse and human iPSCs into neurons through both physical (topography) cues and controlled release of biologically active agents (small molecules and growth factors) as chemical cues.

Specific research aim 1

We hypothesize that solution electrospun PCL nanofibers can promote the differentiation of mouse iPSCs into neuronal cells through the topography of fibers (physical cues) and controlled release of a small molecule (chemical cues).

Objective 1: To demonstrate controlled release of retinoic acid (RA) from encapsulated PCL nanofiber scaffolds with varied topographies.

Objective 2: To determine if blank and encapsualated scaffolds with randomly-oriented and aligned topography could support the neuronal differentiation of mouse iPSCs.

In Chapter two, we study how solution electrospinning can be used to fabricate nanofiber-based biomaterial scaffolds which present chemical and physical cues to promote and direct the neuronal differentiation of mouse iPSCs. These scaffolds fabricated out of PCL have different topographies and they contain different concentrations of RA, a small molecule that regulates neural development. Such scaffolds are expected to support the differentiation of neural progenitors derived from mouse iPSCs into neurons.

Specific research aim 2

We hypothesize that melt and solution electrospun PCL microfibers and bimodal scaffolds can promote the differentiation of hiPSCs into neuronal cells through the topography of microfibers (physical cues) and also the controlled release of RA from nanofibers (chemical cues).

Objective 1: To engineer melt electrospun scaffolds with various topographies and further functionailze them with encapsulated nanofibers to study their ability to support the neuronal differentiation of human iPSCs.

Objective 2: To determine how topographical properties of scaffolds such as fiber diameter and its orientation influence the neurite outgrowth of neural progenitors derived from human iPSCs seeded on such scaffolds.

In Chapter three, we investigate how physical cues affect the neuronal differentiation of human iPSCs. The effect of micro and nanoscale scaffold topography for promoting neuronal differentiation of human iPSCs will be studied. We use melt electrospinning and solution electrospinning together to fabricate multiscale novel PCL scaffolds with engineered properties. Specifically, we focus on how such scaffolds guide and control the orientation and length of neurites outgrowth from neural progenitors derived from human iPSCs. We also aim to show how novel bimodal scaffolds (combination of PCL microfibers and RA encapsulated PCL nanofibers) support the neuronal differentiation of human iPSCs as they present to cells both a physical and chemical cue to encourage their differentiation.

Specific research aim 3

We hypothesize that solution electrospun PCL nanofibers with varied topographies can be encapsulated with growth factors for neural tissue engineering applications. Aligned GDNF loaded PCL nanofibers could support human iPSCs differentiation into neurons. Such engineered systems can deliver glial cell-derived neurotrophic factor (GDNF) over a month.

Objective 1: To engineer solution electrospun scaffolds with various topographies to provide the controlled release of GDNF over a month as well as testing the bioactivity of the released GDNF.

Objective 2: To determine if novel GDNF-loaded aligned PCL nanofiber scaffolds can support the neuronal differentiation of neural progenitors derived from human iPSCs seeded on such scaffolds.

In Chapter four, we study how the solution electrospinning technique can be used to encapsulate proteins such as bovine serum albumin (BSA) and GDNF inside PCL nanofibers with varied topographies. We also assay the compatibility of aligned GDNF loaded scaffolds with human iPSCs and if these scaffolds encourage neuronal differentiation when seeded onto such scaffolds.

Finally in Chapter five, conclusions are drawn about the current state of multiscale scaffolds for promoting neuronal differentiation of iPSCs and controlled release of neurotrophic factors as applied to neural tissue engineering along with future directions for the field.

Chapter 2 Multifunctional Electrospun Scaffolds for Promoting Neuronal Differentiation of Induced Pluripotent Stem Cells[8]

Introduction

Pluripotent stem cell lines can be differentiated into any of the specific cell lineages found in an organism, including those found in neural tissue[19, 39, 76]. The two major types of pluripotent stem cells include embryonic stem cells (ESCs), which are isolated from the inner cell mass of blastocysts, and induced pluripotent stem cells (iPSCs), which are produced from adult somatic cells, such as skin cells, by overexpressing specific transcription factors that restore pluripotency[1, 3, 4, 39, 77]. Pluripotent stem cells are often cultured as aggregates called embryoid bodies (EBs) to induce differentiation into mature phenotypes[2, 78]. One of the major challenges when working with pluripotent stem cells is how to control the differentiation process to produce a desired cell phenotype.

Many pre-clinical studies have shown the potential of cell therapy for spinal cord injury (SCI) treatment [1-4, 19, 39, 76-79]. Schwann cells, neural stem/progenitor cells, and bone-marrow stromal cells have been transplanted into *in vivo* models of SCI to promote functional recovery[79]. More recently, transplanting neural progenitors derived from human iPSCs into the injured mouse spinal cord improved functional recovery compared to control animals[12]. Furthermore, neural progenitors derived from murine and human iPSCs were transplanted into a marmoset injury model where they promoted functional recovery after SCI[13]. These cells

[8] The following chapter is from: **Multifunctional Electrospun Scaffolds for Promoting Neuronal Differentiation of Induced Pluripotent Stem Cells.** Mohtaram, N.K., et al. Accepted for publication by the Journal of Biomaterials and Tissue Engineering in July 2014.

were deemed safe as they did not produce tumors post transplantation. These studies indicated that producing neurons from pluripotent stem cells can serve as an appropriate strategy for achieving regeneration and recovery by replacing the cells lost to SCI[39].

To achieve this goal, presentation of chemical and physical cues can be used to direct pluripotent stem cells to differentiate into neurons[22, 23, 25, 38, 42, 43, 56, 76, 80-82]. Chemical cues, such as growth factors and small molecules like retinoic acid (RA), are commonly used to stimulate the differentiation of stem cells into neurons[22, 38, 42, 76]. In particular , RA is a hydrophobic small molecule (molar mass ~ 300 g/mol) that can stimulate the differentiation of ESCs and iPSCs into motor neurons[39]. Physical cues, such as scaffold elasticity and topography, can also influence the differentiation of pluripotent stem cells into specific phenotypes[22, 23, 25, 43, 56, 80, 82-84]. Of these physical cues, nanotopography has been extensively investigated as many tissues found in body have defined nanoscale structures[70]. A pioneering review by Kim *et al.* characterized the nanostructures present in human tissues along with the use of nanofabrication methods for mimicking these nanostructures[70]. Additionally, functionality and morphology of many cells are controlled with nanotopographical properties of scaffolds[70, 85-87]. For example, aligned nanoscale topography significantly enhanced the neuronal differentiation of a variety of cell types, including mouse ESCs, human mesenchymal stem cells, and human neural crest stem cells[22, 23, 25, 56, 82]. While most studies investigate the effects of chemical and physical cues independently of each other, we fabricated and characterized multifunctional biomaterial scaffolds that presented both types of cues as a substrate for promoting iPSC-derived neural progenitors to differentiate into neurons.

While many biomaterial scaffolds exist, scientists often use electrospun nanofibers for various tissue engineering applications[71, 85, 88]. Encapsulated electrospun nanofibers can be fabricated through the use of emulsion electrospinning. This process involves dissolving specific chemical cues into the desired polymer solution, which is then electrospun into nanofibrous scaffolds[24]. However, adding chemical cues to the polymer solution alters its properties, making it challenging to obtain bead-free nanofiber morphology during the electrospinning process. To alter the physical properties of the nanofiber scaffolds, different fiber collection methods are used to produce different types of nanoscale topography[24, 56]. By tuning operational parameters such as applied voltage and collecting distance, a set of desired physical and chemical properties can be achieved. Ghasemi-Mobarakeh *et al*. showed that polymeric nanofibers could serve as a substrate for the culture of mouse neural progenitors and to enhance neurite outgrowth[89]. Aligned electrospun nanofibers can also regulate adhesion, proliferation, and differentiation of neural crest stem cells toward Schwann cells, highlighting the influence of topography on cell behavior[22, 90]. Neural crest stem cells derived from human iPSCs and human ESCs seeded on aligned nanofiber scaffolds were transplanted into the transected sciatic nerve in a rat model where they accelerated nerve regeneration after 1 month[17]. In addition to the orientation of fibers, the diameter of electrospun fibers could also lead to the modulation of stem cell differentiation into neural phenotypes. For instance, Christopherson *et al.* showed that a higher degree of proliferation and neuronal differentiation of neural stem cells had been achieved when the fiber diameter of electrospun scaffolds decreased[91]. All of these studies show the key roles that such scaffolds play in neural tissue engineering applications[92, 93].

In this study, we demonstrate the controlled release of RA from randomly-oriented and aligned poly (ε-caprolactone) (PCL) electrospun nanofibers and show that these substrates

support the culture and differentiation of iPSC-derived neural progenitors. Our polymer of choice was PCL due to its slow degradation rate, which allows for controlled drug delivery over extended time periods[20]. Using a blending technique, different doses of RA (0.1, 0.2 and 0.3% (*w/v*)) were successfully encapsulated into electrospun PCL nanofibers with different topographies (randomly-oriented and aligned). The controlled release of RA from PCL-RA scaffolds containing 0.2 % (*w/v*) RA from both topographies was characterized for a month, with the randomly-oriented nanofibers releasing RA more rapidly than the aligned nanofibers. Finally, we seeded iPSC-derived neural progenitors upon these scaffolds, where they showed high rates of viability and differentiated into neurons. This work confirms the suitability of these multifunctional scaffolds for stem cell-based tissue engineering applications.

Methods

Nanofiber scaffold fabrication

Poly (ε-caprolactone) (PCL) ($\overline{M_n}\sim45000$) and retinoic acid (RA) (all-trans, ≥98% HPLC, powder form) were purchased from Sigma-Aldrich (St. Louis, MO, USA). Dichloromethane (DCM) (reagent/ACS grade) and methanol (MeOH) were purchased from VWR International (Edmonton, AB, Canada). Phosphate buffer saline (PBS, 1X) solution was purchased from Life Technologies (Burlington, ON, Canada). A mixture of DCM/MeOH at a volume ratio of 8:2 was prepared to dissolve PCL granules to make a 10% PCL (*w/v*) solution. This solution was mixed overnight using a magnetic stir bar on a stirring hotplate (Corning PC-420D). For PCL solutions containing RA, an RA stock solution of 2.5 mg/ml was added into the PCL solution to obtain a homogenous solution of PCL-RA with a theoretical loading of 0, 0.1, 0.2 and 0.3 % *w/v*. This mixture was stirred overnight. All solutions were stirred at 500 rpm at room temperature. The solutions were then stored at 4°C before solution electrospinning. Our electrospinning setup

consists of the following: a syringe pump (New Era Pump Systems Inc., USA), a dispensing needle (McMaster Co., USA), a machined water container, and a high voltage power supply (GAMMA High Voltage Research Inc., USA). PCL and PCL-RA solutions were pumped at a constant flow rate of 2 ml/hr through the electrospinning syringe (nozzle) when fabricating randomly-oriented blank PCL and RA-encapsulated PCL scaffolds respectively. Randomly-oriented nanofibers were collected on top of glass cover slips that were placed on the aluminum foil collector plate. The positive terminal of the high voltage power supply was connected to the foil while the ground terminal was connected to the nozzle tip. For the fabrication of aligned blank and encapsulated nanofibers, a rotating drum was placed between the water container and nozzle to collect spun nanofibers. The flow rate (2 ml/hr) was maintained for both topographies. All fibers were collected on cover slips attached on the surface of the drum, which was charged at 10 kV. The collecting distance and speed of the rotating drum were fixed at determined optimal conditions of 5 cm and 4000 rpm. Each scaffold (~10 mg) was dried overnight prior to its use in experiments. The nanofabrication parameters used in the experiment are provided in Table 1. The electrospinning setup for the fabrication of the randomly-oriented and aligned electrospun PCL nanofibers and the chemical structures of PCL and RA are schematically shown in Figure 1.

Topography	Electrospinning Operational Parameters		
	Voltage (kV)	Collection Distance (mm)	Drum Speed (rpm)
Randomly-oriented	15	75	N/A
Aligned	10	50	4000

Table 1 Nanofabrication parameters

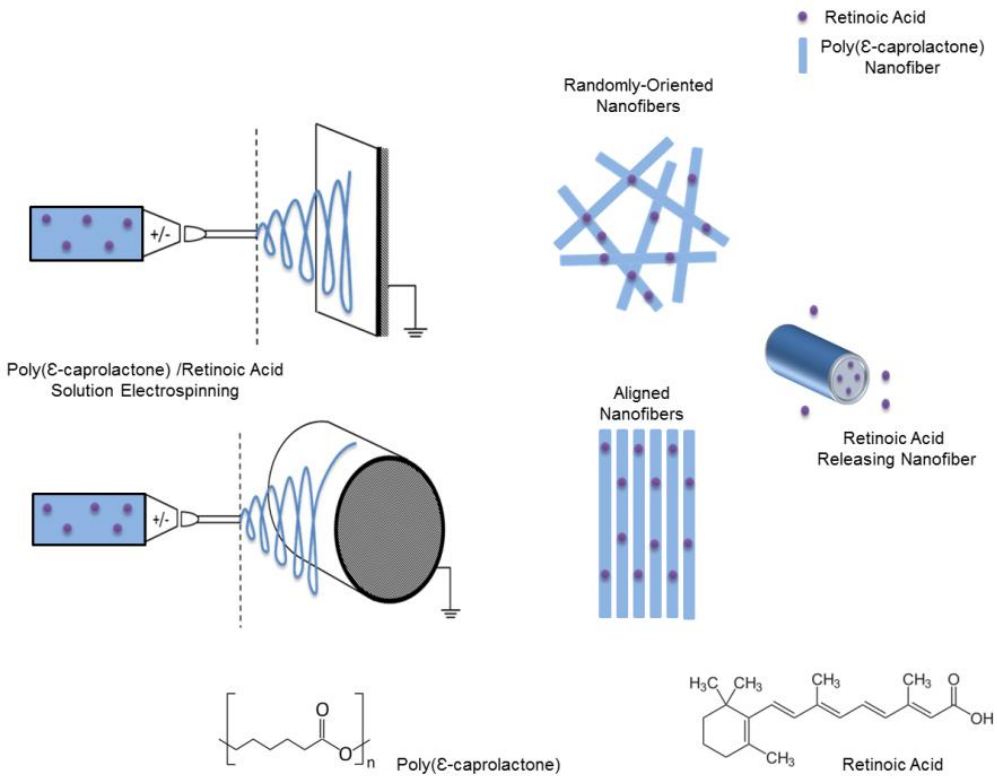

Figure 1 Schematic of the encapsulated nanofibers with varied topographies

Scaffold characterization

The nanofibers were characterized using a Hitachi S-4800 scanning electron microscope (SEM). For each topography, a sample of nanofibers was placed onto an SEM stub mount and sputter coated with the Cressington 208 High Vacuum coater, adding a 3 nm thick carbon layer on the surface of nanofibers. The samples were carbon-sputtered three times for 6 seconds at 10^{-4} $m$bar. Nanofibers were imaged using an accelerated voltage of 1.0 kV and a working distance of 8 mm. The average diameter for each sample was determined using Quartz-PCI Image Management Systems® software. For each sample, 50 fibers were characterized from 3 different SEM images.

In vitro retinoic acid release studies

Encapsulated nanofibers (~10 mg, $n = 3$) were put in 1.5 mL microfuge tubes, suspended in 1 mL PBS, and incubated at 37°C. Release samples were taken at days 1, 2, 6, 10, and 14 for initial release studies, replaced with fresh medium, and stored at -20 °C until analysis. An Ultrospec 3000 spectrophotometer (Pharmacia Biotech®) was used to determine the absorbance of the samples and standards (0.05, 0.1, 0.5, 1, 2.5 and 5 μg/ml of RA) at 316 nm. To determine the amount of RA left in the nanofibers at the end of the experiment, the scaffolds were placed in a 45 mL conical tube with 500 μL of DCM and 2 mL of MeOH added to dissolve the PCL while vortexing for 1 minute. Afterwards, to allow for extraction of loaded RA into the solution, a mixture of PBS and MeOH was added to the conical tube and vortexed for 15 seconds. Encapsulation efficiency was calculated by taking the ratio of the actual encapsulated RA divided by the amount of RA originally added in to the solution. *In vitro* release studies were carried out in triplicate and data was analysed as a mean ± standard deviation (SD).

Stem cell culture and differentiation

All reagents were purchased from Invitrogen unless otherwise specified. Mouse iPSCs (System Biosciences) were cultured at 37˚C and 5% CO_2 on mouse embryonic fibroblast feeder layers in stem cell media as described previously and then passaged accordingly[23]. Embryoid bodies (EBs), which are aggregates containing cells at early stages of differentiation, were formed using a previously described retinoic acid and purmorphamine treatment protocol[82]. Undifferentiated iPSCs were added to non-adhesive plates containing LIF-free media and were cultured as EBs for six days, being dosed with 500 nM retinoic acid (Sigma) and 1 μM purmorphamine (StemGent) during the last four days. Media changes were performed every other day.

Seeding embryoid bodies on nanofiber scaffolds

Sheets of PCL and RA-encapsulated PCL nanofiber scaffolds were sterilized via exposure to UV light for 10 minutes. Under aseptic conditions, the scaffolds were added to 6-well polystyrene tissue culture plates, followed by the addition of 2 mL LIF-free media. EBs were manually seeded onto the surface of each scaffold using a micropipette. The cultures were maintained for 10 days without media change before analysis.

Cell viability analysis

The viability of EBs seeded on the nanofiber scaffolds was analyzed qualitatively after 10 days using a LIVE/DEAD® Viability/Cytotoxicity Kit (Invitrogen). The details of the staining are previously described[25, 38, 94]. Immediately prior to use, calcein AM and ethidium homodimer-1 were diluted in the same solution of D-PBS (Invitrogen) to concentrations of 2 μM and 4 μM, respectively; 200 μL of the stain solution was then added to each well and incubated at room temperature for 45 minutes. Each well was imaged using a fluorescent microscope with images captured at 515 nm for green fluorescence and 635 nm for red fluorescence. Images were overlaid at layer opacity of 50%. In order to quantify the live/dead analysis, an IncuCyte® ZOOM Essen BioScience® fluorescent microscope was used to measure the green fluorescent intensity in the image. Three EBs were selected per group for analysis using the IncuCyte® ZOOM Fluorescent Processing Software.

Immunocytochemistry

Neuronal differentiation was qualitatively assessed by immunocytochemistry targeting the neuron-specific protein β-III-tubulin (TUJ1), as previously described[25, 38, 94]. Cells were fixed with a 10% formalin (Sigma) solution for 1 hour at room temperature, permeabilized with

0.1% Triton-X (Sigma) solution for 45 minutes at 2 – 8 ˚C, and blocked with a 5% solution of normal goat serum (Millipore) for 2 hours at 2 – 8 ˚C. Primary TUJ1 antibody (Millipore) was applied at a dilution of 1:500 and incubated for 12 hours at 2 – 8 ˚C followed by a set of PBS washes. Secondary antibody (Invitrogen) was applied at a dilution of 1:200 and incubated at room temperature for 4 hours followed by a set of washes. Images were captured at 515 nm for green fluorescence.

Statistical analysis

Data are presented as mean values ± standard deviation of the mean. Statistical analysis using STATISTICA 9 applying a standard *t*-test was carried. Significance was considered at the $p < 0.05$ level.

Results

Fabrication and characterization of scaffolds

SEM images of all sets of scaffolds are shown in Figure 2. Morphologies of the randomly-oriented and aligned blank PCL nanofibers are shown in Figures 2A and 2E. The topography of both sets of nanofibers showed a very porous structure with the absence of polymer beads. Due to its crystallinity, the polymer chains tend to be stretched uniaxially along the flow direction, which is induced by the rotating drum at 4000 rpm speed. The fiber diameter was measured as 103 ± 27 nm (*n=50*) and 263 ± 97 (*n=50*) nm for randomly-oriented and aligned topography respectively. For both topographies, the fibers had non-uniform diameters as the fiber diameter changed along the length of individual nanofibers.

Figure 2C and 2G show the topography of the randomly-oriented and aligned electrospun PCL nanofibers containing 0.2 % *w/v* of RA. The average fiber diameter was measured as 517 ±

220 nm (*n=50*) and 617 ± 201 nm (*n=50*) for randomly-oriented and aligned topography respectively from 3 different distinct SEM images for scaffolds containing the same dosage, that being 0.2 % *w/v* of retinoic acid. The resulting electrospun meshes contained no beads. Similar to the blank PCL nanofibers, the fiber diameter varied along an individual fiber. All aligned electrospun RA-encapsulated PCL nanofibers had significantly larger diameters and fiber distribution compared to the blank PCL nanofibers. In the case of randomly-oriented nanofibers, there were significant differences between RA-encapsulated PCL nanofibers and blank nanofibers. Similar results have been reported for the encapsulation of other drugs inside PCL nanofibers. Valmikinathan *et al.* hypothesized that this variation in diameter is due to the phase separation of PCL and nerve growth factor[53]. We assume that this variation in diameter could be also due to the change of PCL solution properties such as viscosity and polarity in the presence of RA. As shown in Figure 2I, the average fiber diameter of aligned PCL-RA scaffolds containing 0.1 % *w/v* of RA is significantly larger compared to the aligned blank PCL scaffolds. There are no significant differences in topography between the blank scaffolds and the encapsulated scaffolds containing 0.2 % *w/v* of RA. This effect might be due to the fact that RA is hydrophobic like PCL. Thus, the affinity of RA to bond physically with PCL chains would be influenced by its concentration. If the concentration of RA is either too low or too high, RA could accumulate inside of the PCL nanofibers, leading to an inconsistency in the diameter of the nanofibers. From the fabrication point of view, the encapsulated scaffold containing 0.2 % w/v of RA was the optimized scaffold in terms of RA loading since there is no significant difference in fiber diameter between two topographies of the scaffold.

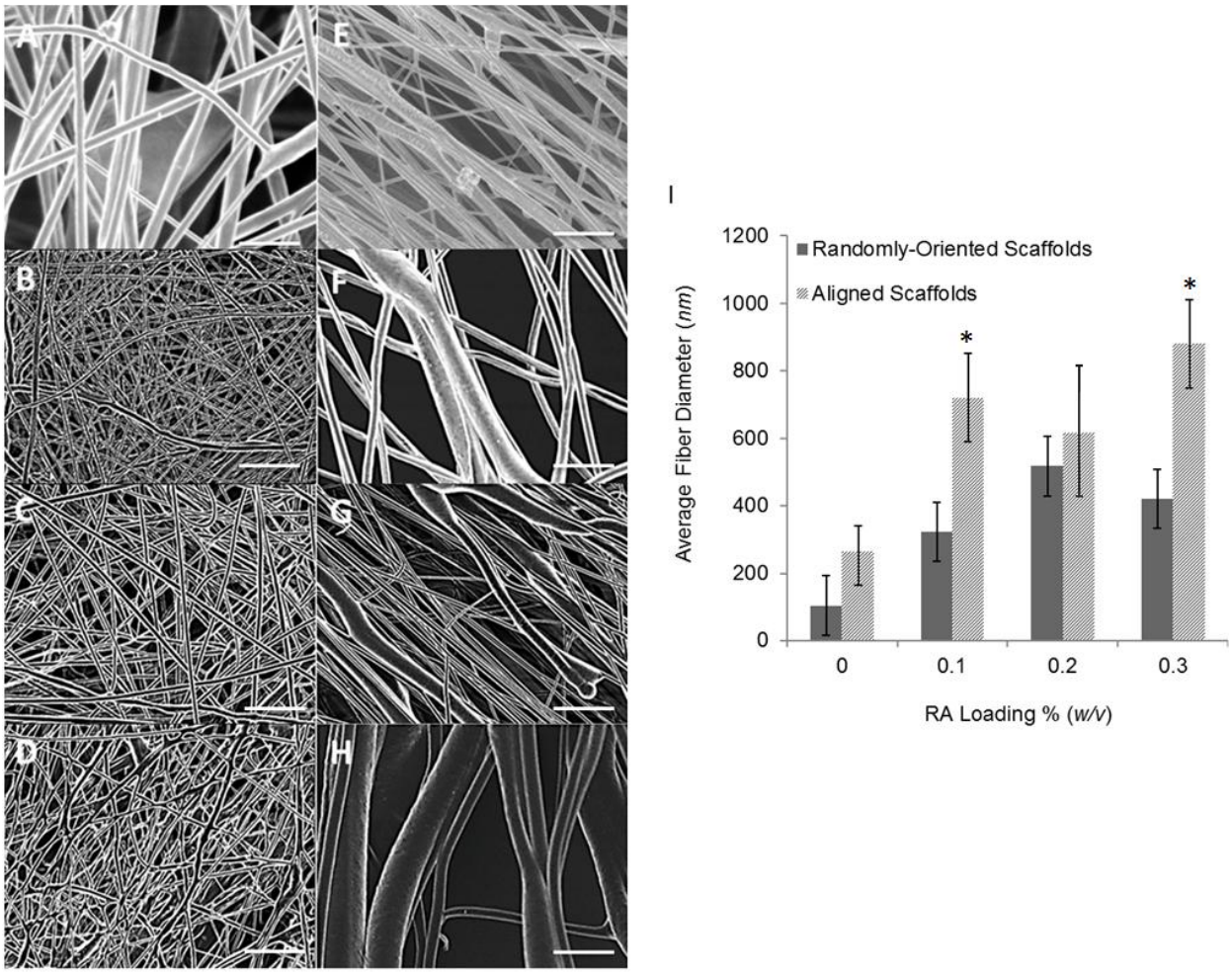

Figure 2 Scanning electron microscopy images of poly (ε-caprolactone) nanofiber scaffolds. (A), (B), (C) and (D) randomly-oriented scaffolds containing 0, 0.1, 0.2, ad 0.3% retinoic acid (w/v) respectively. (E), (F), (G) and (H) aligned scaffolds containing 0, 0.1, 0.2 and 0.3 % retinoic acid (w/v) respectively. Scale bar is 5 µm. (I) Average fiber diameter of randomly-oriented and aligned nanofibers vs. different RA loading. Randomly-oriented nanofibers were spun at 15 kV and the collecting distance was fixed at 7.5 cm since the aligned nanofibers were fabricated at 10 kV and 5 cm. * indicates $p<0.05$ versus two topographies.

Retinoic acid release kinetics

Table 2 shows the encapsulation efficiency for all RA-containing scaffolds. Each RA-containing scaffold was characterized for its ability to release RA over 14 days. The total released RA was 19.4 ± 1.2 % (*n=3*) and 14.94 ± 1.7 % (*n=3*) from PCL nanofibers containing 0.1 *w/v* of RA for the randomly-oriented and aligned scaffolds respectively. For scaffolds

containing 0.3 *w/v* RA, these amounts were 12.47 ± 1.1 % and 9.66 ± 0.95 % for the randomly-oriented and aligned scaffolds respectively. Due to their low encapsulation efficiency, it is possible that the encapsulated RA was not released from inside of the nanofibers, but represents the release of RA present on the surface of nanofibers. The encapsulation efficiency of RA in aligned scaffolds containing 0.2 % *w/v* of RA was 40 ± 5 %, and in randomly-oriented scaffolds this amount was 70 ± 11 %. Since PCL nanofibers containing 0.2 % *w/v* of RA had the highest encapsulation efficiency and the nanofiber morphology consisted of smooth topography, this formulation was used for our 30 day release study and for our cell culture experiments.

Topography	RA % (*w/v*)	Encapsulation Efficiency %
Randomly Oriented	0.1	42 ± 4
	0.2	70 ± 11
	0.3	30 ± 6
Aligned	0.1	25 ± 3
	0.2	40 ± 5
	0.3	20 ± 3

Table 2 Encapsulation efficiency of encapsulated scaffolds with two topographies (n=3).

Due to their porous structure and small fiber diameter, RA-containing PCL electrospun nanofibers have a high surface area, enabling them to serve as proper scaffolds for neural tissue engineering applications. We fabricated bead-free nanofibers while controlling scaffold morphology. Controlled release of RA from PCL nanofibers with both topographies was observed over 30 days at a rate of 0.3 ± 0.1% and 0.6 ± 0.2 % per day for the aligned and randomly-oriented PCL-RA scaffolds respectively (Figure 3). Within 1 day, 0.32 ± 0.01 % of RA was released from the aligned scaffolds since this amount was almost 2 times greater for the

randomly-oriented scaffolds (0.6 ± 0.2%); no burst release was observed. The total RA released over 30 days was 8.5 ± 2.4 % (~ 6.6 μg or ~ 0.2 μg per day) and 17.8 ± 5.4 % (~ 12.5 μg or ~ 0.4 μg per day) for the aligned and randomly-oriented topographies respectively. As previously reported, the standard concentration of RA used for promoting neural differentiation is 1 μM (0.3 μg/mL)[91]. Our scaffolds could provide 0.2 - 0.4 μg/ml of RA per day depending on their topography, which would be an ideal concentration for promoting the neuronal differentiation of stem cells.

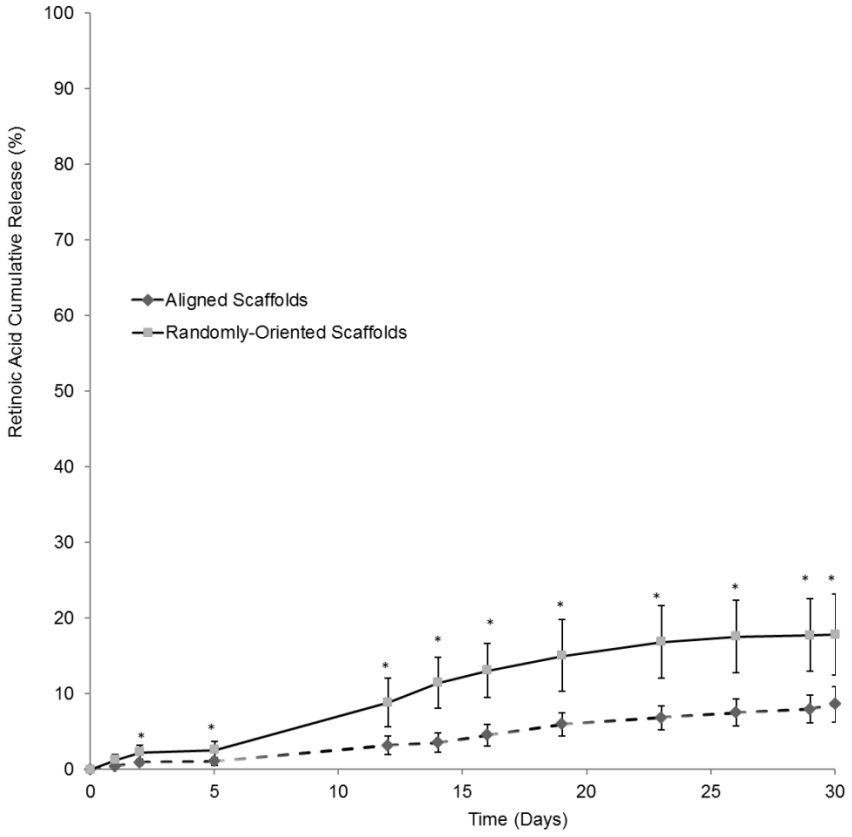

Figure 3 Controlled release data for retinoic acid in randomly-oriented and aligned scaffolds containing 0.2 % retinoic acid (w/v) over 30 days. Error bars indicate standard deviation. * indicates $p<0.05$ versus two topographies with (n=3).

Evaluating the compatibility of multifunctional nanofiber scaffolds with iPSC culture and differentiation

The randomly-oriented and aligned electrospun blank PCL and RA-loaded nanofiber scaffolds were seeded with iPSC-derived neural progenitors to determine their suitability as a stem cell culture substrate. After 10 days, these neural progenitors displayed high levels of viability when seeded upon blank and encapsulated scaffolds, independent of topography (Figure 4). Figure 4E shows the intensity of green fluorescence (representing % of live cells in each respective EB), which was above 80% for all cultures. These cultures were also stained for the neuronal marker Tuj1 after 10 days of culture.

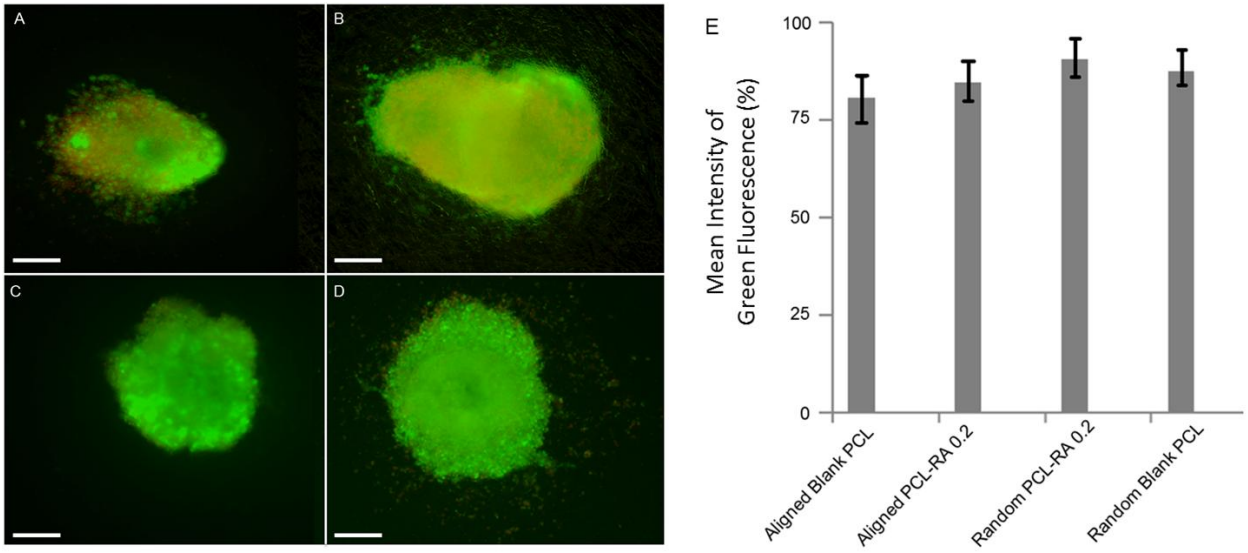

Figure 4 Representative images showing the (A,B) cell viability of mouse iPSC-derived EBs seeded on aligned PCL and PCL-RA nanofibers after 10 days of culture as determined by live/dead assay. Representative images (C,D) showing the cell viability of mouse iPSC-derived EBs seeded on random PCL and PCL-RA nanofibers after 10 days of culture as determined by live/dead assay. Scale bar is 100 μm (n=3). (E) Quantitative Live/Dead Analysis after seeding onto scaffolds after 10 days of culture as determined by IncuCyte ZOOMTM Fluorescent Processing Software. Mean intensity of green fluorescence represents the percentage of cells that were viable.

Figure 5 shows representative images of this staining, which indicates that these iPSC-derived neural progenitors differentiated into neurons. Neurite outgrowth was observed for

aligned blank and encapsulated scaffolds (Figure 5A and 5B). The image displays a clear neuronal phenotype differentiated from the mouse iPSC-derived EBs seeded onto these scaffolds. Outgrowth of neurites along the aligned nanofibers was observed in Figures 5A and B. In the case of random fibers, the cells remained more localized around the EBs. These results suggest that the nanofiber scaffolds direct mouse iPSC-derived neural progenitor migration.

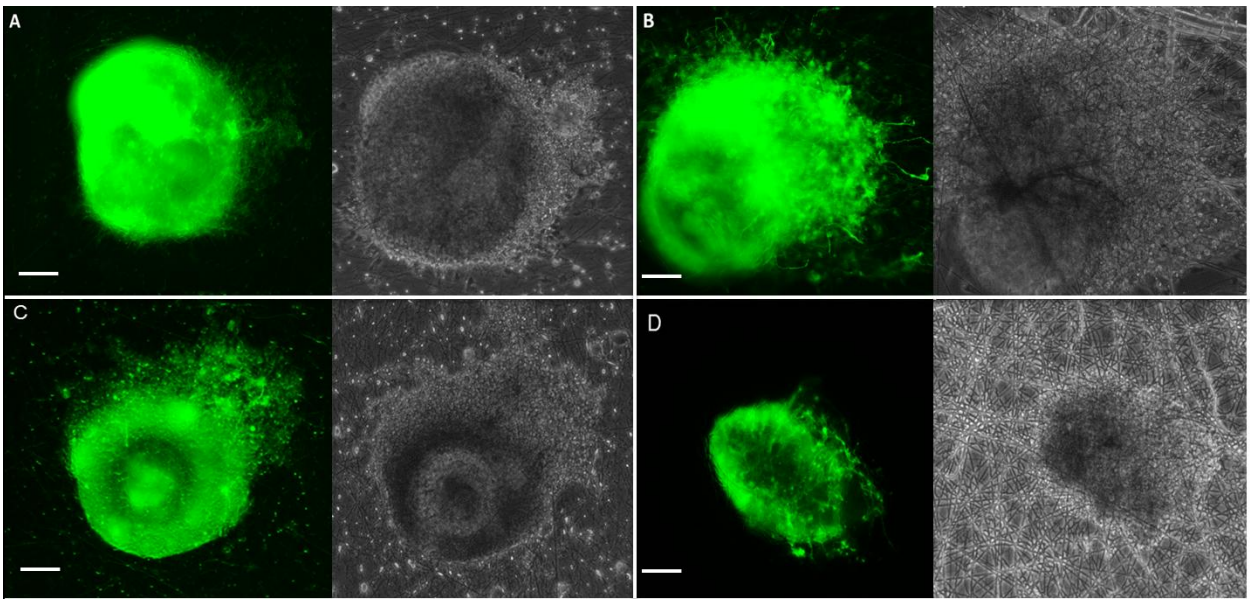

Figure 5 Representative images showing neuronal differentiation of mouse iPSC-derived EBs seeded on (A,B) aligned PCL and PCL-RA nanofibers along phase contrast images and (C,D) random PCL and PCL-RA nanofibers along phase contrast images. Scale bar is 100 μm (n=3).

Discussion and conclusions

While many techniques exist for fabricating biomimetic scaffolds, solution electrospinning can be used to encapsulate bioactive agents inside scaffolds while controlling their topography[21, 24, 25, 43, 56]. For example, Jiang *et al.* reported that PCL nanofibers containing 0.3 % (*w/v*) RA could provide controlled release of RA for 14 days[56]. The released RA enhanced the differentiation of mesenchymal stem cells into neural lineages, demonstrating its bioactivity. Building upon this work, we report similar results when using such multifunctional

scaffolds in combination with iPSC-derived neural progenitors. We have chosen to work with iPSCs since they can continuously self-renew, making cell sourcing feasible for scale-up studies, and they also enable the possibility of patient specific engineered tissues while avoiding the ethical issues associated with ESCs.

Another important factor when designing electrospun scaffolds is the choice of topography. Several studies have demonstrated the effect of aligned topography as a method for directing the migration of both fibroblasts and nerve cells derived from dorsal root ganglion[95, 96]. Xie *et al.* demonstrated that aligned PCL electrospun nanofibers enhance the differentiation of mouse ESCs into neural lineages while influencing cell migration[25]. Another study showed that even random topography can promote neuronal differentiation of human ESCs[97]. Our study focused on the fabrication and characterization of PCL nanofibers containing RA with different topographies and then determining if these scaffolds were compatible with neural progenitors derived from mouse iPSCs. We were able to successfully fabricate such scaffolds containing different concentrations of RA and with different topographies. The aligned scaffolds released RA at slower rate compared to the randomly-oriented scaffolds, suggesting that topography influences release rate. We also showed extended release of RA from our nanofiber scaffolds over 30 days compared to previous reports of a 14-day release[56]. Our encapsulation efficiency ranged from 20 to 70%, demonstrating the inherent variability in the electrospinning process. In order to increase the encapsulation efficiency and improve reproducibility, coaxial electrospinning could be explored as a viable alternative[98].

Our multifunctional scaffolds supported iPSC-derived neural progenitor survival and differentiation. Interaction with the physical environment influences cell behaviour, with aligned topographies enhancing neural differentiation and directing the growth of neurons as seen in

Figure 5A and B. RA can promote neuronal differentiation, making it useful for neural tissue engineering applications. Together, the physical cues from scaffold topography and the chemical cues from controlled drug release are designed to mimic the complex extracellular environment that regulates cell behaviour *in vivo*. Multifunctional scaffolds can be precisely tuned in order to support the differentiation of stem cells into desired phenotypes. While there is a significant body of research that elucidates this behaviour for ESCs, the recent emergence of iPSCs presents new possibilities, including the potential to produce patient-specific engineered tissues[21, 25, 43, 56, 99]. Here, neuronal differentiation of mouse iPSCs and neurite outgrowth from EBs were observed, suggesting our drug-releasing nanofiber scaffolds serve as a proper substrate for stem cell-based neural tissue engineering strategies.

Although we only stained for the neuronal differentiation, it is also important to consider what other cell phenotypes are present in these cultures. Our future work will further characterize these cultures to determine their cellular composition. Of particular concern is the presence of undifferentiated pluripotent stem cells, which could trigger tumor formation[97]. Previous studies have analyzed the cellular composition of EBs containing neural progenitors derived from mouse ESCs at similar timescales[17, 25]. For instance, Xie *et al.* showed that amount of undifferentiated cells indicated by SSEA-1 staining (~15%) and the amount of neural progenitors indicated by nestin staining (~40%) were comparable between blank PCL aligned and randomly-oriented nanofibers[25]. For transplantation studies, this SSEA-1 population would need to be removed using cell sorting to reduce the risk of tumor formation. This same study reported these neural progenitors differentiated into neurons based on Tuj1 expression and oligodendrocytes based on O4 expression at similar levels regardless of nanofiber alignment, but the cells cultured on the randomly aligned scaffolds had higher rates of GFAP expression, indicating more

differentiation into astrocytes[25]. It has been shown that iPSC and ESC lines have different efficiency in forming different neural phenotypes[97], suggesting our cultures may contain less mature phenotypes compared to using mouse ESC-derived embryoid bodies grown on similar scaffolds.

We confirmed that RA encapsulated electrospun PCL nanofibers could support the neuronal differentiation of mouse iPSCs-derived neural progenitors. Compared to other studies, our novelty was the fabrication of RA encapsulated electrospun PCL nanofibers with different dosages and topographies that support the neuronal differentiation of mouse iPSCs. Obtaining consistent morphology while controlling fiber diameter when encapsulating bioactive agents during the electrospinning process remains as a challenge to solution electrospinning. Multiple studies have reported difficulty in obtaining a uniform distribution of fiber sizes[24, 100]. We also observed variability in fiber diameter depending on the fabrication conditions. Additionally, obtaining a high degree of fiber orientation can be challenging when using solution electrospinning to align nanofibers, as seen in our study and in other reports[21]. For instance, Yoshimoto *et al.* reported a broad fiber diameter distribution for PCL nanofibers (400nm ±200 nm)[100]. This variation in diameter may be due to the fast phase separation of PCL and the uncontrollable evaporation of volatile solvent (DCM/MeOH) during electrospinning.

Our proof-of-concept data showed that these multifunctional scaffolds that release RA over a month can be combined with iPSCs-derived EBs containing neural progenitors to support their culture and differentiation into neurons. Neuronal differentiation and outgrowth from EBs were observed. Our work combining stem cells and electrospun encapsulated PCL nanofibers demonstrates a viable method of producing biomimetic scaffolds in regenerative medicine and novel drug delivery systems. In terms of future work, we will investigate the effects of aligned

scaffolds on controlled delivery of growth factors, such as glial derived neurotrophic factor (GDNF), from our scaffolds to further enhance their utility. Similar studies by Chew *et al.* used aligned PCL and ethyl ethylene phosphate electrospun nanofibers for controlled release of nerve growth factor (NGF)[67]. However, their work reported that the encapsulation efficiency of the growth factor inside the nanofibers was very low (~4%). We hope to use our knowledge from these studies to improve the efficiency of the protein loading process and eventually deliver protein cues to these multifunctional scaffolds. We also plan to evaluate these multifunctional scaffolds as substrates for human iPSCs with an end goal of implanting these engineered tissues in an *in vivo* model of a spinal cord injury to determine their efficacy.

Chapter 3 Neuronal Differentiation of Human Induced Pluripotent Stem Cells Using Electrospun Scaffolds with Varied Topographies [9]

Introduction

Human pluripotent stem cells (PSCs) can become any cell type found in the body, making them a powerful tool for engineering tissues. Additionally, PSCs, including embryonic stem cells (ESCs) and induced pluripotent stem cells (iPSCs), continuously self-renew, enabling the generation of large quantities of cells for transplantation[2, 3]. Human iPSCs are generated from somatic cells, such as fibroblasts, which are reprogrammed by introducing transcription factors that cause the cells to function like ESCs. One advantage of using human iPSCs as a possible alternative to human ESCs is that such cell lines could be generated from patients, reducing the probability of immune rejection. The use of iPSCs also avoids the ethical issues associated with using embryos to derive human ESCs[101, 102].

Many studies have differentiated human iPSCs into neural phenotypes for a variety of applications[10-16]. The Li group showed that transplanted neural crest cells derived from human iPSCs promoted accelerated regeneration of the sciatic nerve in a rat injury model[17]. They observed no tumor formation for a 1 year after transplantation of these cells. Neurospheres derived from human iPSCs have been transplanted into the spinal cord injury of mice models where they differentiated into three major neural lineages, neurons, astrocytes, and oligodendrocytes and promoted a significant increase in functional recovery compared to control

[9] The following chapter is from: **Neuronal Differentiation of Human Induced Pluripotent Stem Cells Using Electrospun Scaffolds with Varied Topographies**. Mohtaram, N.K., et al. Under review at the Journal of Biomedical Materials Research. Copyright Permission Pending.

animals[12]. The other study differentiated human iPSCs into neural crest cells *in vitro* and then transplanted these cells into a fetal lamb model of spinal cord injury[18]. These cells survived and differentiated into neurons after transplantation and no tumor formation was observed. Generally, a large body of work presents the potential of using human iPSCs to produce neural phenotypes for different neural injuries.

One of the major challenges when using human iPSCs for tissue engineering applications is how to control the differentiation process to produce three dimensional structures similar to those found in healthy tissue. Stem cell behavior can be significantly modulated by mechanical and topographical physical cues[103-106]. This area remains relatively understudied compared to the wide body of literature describing the use of chemical cues for promoting stem cell culture and differentiation. The differentiation of human ESCs into the three germ layers when seeded on salt leaching fabricated porous scaffolds with different stiffness increased when scaffold stiffness increased[107]. The biophysical microenvironment also influences the rate of reprogramming of somatic cells into iPSCs[104]. Scaffold topography can also control the differentiation of PSCs into specific phenotypes[25, 105, 108]. For instance, the differentiation of human iPSCs into neuronal lineages was significantly influenced by the topography of nano/microstructured scaffolds[105]. Using silicon grating structures with different widths, they found that the human iPSCs seeded on a nanoscale structure could induce a significant up regulation of neuronal markers, compared to microscale structures, indicating the influence of nanotopgraphy on the induction of neuronal lineage.

Electrospun fibers have been evaluated for different neural tissue engineering applications as they can present both chemical and physical cues[43, 56, 92, 93, 109-111]. Xie *et al.* showed aligned nanofibers reduce the fraction of cells that differentiated into astrocytes, which are

undesirable when treating spinal cord injury[25]. The same study reported that mouse ESC-derived neurons seeded on the aligned fibers showed longer neurite outgrowth compared to the same cells seeded on the randomly-oriented nanofibers. Other researchers have shown that seeding human ESC-derived neural cells onto aligned nanofibers enhanced neuronal differentiation compared to randomly orientated nanofibers[43]. Additionally, small molecules and growth factors can be encapsulated inside of such nanofiber scaffolds[24, 56, 109, 111]. For instance, Madduri *et al.* used electrospun nanofibers to encapsulate glial cell line-derived neurotrophic factor (GDNF) and nerve growth factor (NGF) with varied topographies to develop multifunctional scaffolds for peripheral nerve regeneration[109]. In another study, retinoic acid (RA) releasing nanofibers enhanced the differentiation of mesenchymal stem cells into neural lineages[56]. In our previous study, controlled release of RA from PCL nanofibers was provided over one month and such scaffolds were able to promote the neuronal differentiation of mouse iPSCs[111]. Overall, studies on electrospun fibers continue to play a key role in the neural tissue engineering and controlled release of neural drugs for the development of on-going strategies for clinical applications.

These aforementioned studies all used solution electrospinning to fabricate such scaffolds. However, melt electrospinning provides a better way to control the topography of fibrous scaffolds[23, 34, 111-113]. The process of melt electrospinning involves melting a polymer to generate flow for producing fibers with a high degree of reproducibility compared to the more commonly used solution electrospinning. Melt electrospinning does not require a solvent whereas most solvents used in solution electrospinning are cytotoxic, providing an additional key advantage.

Melt electrospinning can be used as a powerful tool to fabricate cell invasive scaffolds with varied architecture for tissue engineering applications[23, 33]. The successful attachment and cell viability of fibroblast cells seeded on PCL melt electrospun scaffolds has been reported[33]. Also, our group recently reported that melt electrospun PCL scaffolds could support the neuronal differentiation of murine ESCs[23]. Generally, the topography of scaffolds can be custom tailored by the tuning of parameters such as flow rate, applied voltage, nozzle size and spinning temperature.

In order to successfully translate PSC-based engineered tissues for clinical applications, the culture and differentiation methods should be reproducible and avoid the use of animal products as they can induce immune responses post transplantation[114-116]. Accordingly, we cultured our human iPSCs in completely defined conditions to maintain their levels of pluripotency. These undifferentiated iPSCs were seeded into microwells in the presence of chemically defined neural induction media to form neural aggregates with uniform diameters, increasing the reproducibility of this process compared to tradition methods for forming embryoid bodies[115]. Thus, both our iPSC-derived neural progenitors and our fibrous scaffolds would be suitable for further translation in terms of pre-clinical and clinical studies.

In this work, we investigated how the topography of PCL melt electrospun scaffolds, including loop mesh and biaxial aligned topographies, influenced the differentiation of these human iPSC-derived neural aggregates into neurons and the resulting neurite outgrowth. Due to its low melting point (~60 ^{o}C), PCL can be easily electrospun into varied topographies[23, 113]. It is also a biocompatible polymer and can serve as a proper scaffold for stem cell culture[23, 25, 111]. We have chosen to focus on generating neurons due to their therapeutic potential for the treatment of spinal cord injuries[117]. We studied the effects of fiber diameter on neuronal

differentiation of human iPSCs using two different fiber diameters in the loop mesh scaffolds. Additionally, we also successfully engineered a novel class of scaffold, biaxial aligned microfibers, for further investigating the effect of physical cues on the neuronal differentiation of human iPSCs. The combination of encapsulated nanofibers with biaxial aligned PCL scaffolds also supported the differentiation of human iPSCs. The differentiated neurons from human iPSCs seeded on these novel tissue-engineered scaffolds could serve as a new strategy for neural tissue engineering applications.

Materials and methods

Melt and solution electrospinning setup

Poly (ε-caprolactone) (PCL, average M_n ~ 45,000) and retinoic acid (RA) (*all-trans*, ≥98% HPLC, powder) were acquired from Sigma-Aldrich Corporation (St. Louis, MO, USA). Dichloromethane (DCM) (reagent/ACS grade) and methanol were purchased from VWR International (Edmonton, AB, Canada). The melt and solution electrospinning setups used for the fabrication of microfibers and encapsulated nanofibers were previously reported[23, 111]. Scaffolds with loop mesh morphology were fabricated by melt electrospinning using 200 µm and 500 µm nozzle sizes and shall be referred to as loop mesh 200 and loop mesh 500 respectively. We had showed previously that fiber diameter increased with the nozzle diameter, enabling fabrication of scaffolds with different fiber diameters[23]. Biaxial aligned scaffolds were fabricated using a 200 µm nozzle for fiber extrusion. Bimodal scaffolds were fabricated by using solution electrospinning to overlay nanofibers containing RA over the biaxial aligned microfibers. The details of electrospinning parameters for each topography are given in Table 3. The composition of our 0.2 % (*w/v*) PCL-RA solution was previously reported[111].

Parameters	Loop Mesh 200 Melt Electrospinning	Loop Mesh 500 Melt Electrospinning	Biaxial Aligned Melt Electrospinning	Bimodal* Solution Electrospinning
Voltage (kV)	20	20	15	15
Distance (cm)	5	5	5	7.5
CNC Speed (mm/s)	200	200	1700	N/A
Temperature (^{0}C)	80	80	80	23
Nozzle size (μm)	200	500	200	N/A

Table 3 Melt and solution electrospinning operational parameters. * In terms of bimodal scaffolds, all melt electrospinning parameters have been set as biaxial aligned scaffolds. Solution electrospinning parameters are given in the table for bimodal scaffolds**.**

Micro and nanostructure characterization

Characterization of topography was performed using a cold emission Hitachi S-4800 FE scanning electron microscopy (SEM) machine to image all scaffolds at low and high magnification. The details of SEM protocol were reported[23, 111]. For each scaffold, three distinct images were captured at 30x magnification with 50 fibers measured to determine the average fiber diameter of each scaffold. For nanofiber characterization, images were captured at 10,000x magnification.

Human iPSC culture and formation of neural aggregates

All reagents were purchased from STEMCELL Technologies™ unless otherwise specified. Human iPSCs (the 1-MCB-01 line) generated from human foreskin cells were received from the WiCell Research Institute[101]. Human iPSCs were cultured at 37˚C and 5% CO_2 on Vitronectin XF™ coated surfaces[114]. To maintain pluripotency, cells were cultured in the presence of TeSR™-E8™ media in 6 well plates[116]. Undifferentiated human iPSCs were

dissociated into a single cell solution using Gentle Cell Dissociation Reagent (STEMCELL Technologies™), which was then distributed into a single well of an Aggrewell™ 800 plate in the presence of 2 mL of STEMdiff™ Neural Induction Medium (NIM, STEMCELL Technologies) (STEMCELL Technologies™)[115]. These plates enable formation of consistent, neural aggregates containing 4000-5000 cells. 1.5 mL of media was replaced with fresh NIM daily.

Neural progenitor cell seeding onto scaffolds

After 5 days, the aggregates containing neural progenitor cells were seeded onto the scaffolds. Approximately 4 neural aggregates were seeded into each well of the 6-well plates containing loop mesh or biaxial aligned or bimodal scaffolds. 1 mL of NIM was added to each well and the cultures and scaffolds were incubated at 5% CO_2 and 37 ºC for 12 days.

Cell viability and immunohistochemistry analysis

The viability of human neural aggregates seeded on the PCL scaffolds was analyzed qualitatively after 12 days by using a LIVE/DEAD® Viability/Cytotoxicity Kit (Invitrogen). The details of our protocol have been previously published[25, 38, 111]. Briefly, 12-day-old neural aggregates grown on the scaffolds were treated with calcein AM, which is enzymatically converted to green fluorescing calcein by the naturally present intracellular esterase activity in live cells. They were also treated with a stain for cytotoxicity, ethidium homodimer-1, which fluoresces red upon binding to nucleic acids accessed through the ruptured cell membranes of dead cells. Media was first removed and then each well was gently washed twice with Dulbecco's phosphate buffered saline (D-PBS) (Invitrogen). Diluted stain solution was then added to each well of a 6-well-plate and the cells were incubated at room temperature. After 45

minutes, we then imaged each well by using IncuCyte® ZOOM Essen BioScience® fluorescent microscope and LEICA 3000B inverted microscope containing an X-cite series 120Q fluorescent light source (Lumen Dynamics) coupled with a Retiga 2000R fast-cooled mono 12-bit camera (Q-imaging). Quantitatively, an IncuteCyte® ZOOM Essen BioScience® fluorescent microscope was used to measure the green fluorescent intensity in each image, corresponding to the percentage of viable cells present. Three distinct cell/scaffold images were selected per scaffold for analysis using the IncuteCyte® ZOOM Fluorescent Processing Software.

We qualitatively assessed the differentiation of human iPSCs using immunocytochemistry to detect the neuron-specific protein β-III-tubulin as previously reported. Briefly, differentiated cells were fixed with a 10% formalin solution (Sigma-Aldrich, St. Louis, MO, USA) for 1 hour at room temperature and then permeabilized with 0.1% Triton-X solution (Sigma-Aldrich, St. Louis, MO, USA). Wells then were blocked with 5% normal goat serum (NGS, Millipore) at 2 - 8 ˚C for 2 hours. The primary antibody for β-III-tubulin (Millipore, 1:500 dilution) was added to each well. Three washes with PBS were performed and the Alexafluor488-conjugated secondary antibody was added and incubated for 4 hours. After an additional set of washes, images were captured at 515 nm for green fluorescence.

Quantitative analysis of neurite extension and cell-body cluster area

An IncuCyte® ZOOM Essen BioScience® fluorescent microscope was used to analyze fluorescent images of Tuj-1 stained neural progenitors seeded on all sets of scaffolds at 20X magnification. Three EBs per scaffold were selected per group and 14 stacks of images were collected for analysis using the IncuCyte® ZOOM NeuroTrack Software™. Maximum neurite length and cell body cluster area of neural progenitors were calculated for each neural progenitor per scaffold. The maximum neurite length is defined by the length of the longest neurite that

extended from the neural aggregate. The cell-body cluster area is the size of the neural aggregates and their extended neurites after 12 days of culture.

Real time quantitative polymerase chain reaction (qPCR) analysis

For each set of scaffolds, total RNA was extracted from cultures using an RNeasy kit (Qiagen), and cDNA was synthesized from 1 µg of total RNA using a High-Capacity cDNA Reverse Transcription Kit (Life Technologies). Quantitative real-time polymerase chain reaction (qPCR) was then performed with 50 ng of the reversely transcribed cDNA through the comparative Ct method and by using fast mode in the StepOnePlus™ Real-Time PCR System (Life Technologies), employing TaqMan® Fast Advanced Master mix and TaqMan® Gene Expression Assays (Life Technologies). Real time qPCR analysis was done to study the expression of Oct4 pluripotency marker, Lin28 (expressed by undifferentiated human embryonic stem cells), Nestin (expressed by neural stem/progenitor cells), and Pax6 (a neuroectoderm marker for human pluripotent stem cells) markers. For the relative quantification of the target gene expression, cycle threshold (C_t) values of the target genes were normalized against that of the endogenous housekeeping gene, 18S rRNA. $\Delta\Delta C_t$ (=ΔC_t sample (differentiated cells) – ΔC_t reference (undifferentiated human iPSCs)) values were plotted as relative levels of gene expression and the data is reported as mean ± standard error of the mean.

Statistical analysis

Data are presented as mean values ± standard deviation of the mean except where previously stated. Statistical analysis was performed using STATISTICA 9 by applying a standard *t*-test and ANOVA to compare data between the groups. Significance was considered at the $p < 0.05$ level.

Results and discussion

Topographical characterization of scaffolds

We fabricated loop mesh 200, loop mesh 500, biaxial aligned scaffolds and bimodal scaffolds using melt and solution electrospinning. The loop mesh 200 scaffolds had an average fiber diameter of 43.7 ± 3.9 µm. Loop mesh 500 scaffolds had an average fiber diameter of 85 ± 4 µm (*n=50*). Low and high magnification SEM images of both sets of loop mesh scaffolds are shown in Figures 6A, 6B, 6C and 6D. Loop mesh scaffolds have a controllable porosity and fiber diameter, and were previously shown to be capable of supporting mouse ESC differentiation into neurons. Figures 6E and 6F show the topography of the biaxial aligned electrospun PCL microfibers fabricated by using 200µm nozzle tip diameter. Highly aligned and stretched microfibers can be fabricated if the speed is set to be faster than the depositing viscous jet. The biaxial aligned scaffold consisted of 20 layers of evenly spaced and fully aligned microfibers. For biaxial aligned scaffolds, the average fiber diameter was measured as 42.3 ± 2.8 µm (*n=50*). From these measurements, the average separation distance, the distance between two individual fibers, for each scaffold was calculated (Table 4). Fabrication of biaxial aligned scaffolds with different diameters (like loop mesh scaffolds) was not possible as the microfibers did not attach to each other when the fiber diameter increased. Figure 6G shows the topography of our novel bimodal scaffolds. Our previous study showed that successful encapsulation of RA inside PCL nanofibers led to month long controlled release of RA. Since biaxial aligned PCL microfibers are porous in nature, RA-encapsulated PCL nanofibers were spun on such structures to increase the efficiency of cell adhesion by increasing the surface area for migrating cells, allowing them to adhere to the surface of fibers in such scaffolds. Figure 6H shows the topography of well-aligned RA-encapsulated PCL nanofibers that have been stretched and parallelized by being spun

between biaxial aligned PCL microfibers. The average fiber diameter for RA encapsulated PCL nanofibers was measured as 344.9 ± 33.6 nm (*n=100*).

Scaffold Type	Fiber Diameter ± SD (μm)	Separation Distance ± SD (μm)
Loop Mesh 200	43.7 ± 3.90	177.9 ± 106.4
Loop Mesh 500	85 ± 4	141.1 ± 54.2
Biaxial Aligned	42.3 ± 2.8	161.1 ± 99.2
Bimodal*	42.3 ± 2.8	161.1 ± 99.2

Table 4 Micro and nanostructure topographical properties of scaffolds (*n=50*). * The average nanofiber diameter for bimodal scaffolds was 344.9 ± 33.6 nm (*n=100*).

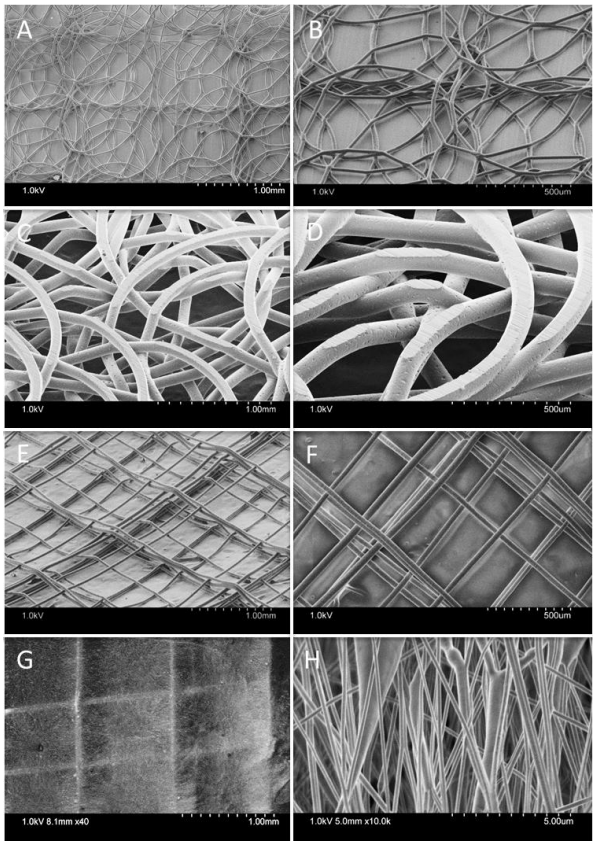

Figure 6 Scanning electron microscopy images of electrospun scaffolds. (A), (B) Low and high magnification images of loop mesh 200 scaffolds. (C), (D) Low and high magnification images of loop mesh 500 scaffolds. (E), (F) Low and high magnification images of biaxial aligned scaffolds fabricated with 200 μm nozzle. (G) Low magnification image of bimodal scaffolds. (H) Retinoic acid encapsulated in poly (eta-caprolactone) nanofibers spun on top of biaxial aligned microfibers, resulting in novel bimodal scaffolds.

The effect of loop mesh topography on the behavior of human iPSC-derived neural progenitors

Neural aggregates containing human iPSC-derived neural progenitor cells were cultured on both sets of loop mesh scaffolds for 12 days. Figure 7A and 7B show the bright field and live/dead images of seeded cells onto loop mesh 200 scaffolds. The neural progenitors were able to adhere to these scaffolds and migrate along the fibers migration. After 12 days, these neural progenitors displayed high levels of viability when seeded upon loop mesh scaffolds (Figure 7B). A subset of the seeded cells stained positive for the neuronal marker Tuj1, indicated successful differentiation into neurons (Figure 7D). After 12 days, the cells had started to migrate outward from the spherical neural aggregate along the looped fibers, with distance of migration dependent on the scaffold morphology. Bright field, live/dead, and immunocytochemistry images of cells seeded on loop mesh 500 can be seen in Figures 7E, 7F, 7G, and 7H, respectively. Compared to the loop mesh 200 scaffolds, the cells were not elongated, possibly due to the thick fibers acting as an obstacle to migration. The cells are located in the gap between of fibers (Figure 7G) and tend not to differentiate or migrate out in any particular fiber direction. In fact, human iPSCs did not respond strongly to loop mesh 500 scaffolds. In contrast, human iPSCs seeded on loop mesh 200 scaffolds were oriented and elongated along fibers (Figure 7D). These results suggest that the loop mesh 200 scaffolds served as a better substrate for human iPSC-derived neural progenitors compared to the loop mesh 500 scaffolds.

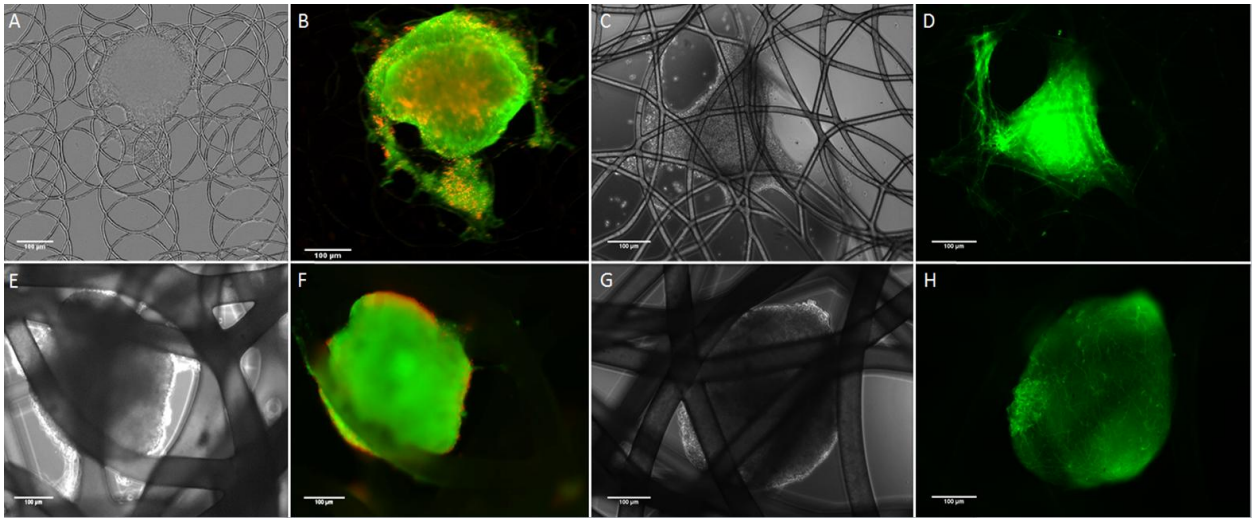

Figure 7 Neural progenitors seeded on loop mesh scaffolds after 12 days of culture. (A),(B) Bright field image and fluorescence image showing live and dead staining of cells seeded on loop mesh 200 scaffolds. (C), (D) Bright field image and fluorescence image showing staining for the neuronal marker Tuj1 expressed by cells seeded on loop mesh 200 scaffolds. (E), (F) Bright field image and fluorescence image showing live and dead staining of cells seeded on the loop mesh 500 scaffold. (G), (H) Bright field image and fluorescence image showing staining for the neuronal marker Tuj1 expressed by cells seeded on loop mesh 500 scaffolds.

Biaxial aligned and bimodal scaffolds

Both biaxial aligned and bimodal scaffolds were able to support the culture and differentiation of human iPSC-derived neurons (Figure 8 and 9). The live/dead images demonstrate that biaxial aligned scaffold topographies are viable substrates for human iPSCs because the majority of the seeded cells fluoresced green (Figure 8B). Figure 8D shows that scaffold topography serves to direct neurite extension as seen by the large number of cells staining positive for the neuronal marker Tuj1. The neurons extend along the fibers of biaxial aligned scaffolds and there appears to be regions of dense cell growth, which shows the areas that have the most extracellular support. As can be seen (Figure 8D), neural progenitors of human iPSCs were elongated along the axis of microstructured PCL biaxial aligned scaffolds. This cell behaviour was totally dependent on topography as the neurite outgrowth correlated with fiber direction. The interactions and infiltration between cells into bimodal scaffolds can be seen in Figure 9C and 9D. In Figures 9A and 9B, the cells had properly attached to the scaffolds and

the scaffolds were able to support the adhesion of cells. Figure 9C and 9D show the neuronal differentiation of single neural progenitors seeded on our scaffolds. Figure 9E and 9F show the interactions of two human iPSC-derived neural progenitors. For these scaffolds, the neurites extend in all directions, possibly due to the presence of the nanofibers.

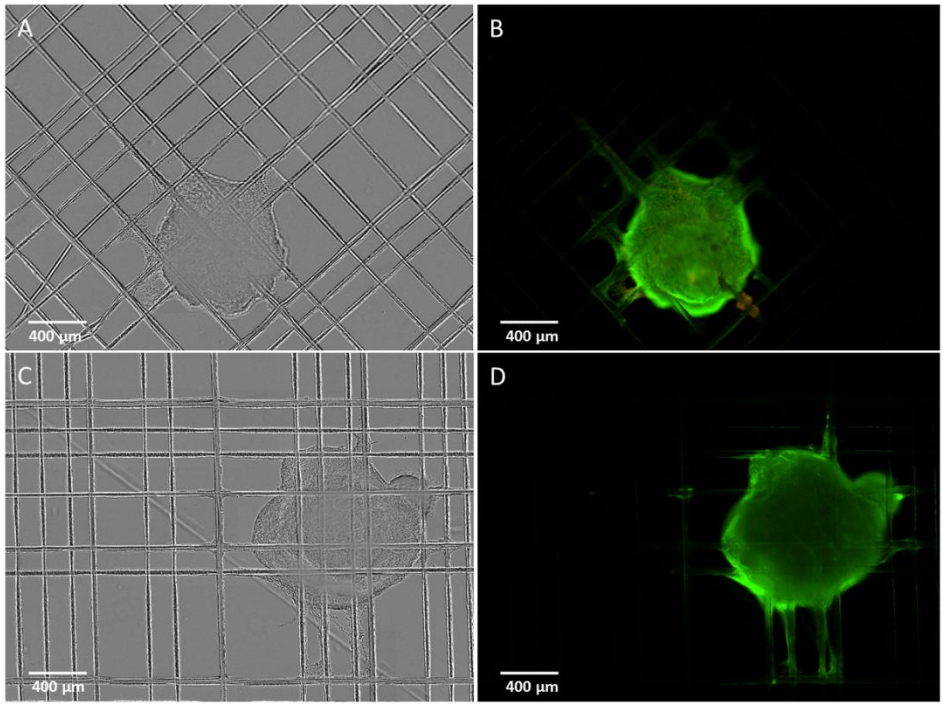

Figure 8 Neural progenitors seeded on biaxial aligned scaffolds fabricated using a 200 µm nozzle after 12 days of culture. (A),(B) Bright field image and fluorescence image showing live and dead staining of cells. (C), (D) Bright field image and fluorescence image showing staining for the neuronal marker Tuj1 expressed by cells.

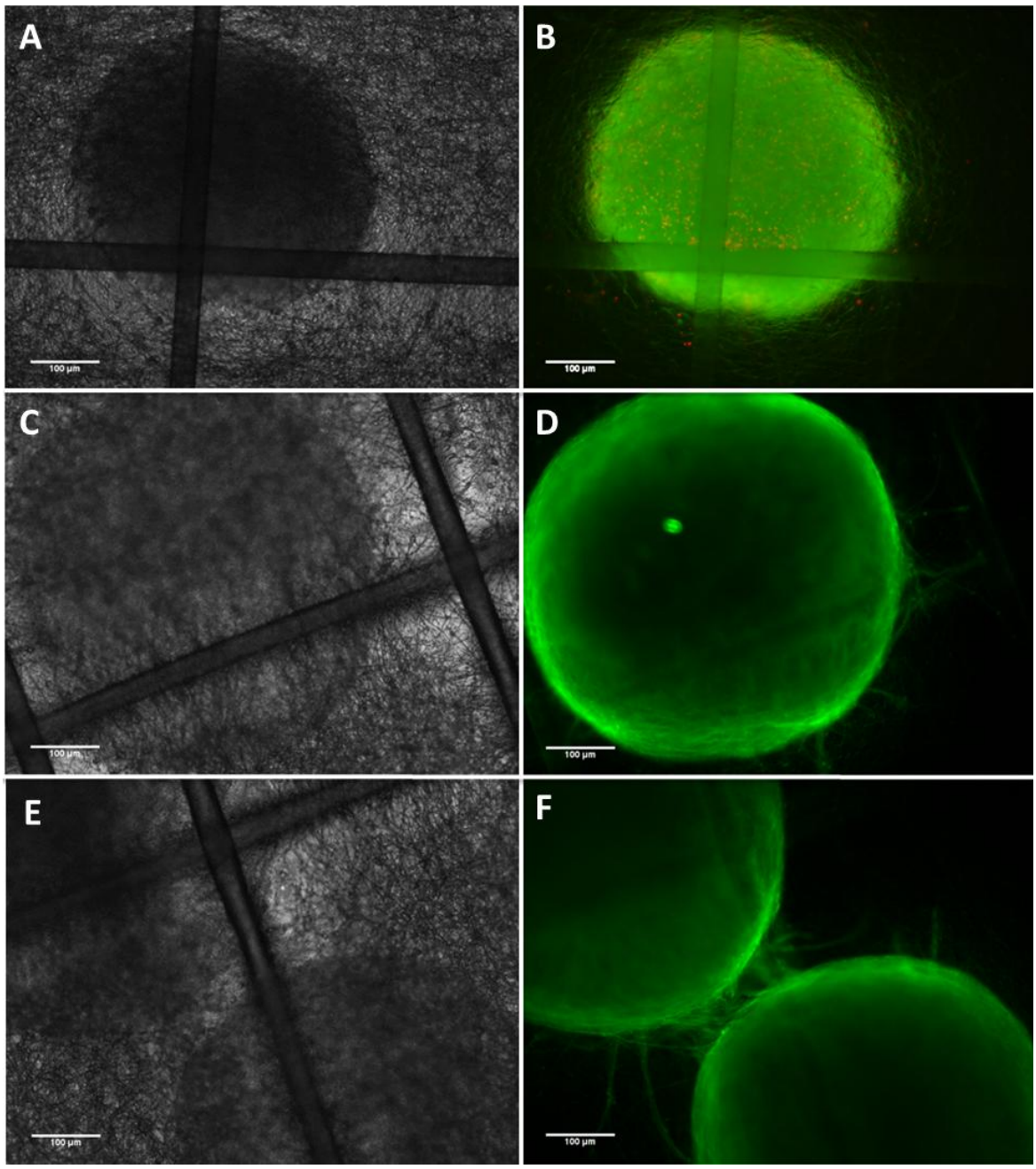

Figure 9 Neural progenitors seeded on bimodal scaffolds after 12 days of culture. (A), (B) Bright field image and fluorescence image showing live and dead staining of cells seeded on bimodal scaffolds. (C), (D) Bright field image and fluorescence image showing neuronal marker Tuj1 staining for two adjacent neural aggregates seeded on bimodal scaffolds that have neuronal interconnections.

Quantitative analysis of cell viability, neurite outgrowth and differentiation

Figure 10A shows the intensity of green fluorescence (representing % of live cells in each respective neural aggregate) for all cultures. Loop mesh 200 and 500 scaffolds displayed the

intensity of green fluorescence around 81 ± 8% and 70 ± 1 % respectively. After 12 days of seeding, the intensity of green fluorescence was 87.2 ± 6 % for the neural progenitors seeded onto biaxial aligned scaffolds. The intensity of green fluorescence was 95.1 ± 2 % for the neural progenitors seeded onto bimodal scaffolds. The neural progenitors seeded onto bimodal scaffolds displayed the highest levels of viability. Cell body cluster area and maximum neurite field were calculated for each neural progenitors seeded on loop mesh 200, loop mesh 500, biaxial aligned and bimodal scaffolds (Figure 10B and 10C). As it can be seen from Figure 5B, the neural progenitors cultured on loop mesh 200 scaffolds exhibited a higher cluster area compared to those seeded on loop mesh 500 scaffolds, but no significant difference was observed in terms of maximum neurite extension (Figure 10C). The cell body cluster area of neural progenitors cultured on biaxial aligned samples was significantly, ~1.7 mm^2 larger than that of neural progenitors seeded on bimodal scaffolds. The maximum neurite length for neural progenitors seeded on biaxial aligned scaffolds was also significant longer (~ 280 %) compared to the cells seeded on bimodal scaffolds, showing that the biaxial aligned scaffolds enhanced the neurite outgrowth of neural progenitors compared to other scaffolds. Significantly, such scaffolds also showed the maximum cell body cluster area and the maximum neurite length compared to other type scaffolds. Overall, these results propose that biaxial aligned scaffolds would serve as the best substrate for promoting spreading and guidance of differentiated cells.

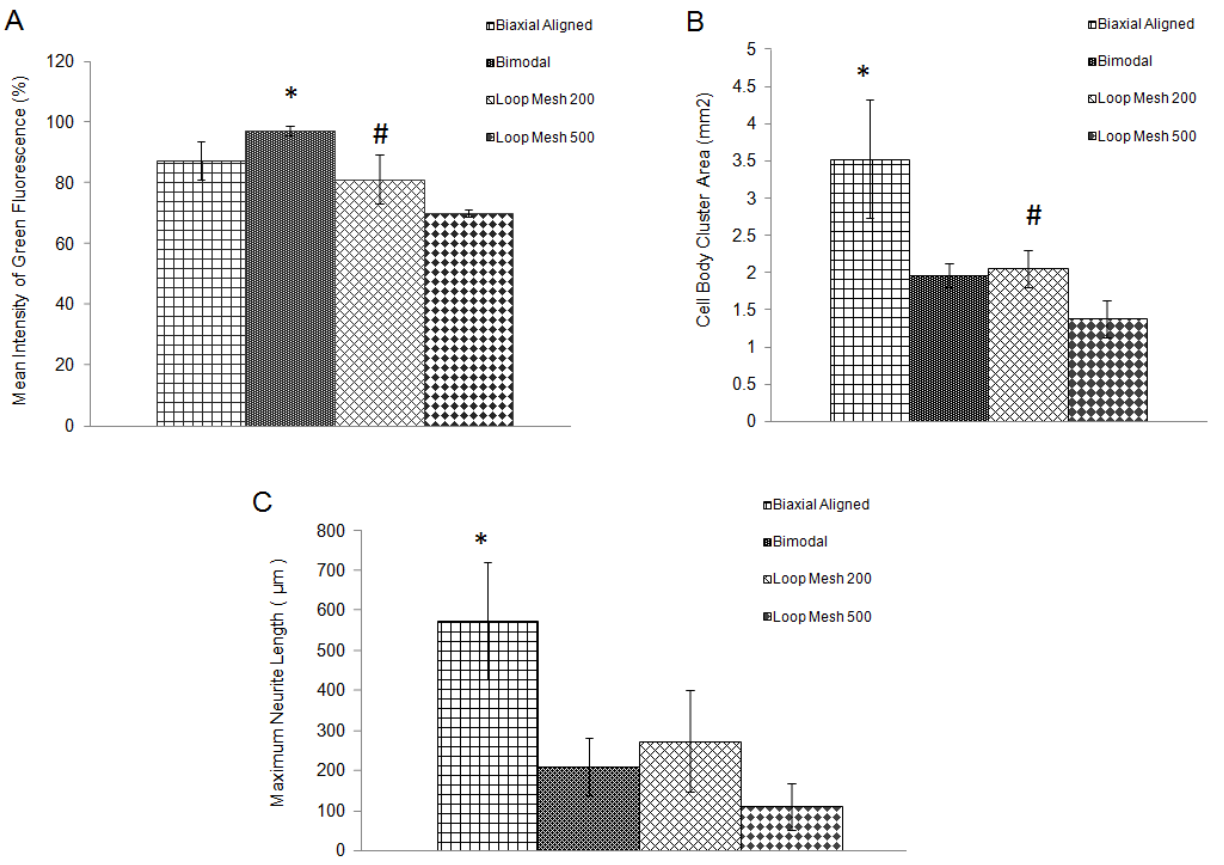

Figure 10 (A) Mean intensity of green fluorescence. (B) Cell body cluster area. (C) Maximum neurite length. * indicates $p<0.05$ versus other scaffolds. N=3.

Quantitative polymerase chain reaction was used to examine the following markers: Oct4 (transcription factor associated with the self-renewal of pluripotent stem cells), Lin28 (microRNA involved in self-renewal of pluripotent stem cells), Nestin (cytoskeletal protein expressed by neural stem/progenitor cell), and Pax6 (protein that regulates the development of neuroectoderm marker). The mRNA expression of Oct4 (2.6-7.2 fold change) and Lin28 (2.5-5.9 fold change) decreased, and the expression of Pax6 (12.0-16.2 fold change) and Nestin (2.0-3.0 fold change) increased in the differentiated cells (12 days) compared to undifferentiated cells (Figure 11). The decreased level of the pluripotency markers is expected as the cells differentiate into mature phenotypes. Nestin is expressed much earlier than Pax6; its expression being up

regulated would suggest the cells are further along in the differentiation process. The expression of Oct4 for cells seeded on biaxial aligned scaffolds decreased significantly compared to the cells cultured on other scaffolds. There is a significant difference between loop mesh 200 and other scaffolds for the expression of Oct4. Gene expression of Nestin positive cells has not shown a significant difference between biaxial aligned and bimodal scaffolds. However, gene expression of Pax6 positive cells increased significantly from other scaffolds to the biaxial aligned scaffolds, indicating that the differentiation of cells was enhanced on biaxial aligned scaffolds versus the loop mesh 200. The expression of Pax6 for biaxial aligned scaffolds was ~13.5 %, which was increased to the loop mesh scaffolds. The cells cultured on loop mesh 200 scaffolds with an average fiber diameter of 43.7 ± 3.9 μm showed 11.2 % more Pax6 marker expression when compared to loop mesh scaffolds with an average fiber diameter of 85 ± 4 μm, indicating the significance of fiber diameter on neural differentiation of human iPSCs. Interestingly, cells seeded on biaxial aligned scaffolds showed more expression of Pax6 when compared to bimodal scaffolds. The gene expression of cells expressing Pax6 marker was higher (~ 11 %) on loop mesh 200 scaffolds compared to loop mesh 500 scaffolds. These results suggest that the orientation of microfibers and their average diameter influenced the differentiation of human iPSCs when seeded on such scaffolds through mechanical cues. Overall, biaxial aligned scaffolds have the most expression of Pax6 (~ 16.2 fold increase over controls), indicating such scaffolds enhanced the neural differentiation of human iPSCs compared to the other scaffolds.

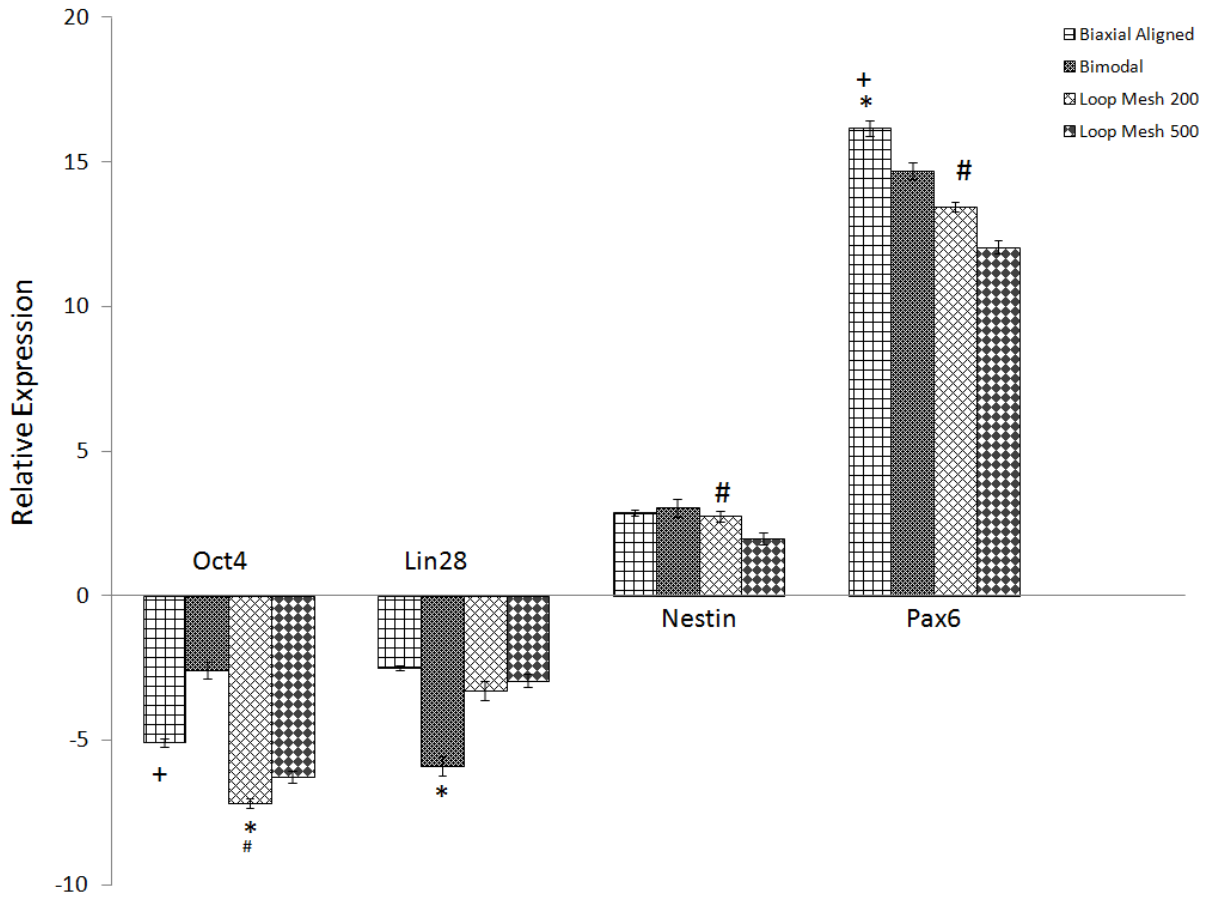

Figure 11 qPCR Analysis of neural progenitor cultured on scaffolds for 12 days. The markers examined were Oct4, Lin28, Nestin, and Pax6 for differentiated human iPSCs. * indicates $p < 0.05$. Data plotted VS. Undifferentiated human iPSCs data as control. The expression levels are normalized to undifferentiated human iPSCs

Discussion and future work

The major advantage of melt electrospun scaffolds for tissue engineering applications is the level of control that can be achieved in terms of fiber diameter and topography. Studies have shown that melt electrospinning can be used as a powerful fabrication technique to construct various structures while controlling their topography with an excellent degree of repeatability[23, 32-34, 111, 118]. We have previously used melt electrospinning to fabricate loop mesh scaffolds with varied topographical and mechanical properties[23]. Such loop mesh scaffolds have been shown to be an excellent substrate to support the attachment and neuronal differentiation of

neural progenitors derived from murine ESCs. Based on these promising results, we now investigated the effect of such topographical properties on the neuronal differentiation of human iPSCs. We seeded human iPSC-derived neural aggregates onto two different loop mesh scaffolds, where they could survive, migrate, and differentiate into neurons. The cells cultured on loop mesh 200 scaffolds were able to migrate along the fibers migration. Since the loop mesh 200 scaffolds served as a better substrate for human iPSCs culture, we used the 200 µm nozzle size and increased the speed of the melt deposition from 200 to 1700 mm/s, to fix the fiber diameter (~ 45 µm) and to control the alignment of scaffolds while converting the topography from loop mesh to highly aligned biaxial scaffolds. In addition to the loop mesh scaffolds, we also successfully designed and tested the biaxial aligned scaffold topography in order to report its promising ability to provide physical cues for the differentiation of pluripotent stem cells.

Although using melt electrospinning for drug delivery applications has been reported[119], it is not commonly used to produce controlled release of drugs from fibrous scaffolds unlike solution electrospinning. Therefore, many groups are still using solution electrospinning to encapsulate bioactive agents into nanofibers for neural tissue engineering applications[24, 56, 111]. Here, we combined the advantages of both techniques, by using the control over topographical features offered by melt electrospun microfibers and the encapsulation of drugs and controlled release offered by solution electrospun nanofibers.

PSCs have previously been shown to respond to various physical cues[25, 43, 105, 111]. In this work, we studied how human iPSCs seeded onto electrospun scaffolds would respond to changes in micro and nanotopography features. Here, on loop mesh 200 scaffolds (43.7 ± 3.9 µm), human iPSCs were well elongated and migrated outward from the neural aggregates along the fibers direction (Figure 7D) while cells have shown to be located between the gap of fibers

when seeded onto loop mesh 500 scaffolds (85 ± 4 µm) without any migration, indicating how decreasing fiber diameter could enhance the neuronal differentiation of such cells. Similar to our results, Pan et al have shown that the morphology of human iPSCs had been strongly structure dependent, and they have qualitatively and quantitatively shown that the cells seeded on the smallest topography (on a 350 nm substrate) had the highest neuronal differentiation[105]. In addition to fiber diameter, our novel biaxial aligned scaffolds also demonstrated that the orientation of fibers could strongly control the direction or neurites outgrowth from human iPSCs. When the neural progenitor cells derived from human iPSCs were differentiated on the biaxial aligned scaffolds, cells drastically aligned and elongated along the direction of the microstructure. In sense of nanoscale, aligned electrospun nanofiber scaffolds have previously shown to guide the neurite outgrowth from mouse ESCs and iPSCs when seeded on such scaffolds[25, 111]. Mahairaki et al. have proved that the human ESC-derived neural precursors cultured on aligned micro- and nanofibers had shown a higher rate of neuronal differentiation than other random micro and nanofibers[43]. We have previously shown that interaction with the physical cues had effected cell behaviour, while aligned topographies directed the outgrowth of neurons from mouse iPSCs[111]. However, we believe that flow cytometry should be also used to quantify the presence of differentiated cell phenotypes on our current scaffolds to further investigate the topographical cues on the neural differentiation of human iPSCs .

Neural progenitor cells derived from human iPSCs cultured on biaxial aligned microfiber scaffolds demonstrated the longest degree of neurite outgrowth (~573µm) compared to those seeded onto other scaffolds. Outgrowth of human iPSCs-derived neurons has been demonstrated to be strongly directed by physical cues including the orientation of fibers along their average diameter. Although, our present study showed that the biaxial aligned microfiber scaffolds could

enhance the differentiation of cells into neurons, the maximum neurite outgrowth (~573μm) is still smaller than previous findings for the maximum neurite length (~1600 μm) which were reported for mouse ESCs seeded onto aligned nanofibers[25]. On the other hand, studies on nanofibers scaffolds fabricated using solution electrospinning have been limited to only randomly-oriented and aligned topographies with very low degree of repeatability and controllability, excluding the influence of other scaffold architectures such as highly controllable biaxial aligned scaffolds, loop mesh and other possible designs. However, we believe that decreasing the fiber diameter to nanoscale will be doable by tuning melt electrospinning parameters with the aim of fabricating biaxial aligned nanofiber scaffolds to further promote the maximum neurite length of seeded neural progenitor cells derived from human iPSCs onto such scaffolds.

We reported that micro scale topography could significantly promote the expression of neural marker Pax6 in our human iPSCs culture. This indicates that the induction of neural lineages of human iPSCs was significantly controlled by melt electrospun topography. Neural progenitors of human iPSCs seeded on biaxial aligned scaffolds were elongated along the fibers and showed the highest expression of Pax6. However, the cells cultured on the bimodal scaffolds had higher rates of Pax6 expression compared to all loop mesh scaffolds. Our bimodal scaffolds were fabricated in order to determine if PCL nanofibers encapsulating RA would assist the iPSCs in further expression of neural marker Pax6. Compared to biaxial scaffolds without any RA nanofibers, the bimodal scaffolds showed that the iPSCs expressed less Pax6 and therefore bimodal scaffolds show no advantage over simple biaxial aligned scaffolds. However, our bimodal scaffolds could support the interactions of two human iPSC-derived neural progenitors and such scaffolds demonstrated the highest % of live cells in their neural aggregate (~ 95 %) compared to the other

scaffolds which could be due to the presence of bioactive nanofibers filling the gap between blank PCL microfibers.

We have shown that human iPSCs can differentiate into neurons when seeded onto fibrous melt electrospun and bimodal PCL scaffolds. We investigated the physical cues of electrospun microfiber scaffolds on the neuronal differentiation of human iPSCs. All loop mesh, biaxial aligned and bimodal scaffolds supported neuronal differentiation as the seeded cells expressed the neuron specific protein β-III-tubulin. Particularly, neurite outgrowth was directed by the scaffold topography of our biaxial aligned scaffolds. This study has been completely chemically defined and would be introduced as a promising approach for neural tissue engineering clinical applications. The next step in this research would be to generate more quantitative results using flow cytometry and looking at other phenotypes present. We will only focus on neurons since for stem cell treatment applied at the injury site, it is important that the cells be directed to become neurons which will promote regeneration rather than other cell types such as astrocytes that will contribute to the scar tissue. We would also recommend analyzing wells at specific time intervals throughout the 12-day seeding period. Progressive, quantitative data could yield a greater understanding of the mechanisms behind human iPSC neural differentiation. Additionally, we will aim to encapsulate larger molecules such as growth factors, like glial derived neurotrophic factor (GDNF), inside bimodal scaffolds to further enhance neuronal differentiation of human iPSCs.

Conclusion

We were able to successfully fabricate 4 types of scaffolds with varying topographies using electrospinning, including loop mesh 200, loop mesh 500, biaxial aligned and bimodal scaffolds coated with RA-releasing nanofibers. All of these scaffolds supported the culture of human

iPSC-derived neural progenitors with a degree of viability and their differentiation into neurons. Scaffold topography influenced the length of neuronal processes as neurons cultured on the loop mesh 200 scaffolds had longer processes when compared to loop mesh 500 scaffolds. The greatest amount of extension was observed for the cells cultured on the biaxial aligned scaffolds. Overall, this study demonstrated how topography can be used to differentiate human iPSC-derived neural progenitors into neurons while being able to direct neurite outgrowth as well. It further demonstrates how melt electrospinning can be used to fabricate substrates for tissue engineering applications in a reproducible fashion.

Chapter 4 Controlled Release of Glial Cell-Derived Neurotrophic Factor from Random and Aligned Electrospun Nanofibers[10]

Introduction

Neurotrophic factors, such as glial cell-derived neurotrophic factor (GDNF), are proteins that regulate and promote the differentiation, growth, and survival of neurons [24]. Expressed in the central nervous system (CNS), GDNF promotes the survival of motor and dopaminergic neurons, making it a promising therapeutic for the treatment of neurodegenerative diseases [24, 120-127]. For instance, clinical trials are currently underway to determine the efficacy of GDNF for the treatment of Parkinson's disease (PD)[128-132]. GDNF can also be used to enhance cell survival after transplantation in the damaged CNS. For example, Wang *et al*. used GDNF pre-treatment to enhance the survival of grafted neural cells in rat PD model [133]. Olle *et al*. summarized the GDNF trials in PD patients which indicated its potential in nerve protection and regeneration for treatment of the disease [133, 134]. GDNF also has trophic effects on motor neurons, which holds great promise for the applications on spinal cord injuries (SCI)[39].

Based on these aforementioned properties, controlled release of GDNF from different biomaterials serves as a promising strategy for treating diseases and disorders of the CNS. Previous studies have used drug delivery systems, including microspheres, affinity based delivery systems, and hydrogels[24] to generate controlled GDNF release. Agbay *et al*. showed that PCL microspheres could be formulated to release bioactive GDNF over 25 days. The released GNDF was successfully proven to be bioactive since PC12 cells showed the neurite

[10]The following chapter is from: **Controlled Release of Glial Cell-Derived Neurotrophic Factor from Random and Aligned Electrospun Nanofibers**. Mohtaram, N.K., et al. In preparation for submission into the Journal of Neural Engineering.

outgrowth when treated with the release GDNF. As a promising alternative to these aforementioned delivery systems, natural and synthetic polymeric nanofibers play an important role in neural drug delivery applications. Encapsulated nanofibers offer a number of advantages over other delivery systems like microspheres. Virtues include the ease of controlling the structure of nanofibers, the ability to alter their porosity, the ability to tailor their mechanical properties and more importantly, the capability for improving their biological functionality by immobilization of proteins and other signaling molecules on the surface of such nanofibers[24]. Therefore, nanofibers represent a very fascinating biomaterial-based delivery system to encapsulate growth factors and small molecules for not only providing the controlled release of such drugs but also act very effectively in stem cell differentiation and guidance of neurite extension for neural tissue engineering applications.

Solution electrospinning is a nanofiber fabrication process where an applied electric potential stretches out fibers from a viscoelastic flow of polymers. The polymer solution of choice is pumped through a nozzle into an electric field where the force applied by the electric potential balances against the surface tension, causing the droplets to continuously deform in the direction of flow, resulting in fiber formation. Solution electrospinning can be used to prepare nanofiber scaffolds with unique topography from a range of polymers. Previous studies focused on the encapsulation drug factors into electrospun fibers and characterizing the drug release profile of these scaffolds using various polymers and neurotrophic factors[24, 109, 135-141]. For example, nanofiber scaffolds can deliver a ligand that mimics the properties of brain-derived neurotrophic factor[138] while Jiang et al. showed that electrospun nanofiber morphology along with controlled release of retinoic acid promoted the differentiation of mesenchymal stem cells into neural lineages[56]. Wang et al. used coaxial electrospinning to incorporate nerve growth

factor (NGF) into aligned core–shell nanofibers to promote peripheral nerve regeneration in vitro[133]. Valmikinathan et al. showed the sustained release of bovine serum albumin (BSA) and NGF encapsulated from nanofibers after 28 days[53]. These aforementioned studies show that research on encapsulated nanofiber biomaterials holds great promise in the fields of neural drug delivery since encapsulated nanofibers could be used to modulate the wound environment in CNS and enhance nerve regeneration.

Of many natural and synthetic polymers used in the solution electrospinning techniques, poly (ϵ-caprolactone) (PCL) is such a promising biodegradable and biocompatible polymer, approved by the U.S. Food and Drug Administration (FDA) for drug delivery applications. Dash et al. have published a great up-to-date review on PCL based formulations for drug delivery applications[20]. Overall, this body of work on PCL nanofibers continue to play an important role in the controlled release of neural drugs for the development of on-going strategies for neural clinical applications[24].

In this study, we fabricate and characterize PCL-BSA and PCL-BSA-GDNF nanofibers. Then we characterized the controlled release of the GDNF and confirmed that the released GDNF is bioactive. GDNF is a hydrophilic protein with a molecular weight of 30 kDa. The purpose of the work is to show the potential of combination the chemical cues (controlled release of GDNF) and the physical cues (topographies of electrospun nanofibers) to investigate a suitable scaffold for neural tissue engineering applications. Three types of electrospun nanofibers, including PCL, PCL-BSA, and PCL-BSA-GDNF scaffolds, were all fabricated into aligned and random topography. These nanofibers were characterized using scanning electron microscopy (SEM) to show the morphologies, fiber diameter, and then testing the ability of controlled release of BSA and GDNF along assaying bioactivity of the released GDNF using

PC12 cells. Using this assay, the released GDNF was confirmed to be biologically active after 30 days from both types of electrospun nanofibers. This study showed a promising application of aligned and random GDNF encapsulated electrospun nanofiber scaffolds for neural tissue engineering.

Materials and methods

Fabrication of encapsulated nanofibers

Poly (Ɛ-caprolactone) (PCL,Mn: 45,000), bovine serum albumin (BSA) (M_w 66 *kD*a, lyophilized powder) were purchased from Sigma-Aldrich (St. Louis, MO, USA). 1,1,1,3,3,3-Hexafluoro-2-Propanol (HFP), 99 +% was purchased from Alfa Aesar; Phosphate-Buffered Saline (PBS), (pH 7.4 from Gibco®.). Dichloromethane (DCM) (reagent/ACS grade) was purchased from VWR International (Edmonton, AB, Canada). 400 mg of PCL was added to 5 mL of HFP to make 8 % (*w/v*) solution which was mixed overnight. Then 50 mg of BSA was added for the day 2 of mixing to make the final PCL-BSA (80:20) solution. 107 µL of the GDNF stock solution (9.3 mg/ml) was added to make a homogenous solution, resulting in a theoretical loading level of 0.22 *wt*% GDNF in the polymer solution. The solution electrospinning setup for the fabrication of encapsulated nanofibers was previously reported. The PCL, PCL-BSA, and PCL-BSA-GDNF solutions were pumped at the constant flow rate of 2 ml/hr into electrospinning syringe in order to fabricate random and aligned scaffolds respectively. Random nanofibers were collected on top of an aluminum foil and aligned fibers were spun on a rotating drum. The solution electrospinning parameters used in the experiment are summarized in Table 5. Each scaffold (~10 mg total weight) was spun for 5 minutes and dried overnight.

Topography	Scaffold	Collecting Distance (mm)	Voltage (kV)	Drum Speed (rpm)
Random	PCL Blank	5	15	N/A
	PCL- BSA	5	15	N/A
	PCL-BSA-GDNF	5	15	N/A
Aligned	PCL Blank	2.5	12	5000
	PCL-BSA	2.5	12	5000
	PCL-BSA-GDNF	2.5	12	5000

Table 5 Solution electrospinning parameters for nanofibers with varied topographies.

Morphological characterization

The nanofibers were characterized using scanning electron microscopy (SEM) (Hitachi S-4800 SEM). A standard SEM procedure was followed for obtaining high magnification images (20,000 X), including carbon coating the samples prior to imaging as previously reported[111]. The average fiber diameter was determined using Quartz-PCI Image Management Systems® software tools with 100 fibers being measured per sample.

In vitro release studies

BSA encapsulation efficiency and release study

The encapsulation efficiency, the ratio of the amount of BSA incorporated in scaffold to the amount of BSA added to the mixture, was determined by rapidly dissolving the PCL of the nanofibers and measuring the protein released. A measured amount of nanofibers were placed in conical tube containing 8 mL of DCM, this was mixed via vortex mixer (Fisher Scientific) for 2 minutes. 2 mL of PBS was added and the solution was mixed for another 30 seconds. The

resulting solution was centrifuged at 5000 rpm for 20 min, after which the PBS + protein solution was extracted from the tube. The concentration of BSA protein in the collected washes was measured using the Bio-Rad®Protein Assay with a Microtiter Plate Protocol.

Release studies were conducted for every day for 30 days to measure the release of BSA from the nanofibers over time. Initially, nanofibers were immersed in 1 mL of PBS and stored at 37 °C. Every 24 hours the nanofibers were washed by removing the PBS via a needle and syringe. The collected washes were then frozen for later analysis and 1 *m*L of fresh PBS added to each scaffold. The concentration of protein in the extracted solution was measured via the Bio-Rad®Protein Assay with a Microtiter Plate Protocol. For the protein assay protocol standards were made from bovine serum albumin (Sigma Life Sciences) ranging from a concentration of 8 μg/mL to 80 μg/mL. This assay measures the total amount of protein in the sample. The absorbance was measured using spectroscopy (Infinite M200 Pro Softmax Pro version 5.2) at 595 nm. From the absorbance of the samples compared to that of the standards the concentration of protein within the sample could be determined.

GDNF encapsulation efficiency and release study

In order to measure the encapsulation efficiency of GDNF for PCL-BSA-GDNF nanofibers, the encapsulated GDNF per unit weight of nanofibers was also determined by extraction into 2 mL PBS as previously described for BSA extraction. Release studies were conducted every other day for 30 days to measure the release of GDNF from the nanofibers over time. Concentrations of GDNF were determined by Enzyme-linked immunosorbent assay (ELISA) to measure encapsulated GDNF and released GDNF in each sample. Polyclonal goat IgG human GDNF biotinylated antibody, monoclonal rat IgG anti-GDNF antibody, and wash buffer were purchased from R&D Systems (Minneapolis, MN, USA). ImmunoPure® streptavidin horseradish

peroxidase conjugate and fetal bovine serum (FBS) were purchased from Thermo Scientific (Rockford, IL, USA). Good manufacturing practice (GMP) Liatermin (r-metHuGDNF), was provided by MedGenesis Therapeutix Inc. (Victoria, BC, Canada). The release samples were collected every other day to increase the amount of GDNF in each sample for easier detection. Samples were assayed by GDNF ELISA (Amgen procedure #A0195r04). Grenier 96 well plates were coated with monoclonal anti GDNF antibodies in PBS (100 µl/well) and the nonspecific binding sites were blocked by a milk protein solution (0.1% Milk, 0.01% Tween 20 in 1X PBS) (Mandel Scientific). GDNF release samples and standards (100 µL/well) were incubated in capture antibody coated for 1hr on a minishaker (VWR). Detection was done by biotin conjugated polyclonal anti-GDNF antibodies, followed by streptavidin conjugated horse radish peroxidase. Colourmetric analysis was performed by addition of Sureblue Reserve substrate (KPL) for colour development. The reaction was stopped using phosphoric acid and analyzed using an Infinite M200 plate reader at absorptions of 450 and 650nm.

Bioactivity assay

In order to determine the bioactivity of released GDNF, undifferentiated PC12 cells (ATCC) (Rockville, MD, USA) were exposed to GDNF samples retrieved from release points at Day 0, 10 and 30 and the extent of neurite outgrowth was assessed. PC12 cells were grown in suspension using Dulbecco's modified eagle medium (DMEM; 1×, 4.5 g/L D-glucose, L-glutamine) (Invitrogen) supplemented with 15 % FBS (Life Technologies) at 37 °C and 5 % CO2. Cells were passaged with a 22-gauge needle to separate cell clumps. Laminin derived from the basement membrane of Engelbreth-Holm-Swarm murine sarcoma cells and 0.01 % poly-L-ornithine (PLO) solution were purchased from Sigma-Aldrich (St. Louis, MO, USA). 24-well tissue culture plates (Grenier) were first coated with PLO and then with Laminin. The plates

were seeded with PC12 cells at a concentration of 20,000-60,000 cells/mL and exposed to released GDNF at concentrations of 0.01ng/mL and 1.0x10-5 μg/mL corresponding to day 10 and day 30 of the release study. The loaded plates were incubated inside of an IncuCyte® ZOOM Essen BioScience® microscope (Ann Arbor, Michigan, USA) and scanned at 12 hour intervals for neurite outgrowth tracking.

Quantitative analysis of neurite outgrowth

An IncuCyte® ZOOM Essen BioScience® microscope was used to analyze bright field images of seeded PC12 exposed to GDNF washes at 10X objective. 24-well plates were placed inside the Incucyte and each well was scanned every 12 hours for a period of 10 days to study the kinetics of neurite growth. At the end of scanning schedule, images were analyzed using the IncuCyte® ZOOM NeuroTrack Software™. Neurite length was calculated for each day of the 10 day time course and the maximum neurite length after 10 days was calculated.

Stem cell culture and neuronal differentiation

To determine suitability of aligned PCL-BSA-GDNF scaffolds for stem cell culture, human iPSCs (the 1-MCB-01 line from Thomson Lab) were utilized. Human iPSCs were cultured Vitronectin XF™ coated surfaces in the presence of TeSR™-E8™ media in 6 well plates (Global stem, USA) to maintain pluripotency[114, 115]. Undifferentiated human iPSCs were subsequently removed and cultured into a single well of an Aggrewell™ 800 plate in the presence of 2 mL of STEMdiff™ Neural Induction Medium (NIM, STEMCELL Technologies) (STEMCELL TechnologiesTM). During this process, the media is changed with 1.5 mL of fresh NIM every day. The resulting aggregate consists entirely of neural progenitors (after 5 days). Individual neural progenitors were removed from suspension and seeded onto scaffolds. Human

iPSC-derived neural progenitors were cultured on aligned PCL-BSA-GDNF nanofiber scaffolds for 12 days before image analysis. Neuronal differentiation of seeded cells was qualitatively assessed after 12 days by immunocytochemistry targeting the neuron-specific protein β-III-tubulin. The detail of immunohistochemistry is previously published[111]. Images were captured for green fluorescence and fluorescent images were acquired on a LEICA 3000B inverted microscope using an X-cite series 120Q fluorescent light source (Lumen Dynamics) coupled to a Retiga 2000R fast cooled mono 12-bit camera (Q-imaging).

Statistical analysis

Data are presented as mean values ± standard deviation of the mean. Statistical analysis was performed using STATISTICA 9 by applying a standard *t*-test to compare differences between experimental groups. Significance was considered at the $p < 0.05$ level.

Results

Fabrication and characterization of encapsulated nanofibers

We fabricated blank PCL, PCL-BSA, and PCL-BSA-GDNF nanofibers scaffolds using solution electrospinning with random and aligned topographies. By tuning the solution electrospinning parameters such as collecting distance, applied voltage, and the drum speed, we could successfully fabricate nanofibers scaffolds with varied topographies with a very porous structure without any polymer beads or either protein agglomerations. We have previously proved that the degree of alignment of blank and encapsulated electrospun nanofibers with small molecules, can be improved significantly using a rotating drum. SEM images of both topographies for each type of scaffold are shown in Figure 12. The morphology of random and aligned blank PCL nanofibers is shown in Figures 12A and 12B respectively. For random blank

PCL nanofibers, the average fiber diameter was measured as 358.62 ± 95.42 nm (*n=100*) and for aligned blank PCL nanofibers, the average diameter was measured as 202.25 ± 145.87 nm (*n=100*). Random and aligned electrospun PCL-BSA nanofibers were fabricated at 15 kV and 12 kV applied voltage respectively and their structure has shown a very fine bead-free morphology at these aforementioned voltages. Figure 12C and 12D represent the morphology of random and aligned PCL-BSA nanofibers respectively. The average fiber diameter for random and aligned PCL-BSA nanofibers was measured as 625.87 ± 240.48 nm (*n=100*) and 429.57 ± 152.37 nm (*n=100*). Figures 12E and 12F show the topography of the random and aligned electrospun PCL-BSA-GDNF nanofibers fabricated at 5 and 2.5 mm collecting distance. For aligned scaffolds, the average fiber diameter was measured as 247.78 ± 124.66 nm (*n=100*) and for random scaffolds the average diameter was measured as 525.42 ± 193.32 nm (*n=100*).

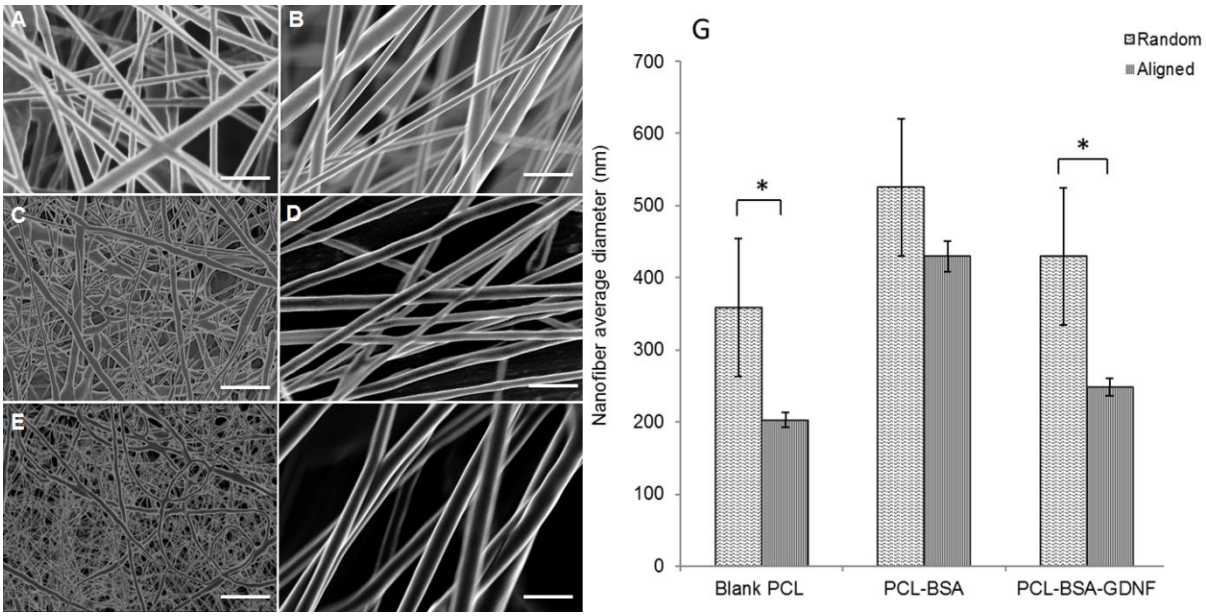

Figure 12 Scanning electron microscopy images of nanofiber scaffolds. (A),(B) Random and aligned blank PCL nanofibers. (C), (D) Random and aligned PCL-BSA nanofibers. (E), (F) Random and aligned PCL-BSA-GDNF nanofibers. Scale bar is 1 µm. (G) Average fiber diameter of random and aligned blank PCL, PCL-BSA, and PCL-BSA-GDNF nanofibers. (*$p<0.05$).

Encapsulation efficiency and release study

Encapsulation efficiency of encapsulated nanofibers scaffolds with two topographies is given in Table 6. We were able to encapsulated BSA and GDND inside bead-free PCL-BSA and PCL-BSA-GDNF nanofibers while varying scaffold topography. The encapsulation efficiency of BSA inside random and aligned PCL-BSA scaffolds was 54.3 ± 3.3 % and 42.2 ± 4.5 % respectively. For random PCL-BSA-GDNF nanofibers the encapsulation efficiency of GDNF was measured as 31.6 ± 2.4 % and for aligned PCL-BSA-GDNF nanofibers the encapsulation efficiency was measured as 27.5 ± 3.7 %.

Topography	Scaffold	Encapsulation Efficiency %
Random	PCL- BSA	54.3 ± 3.3
	PCL-BSA-GDNF	31.6 ± 2.4
Aligned	PCL-BSA	42.2 ± 4.5
	PCL-BSA-GDNF	27.5 ± 3.7

Table 6 Encapsulation efficiency of encapsulated scaffolds with two topographies (*n=3*).

Figure 13A shows the release kinetics of BSA from random and aligned PCL-BSA nanofibers. Random PCL-BSA nanofibers released a maximum BSA amount of 0.5 mg on day 30 of release studies while aligned PCL-BSA nanofibers released a maximum of 0.6 mg BSA on day 30. The cumulative release of BSA over time from aligned PCL-BSA nanofibers were greater significantly compared to the release of BSA from random PCL-BSA nanofibers. Controlled release of GDNF from random and aligned PCL-BSA-GDNF nanofibers was observed over 30 days (Figure 13B). Within 2 day, 0.64 ± 0.14 % of GDNF was released from the random PCL-BSA-GDNF nanofibers since this amount was greater compared to the aligned nanofiber (0.22 ± 0.01%) significantly. The total GDNF released over 30 days was 8.17 ± 0.44

% (~ 0.42 μg) and 4.1 ± 0.43 % (~ 0.73μg) for the aligned and randomly-oriented topographies respectively. GDNF was released at an average rate around 0.28 % and 0.15 % per day for 30 days for the aligned and randomly oriented PCL-RA scaffolds respectively. The release data at each day between the random and aligned PCL-BSA and also the random and aligned PCL-BSA-GDNF nanofibers was significantly different ($p<0.05$). Overall, the PCL-BSA aligned nanofibers showed 118% more release than the randomly oriented fibers and this amount was around ~ 200% when comparing PCL-BSA-GDNF nanofibers to PCL-BSA-GDNF random nanofibers indicting the great potential of such scaffolds for providing quicker release while having aligned topography for tissue engineering applications.

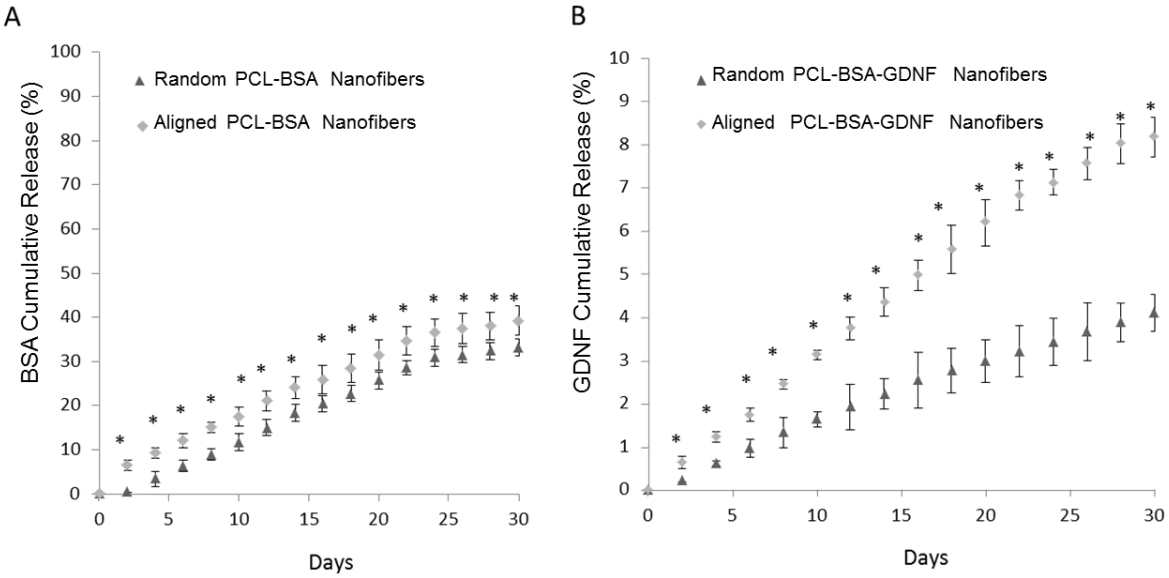

Figure 13 Controlled release profiles. A: In vitro cumulative BSA release from random and aligned PCL-BSA nanofibers. B: In vitro cumulative GDNF release from random and aligned PCL-BSA-GDNF nanofibers. Standard deviations are shown (*n=3*). The release data at each day between the random and the aligned nanofibers was significantly different for each set of encapsulated nanofibers (*$p<0.05$).

Kinetics of neurite outgrowth

The bioactivity of released GDNF from random and aligned PCL-BSA-GDNF nanofibers was evaluated using PC12 cells. Cells were exposed to GDNF washes from day 10 for random and aligned PCL-BSA-GDNF nanofibers, corresponding to 172 ng/ml and 341 ng/ml and also

day 30 for random and aligned PCL-BSA-GDNF nanofibers, corresponding to 23 ng/ml and 14 ng/ml. All cells were scanned every 12 hours for a period of 10 days (240 hours). Figure 14 shows the kinetics of differentiation of neurites from PC12 cells in the presence of GDNF for different dosages and topographies. The GDNF released for both day 10 (~ 341 ng/ml GDNF) and day 30 (~ 23ng/ml GDNF) washes from the random and aligned PC-BSA-GDNF nanofibers initiated the neurite outgrowth of PC12 cells with an approximate length of 300 μm after the first 12 hours of seeding. Figure 14A shows that the maximum neurite length for random PCL-BSA-GDNF nanofibers was reported (~ 523 μm), observed after 96 hours for day 10 of wash (~ 172 ng/ml). Figure 14B shows that the maximum neurite length (~ 556 μm) was observed after 216 hours for day 10 of wash (~ 341 ng/ml GDNF) for the aligned PCL-BSA-GDNF nanofibers. Overall, the released GDNF from aligned PCL-BSA-GDNF nanofibers has induced the maximum neurite outgrowth from PC12, where this highest neurite outgrowth was induced from the highest concentration of GDNF (~ 341 ng/ml GDNF) subsequently. Due to the lower concentration of GDNF washes at 30 (~ 23 ng/ml for random and ~14ng/ml for aligned nanofibers), PC12 cells showed a shorter neurites compared to Day 30 of wash for both set of nanofibers.

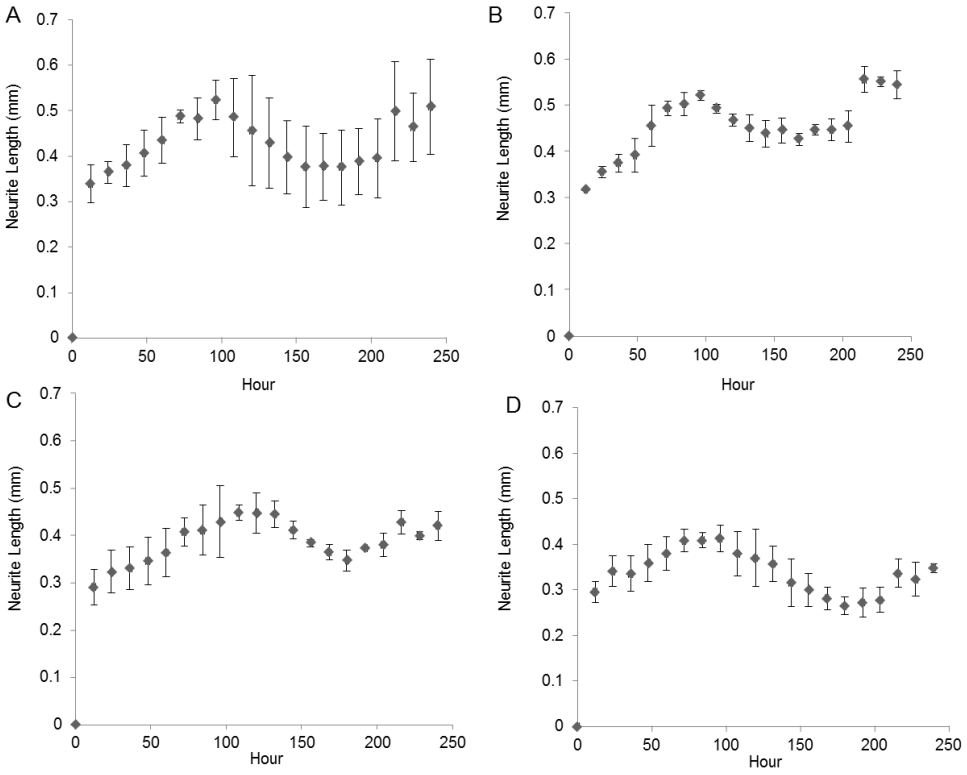

Figure 14 Kinetic of neurite length from PCL12 cells over 10 days. (A) Cells exposed to day 10 wash from random PCL-BSA-GDNF nanofibers. (~ 172 ng/ml GDNF). (B) Cells exposed to day 10 wash from aligned PCL-BSA-GDNF nanofibers (~ 341 ng/ml GDNF). (C) Cells exposed to day 30 wash from random PCL-BSA-GDNF nanofibers (~ 23ng/ml GDNF). (D) Cells exposed to day 30 wash from aligned PCL-BSA-GDNF nanofibers (~ 14 ng/ml GDNF). Standard deviations are shown (*n=3*).

Neurite length analysis

Figure 15 shows the neurite extensions observed at 10x magnification of PC12 cells exposed to the released GDNF from both random and aligned nanofibers. The GDNF released from random and aligned PCL-BSA-GDNF nanofibers at day 30 enhanced extending neurites from PC12 cells (Figure 15C and 15D) compared to the negative control PC12 cells were no GDNF was present (Figure 15A). Quantitatively, we assayed the bioactivity of released GDNF after full 10 days. At the end of assays, we measured the maximum neurite length and also the percentage of cells extending neurites achieved by the end of 10 days scanning for day 30 of wash for both random and aligned nanofibers. Figure 16A shows the maximum neurite length in total cells for days 10 and 30 of wash from both random and aligned PCL-GDNF nanofibers after 10 days of

culture. There was a significant difference between day 10 and day 30 of washes for random GDNF nanofibers. There was no significant difference between the percentage of cells extending neurites for random and aligned PCL-BSA-GDNF nanofibers for day 10 and 30 of wash.

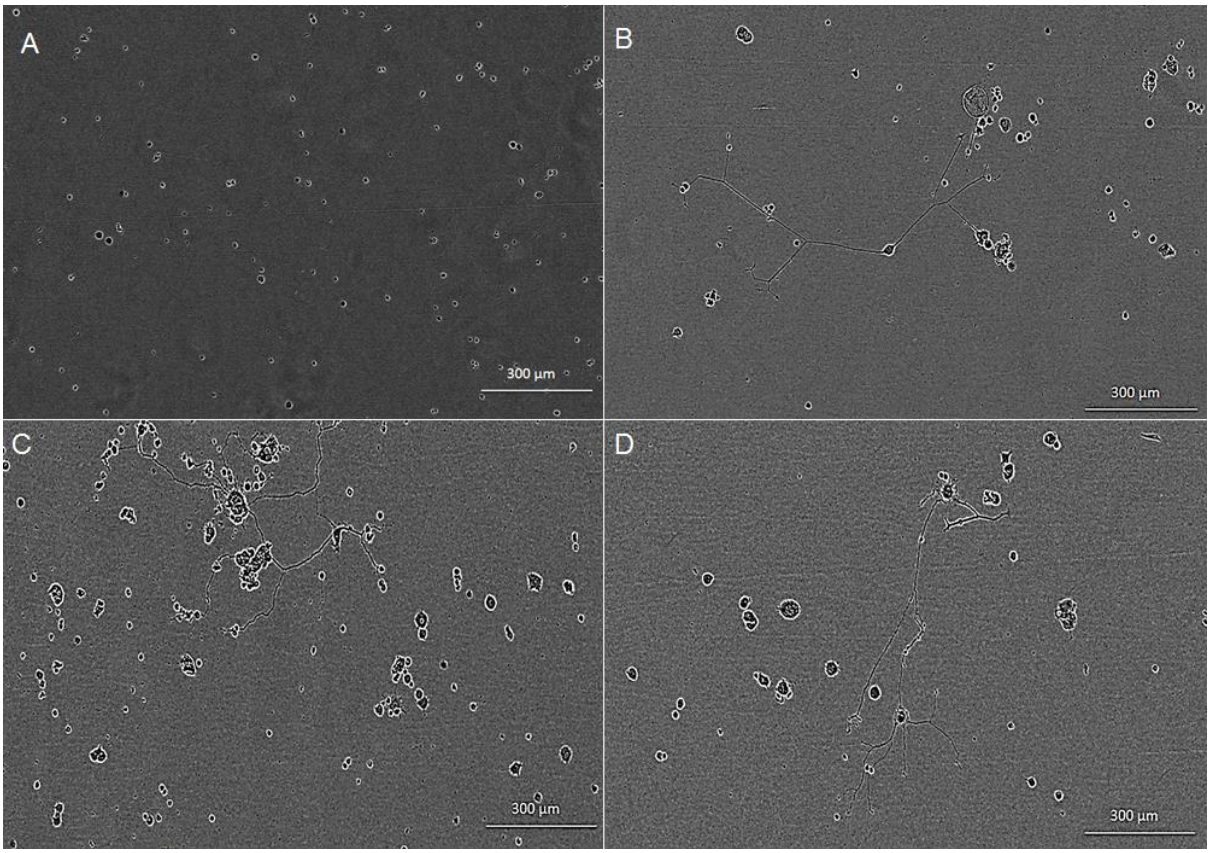

Figure 15 Neurite extensions observed at ×10 magnification of PC12 cells. (A) Negative control. (B) Positive control (25 GDNF ng/ml). (C) Day 30 wash (~ 23 ng/ml GDNF) from random PCL-BSA-GDNF nanofibers. (D). Day 30 wash (~14 GDNF ng/ml) from aligned PCL-BSA-GDNF nanofibers. Cells are photographed in phase contrast after 10 days.

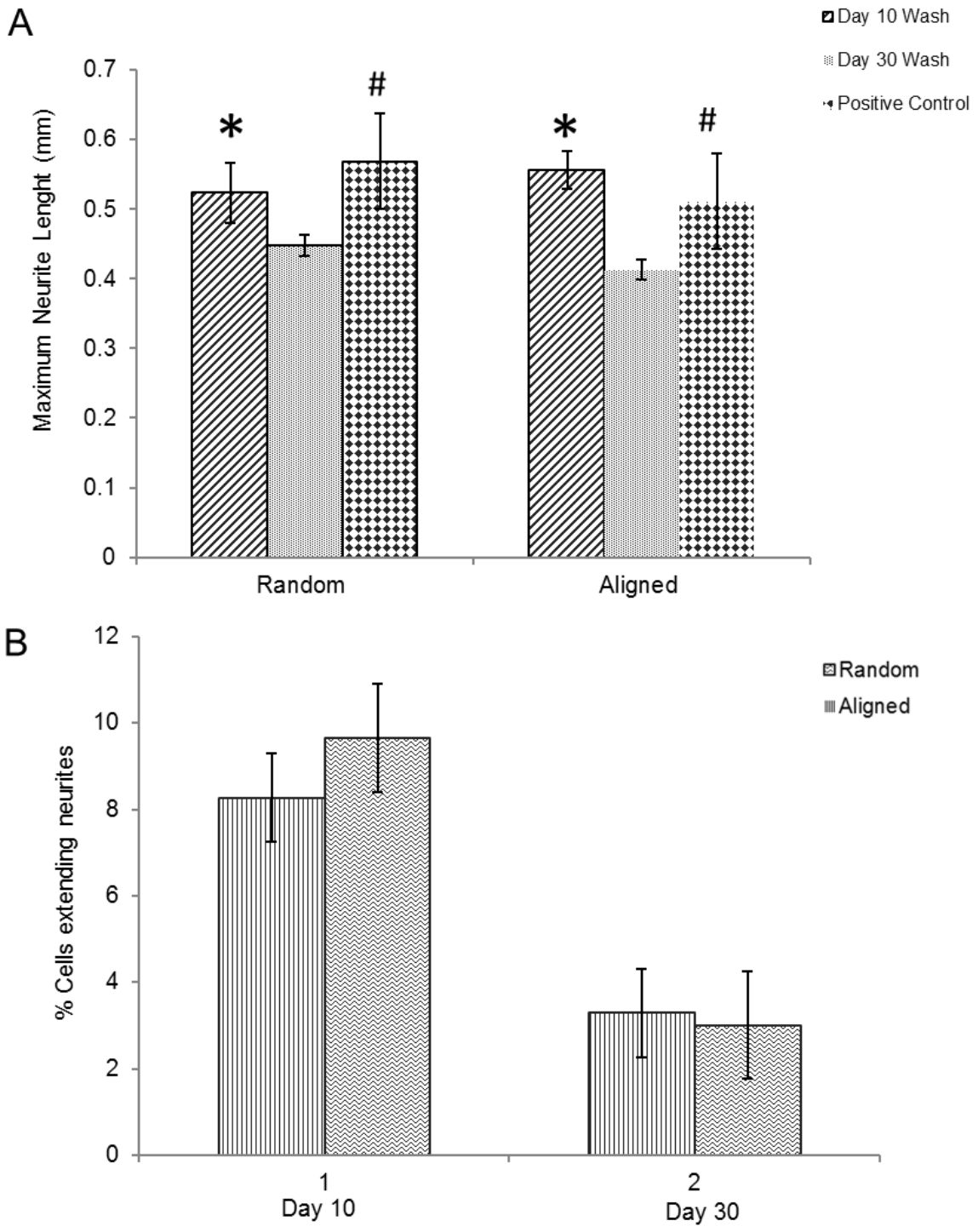

Figure 16 (A) Maximum neurite length in total cells for days 10 and 30 of wash from both random and aligned PCL-GDNF nanofibers. Cells were observed at ×10 magnification. (B) Percentage of cells extending neurites for days 10 and 30 of washes from random and aligned PCL-BSA-GDNF nanofibers. * indicates $p<0.05$ versus day 10 and day 30 of washes. # indicates $p<0.05$ versus day 30 and positive control.

Evaluating the compatibility of aligned GDNF nanofibers with iPSC culture and differentiation

The ability of the aligned PCL-BSA-GDNF nanofiber scaffolds to serve as a stem cell culture substrate was examined through cell seeding experiments. Human iPSC-derived neural progenitors attached to these nanofibers and neuronal differentiation from seeded neural progenitors could be observed after 12 days of culture. Figure 17 presents the results of the differentiation of neural progenitors derived from human iPSCs into neurons when seeded upon such scaffolds. Figure 17A shows a bright field image of the individual neural progenitor. Figure 17B shows the neuronal differentiation of such cells. These images verify that such scaffolds could support the neuronal differentiation of human iPSC-derived neural progenitors. Overall, solution electrospinning encapsulated GDNF nanofibers combined with human iPSC-derived neural progenitors can be seen as a perfect tool for neural tissue engineering.

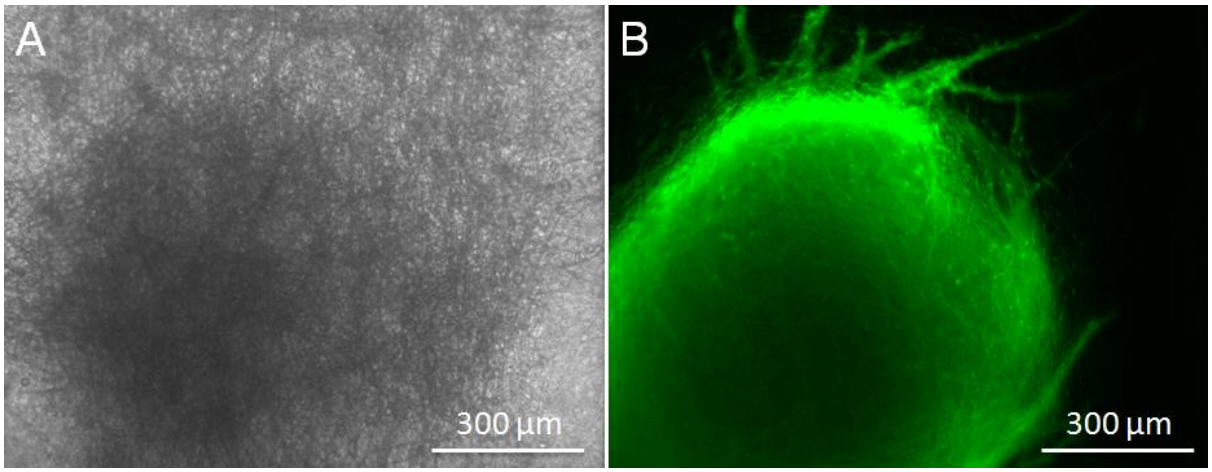

Figure 17 Neural progenitors seeded on aligned PCL-BSA-GDNF scaffolds after 12 days of culture. (A) Bright field image showing cells seeded on scaffolds. (B) Fluorescence image showing neuronal marker Tuj1 staining for neural aggregate seeded on nanofiber scaffolds.

Discussion

There are many methods to design drug delivery systems constructed of biocompatible polymers for providing controlled release of neurotrophic factors. Solution electrospinning can

be used to easily fabricate encapsulated nanofibers to obtain the controlled release of small molecules and also various proteins while tailoring the topography of such scaffolds[24, 111]. Our random and aligned blank PCL, PCL-BSA and PCL-BSA-GDNF nanofiber scaffold had excellent bead-free structure. Due to a tensile force induced by the rotating drum, the aligned nanofibers tend to be stretched uniaxially along the flow direction which results in the aligned nanofibers being thinner when compared to the random nanofibers. For aligned PCL-BSA-GDNF scaffolds, the average fiber diameter was measured as 247.78 ± 124.7 nm (*n=100*) and for random scaffolds the average diameter was measured as 525.42 ± 193.3 nm (*n=100*). For all nanofibers, the fiber diameter changed along an individual fiber so the fibers had non-uniform diameters. Controlling the uniform distribution of fiber size is very challenging. For instance, Yoshimoto *et al.* reported a broad fiber diameter distribution for PCL nanofibers (400nm ±200 nm). This variation in diameter may be due to the fast phase separation of PCL and the uncontrollable evaporation of volatile solvent during electrospinning[100].

We have previously shown how to encapsulate small molecules such as retinoic acid, (RA) inside PCL nanofibers using solution electrospinning to fabricate random and aligned encapsulated nanofibers[111]. Our previous data showed that 8.6 %, and 18 % of RA was released from aligned and random PCL nanofibers respectively over a month. In this paper, we could successfully encapsulate BSA and GDNF proteins inside random and aligned electrospun nanofibers. Our data showed that the controlled release of BSA and GDNF was provided over a month. Our PCL-BSA nanofiber scaffolds were able to provide around 40% and 30% release of BSA from aligned and random nanofibers respectively. Similarly, Valmikinathan et al. have reported almost the same amount of BSA release from their nanofibers. However, they have not studied the effect of topography on BSA release from such scaffolds[53]. Our work has shown

that the random PCL-BSA nanofibers released a maximum BSA amount of 0.5 mg on day 30 of release studies while aligned PCL-BSA nanofibers released a maximum of 0.6 mg BSA on day 30. Madduri et al. used electrospun nanofibers made from natural biomaterial, silk fibroin, to encapsulate GDNF with varied topographies[109]. To our knowledge, we are the first group to develop synthetic encapsulated PCL-BSA-GDNF nanofibers with varied topographies. In order to produce more uniform and higher encapsulated nanofibers, while preserving the bioactivity of GDNF, we co-encapsulate the growth factor with BSA inside the nanofibers. BSA has shown to act as a carrier protein to preserve bioactivity during the solution electrospinning process[53]. Overall, our results demonstrated that GDNF release from nanofibers was much slower than BSA release from such nanofibers with varied topographies. However, this release behaviour was very similar to our recent work on the GDNF encapsulation inside PCL microspheres. However, using coaxial electrospinning would be suggested as an alternative strategy to increase the release rate of proteins from electrospun nanofibers along increasing the encapsulation efficiency.

Despite the advantages of using solution electrospinning to fabricate nanoscale drug delivery systems, one of the main biological concerns is using toxic solvents such as HFP. In order to prove that the encapsulated GDNF has not been denatured in the presence of HFP, we evaluated the bioactivity of released GDNF from random and aligned electrospun nanofibers by quantitative and qualitative assays. For instance, we were able to study the neurite kinetics over 10 days for different washes of GDNF when exposed to PC12 cells to further understand the effect of dosage and time on neurite outgrowth length from such cells. GDNF washes (day 10 and 30) from the both random and aligned PCL-BSA-GDNF nanofibers were observed to initiate PC12 neurite outgrowth after 12 hours of seeding. Day 10 of GDNF wash (~ 172 ng/ml) samples

from random nanofibers yielded longer neurite extensions compared to day 30 of GDN wash (~ 23 ng/ml), and this amount was not significantly different compared to the positive controls at significance for such nanofibers. The same behavior has been demonstrated for the aligned nanofibers as well proving the effect of concentration on the neurite length (Figure 16A). The percentage of cells extending neurites compared to no GDNF (negative control) was not statistically different between random and aligned nanofibers for day 10 and day 30 of washes (Figure 16B). We believe due to the biocompatibility of PCL for drug delivery applications, the released GDNF would be still bioactive as proved by PC12 cells bioactivity assay.

Our work combining human iPSCs and GDNF encapsulated nanofibers demonstrates a promising method of producing biomimetic scaffolds for neural tissue engineering applications and novel drug delivery systems for providing the controlled release of neurotrophic factors. Finally human iPSCs adhesion and their neuronal differentiation on encapsulated GDNF nanofibers were observed. Directed outgrowth from neural progenitors was also observed, suggesting the effect of topography serves as a physical cue for stem cell-based tissue engineering approaches. Our proof of concept data demonstrates the compatibility of stem cells with such scaffolds fabricated via solution electrospinning. Overall, this work demonstrated the promising potential of GDNF aligned electrospun nanofiber scaffolds fabricated via solution electrospinning for neural drug delivery and tissue engineering applications. Our versatile technique to fabricate aligned encapsulated nanofibers via solution electrospinning provided controlled release of GDNF from such scaffolds. On-going work is investigating the quantitative effects of aligned scaffolds and controlled delivery of GDNF from such scaffolds to enhance neural differentiation of pluripotent stem cells.

Conclusions

In this study, the encapsulation of proteins BSA and GDNF into random and aligned PCL electrospun nanofibers scaffolds was investigated. We achieved reasonable encapsulation efficiency of BSA for our random and aligned PCL-BSA nanofibers and GDNF for PCL-BSA-GDNF nanofibers (~30 – 50 %). We were able to fabricate bead-free nanofibers while controlling scaffold topography. Controlled release of GDNF from random and aligned PCL-BSA-GDNF nanofibers with both topographies was observed over 30 days. PC12 cell neurite outgrowth confirmed the bioactivity of released GDNF from such nanofibers. We have also shown how fast the released GDNF from nanofibers could initiate the neurite outgrowth by providing excellent quantitative kinetics data. Finally aligned scaffolds were clearly able to support the adhesion and neuronal differentiation of human iPSCs-derived neural progenitors, making them a useful tool for tissue engineering applications as well. A novel combination of the aligned encapsulated nanofibers with pluripotent stem cells would serve as a pioneer approach for neural tissue engineering and drug delivery applications.

Chapter 5 Overall Conclusion and Future Work

The broad problem statement is how multiscale electrospun scaffolds can promote the neural differentiation of induced pluripotent stem cells by presenting physical cues (topographical properties) and chemical cues (controlled release of small molecules and growth factors). The research presented here addresses this problem statement in three specific ways:

Conclusion of Research Aim 1

Reseach Aim 1 was to combine both the topography of fibers (physical cues) and controlled release of a small molecule (chemical cues) using solution electrospinning technique to fabricate multifunctional PCL nanofibers that can promote the differentiation of mouse iPSCs into neuronal cells.

In Chapter 2, the encapsulation of RA, a small molecule that can regulate the neural differentiation of PSCs, into randomly-oriented and aligned PCL nanofibers was investigated. RA, an important factor in the development, regeneration, and maintenance of the nervous system, could induce the differentiation of neurons, making it extremely useful for neural tissue engineering applications. Due to the porous structure and small fiber diameters, encapsulated PCL electrospun nanofibers had a high surface area which was very valuable for constructing multifunctional scaffolds for neural tissue engineering applications. More importantly, the scaffold's morphology has shown bead-free nanofibers. Controlled release of RA from PCL nanofibers with both topographies was observed over 1 month. In order to test the bioactivity of such scaffolds, murine (iPSCs) -derived neural progenitors was seeded onto electrospun scaffolds. Neural progenitors derived from iPSCs could be differentiated into neurons when seeded onto blank and RA encapsulated electrospun scaffolds with varied topographies include

randomly-oriented and aligned. Alignment of blank and encapsulated nanofibers could direct the neurite outgrowth drastically. A novel combination of the encapsulated nanofibers with stem cells would be introduced as a promising approach for neural tissue engineering applications. We conclude that our versatile technique to fabricate biocompatible nanofibers via solution electrospinning could successfully provide the controlled release of RA with the aim of supporting stem cell growth, proliferation and viability. These promising results are published in the Journal of Biomaterials and Tissue Engineering. Together, the physical cues from scaffold topography and the chemical cues from controlled drug release were designed to mimic the complex extracellular environment that regulates cell behaviour in *vivo*.

Conclusion of Research Aim 2

Research aim 2 was to investigate how topographical properties of engineered melt and solution electrospun fiber scaffolds could affect the neurite outgrowth and the neuronal differentiation of neural progenitors derived from human iPSCs seeded onto such scaffolds.

In chapter three, the effects of topographical cues of neural differentiation of human iPSCs were investigated. The physical properties of melt electrospun microfiber scaffolds on the viability and neural differentiation of human iPS were investigated. Four different scaffold topographies, loop mesh 200, loop mesh 500, biaxial mesh and bimodal, were fabricated using melt and solution electrospinning techniques. Neural progenitors derived from human iPSCs were seeded onto the aforementioned scaffolds. After 12 days of culturing cells on the loop mesh, biaxial mesh and bimodal scaffolds the following conclusions were made. The Live/Dead images proved that all scaffolds were viable substrates to neural progenitor cells due to the high ratio of live cells over dead cells (above 70 %). Loop mesh 200 and biaxial aligned scaffold topographies drastically encouraged cell adhesion and cell migration since bright field images

showed that cells migrated along the fiber morphologies and filled porous structures. Smaller diameter loop mesh scaffolds (loop mesh 200, 43.7 ± 3.9 μm) induced higher expression of the neural markers Nestin and Pax6 compared to thicker diameter loop mesh scaffolds (loop mesh 500, 85 ± 4 μm). The loop mesh and biaxial aligned scaffolds guided the neurite outgrowth of human iPSCs along the topographical features with the maximum neurite length of these cells being longer on the biaxial aligned scaffolds. Lastly, all microfiber scaffolds fostered neural differentiation because a majority of the seeded cells expressed the neuron specific protein β-III-tubulin. Our novel bimodal scaffolds could support the interactions of two human iPSC-derived neural progenitors and these scaffolds demonstrated the highest percentage of viable cells (~ 95 %) compared to the other scaffolds.

Conclusion of Research Aim 3

Research Aim 3 investigated that solution electrospun PCL nanofibers with varied topographies could be encapsulated with growth factors for neural tissue engineering applications. Such engineered systems could provide the controlled release of GDNF over a month. Aligned GDNF loaded PCL nanofibers were also able to support human iPSCs differentiation into neurons.

The use of biodegradable electrospun polymeric nanofibers encapsulated with small molecules and growth factors can serve as novel controlled drug delivery systems, overcoming associated problems with traditional delivery methods such as having burst release effects. PCL has one of the slowest degradation rates, making it an optimal biodegradable polymer for use in systems requiring controlled drug delivery over extended time periods. GDNF supports the survival and differentiation of dopaminergic neurons. In chapter four, PCL nanofibers with different topographies containing encapsulated GDNF were fabricated to provide the controlled

release of GDNF over one month. Firstly, BSA was encapsulated inside of PCL nanofibers to determine the optimal fabrication conditions for producing long term protein release. Then, encapsulation of GDNF into PCL-BSA nanofibers was carried out and in vitro release studies for long term GDNF release (one month) from such nanofibers were performed. Overall, it was reported that GDNF-loaded biodegradable nanofibers using an emulsion electrospinning technique were successfully fabricated. It has also been shown that such nanofibers can be used to deliver proteins over a 30 day time course. These novel BSA-GDNF loaded nanofibers may represent a promising approach to develop drug releasing patches for as artificial dura. PC12 cell neurite outgrowth confirmed the bioactivity of released GDNF from such nanofibers. It has also been shown how fast the released GDNF from nanofibers could initiate the neurite outgrowth by providing excellent quantitative kinetics data. This research demonstrated that electrospun nanofibers with varied topography could be used to deliver bioactive GDNF in a controlled fashion and that aligned substrates supported the culture and neuronal differentiation of human iPSC-derived neural progenitors.

Overall conclusion

This work is representative of an important contribution in the field of neural tissue engineering using mouse and human iPSCs. Our promising results showed how significantly chemical and physical cues could be presented by novel solution and melt electrospun fiber scaffolds to support the neuronal differentiation of iPSCs. Our results contribute into following publications including journal articles, review papers, book chapter and conference oral and poster presentations:

Research Articles:

1. Mohtaram, N., Ko, J., King, C., Sun, L., Muller, N., Jun, M., Willlerth, S.M. **Neuronal Differentiation of Human Induced Pluripotent Stem Cells Using Multiscale Electrospun Scaffolds.** Under review, Journal of Tissue Engineering and Regenerative Medicine.
2. Mohtaram, N., Ko, J., Rattray, D., O'Neil, P., Rajwani, A., Vasandani, R., Agbay, A., Jun, M., Willlerth, S.M. **Controlled Release of Glial cell-derived Neurotrophic Factor from Aligned Electrospun Nanofibers**. In preparation, Journal of Controlled Release.
3. Mohtaram, N., Ko, J., Montgomery, A., Carlson, M., Sun, L., Wong, A., Robinson, M., Jun, M., and Willerth, S.M. **Multifunctional Electrospun Scaffolds for Promoting Neuronal Differentiation of Induced Pluripotent Stem Cells.** Accepted for publication by the Journal of Biomaterials and Tissue Engineering in July 2014.
4. Ko, J., Mohtaram, N., Lee, P.C., Willerth, S.M., and Jun, M. **Using mathematical modeling to control topographical properties of poly (ε-caprolactone) melt electrospun scaffolds II**. Submitted, Journal of Micromechanics and Microengineering
5. Ko, J., Bhullar, S., Mohtaram, N., Willerth, S.M., and Jun, M. **Using mathematical modeling to control topographical properties of poly (ε-caprolactone) melt electrospun scaffolds**. Journal of Micromechanics and Microengineering. 2014 April (24) 065009.
6. Agbay, A., Mohtaram, N., and Willerth S.M. **Controlled release of glial cell line-derived neurotrophic factor from poly (ε-caprolactone) microspheres.** Drug Delivery and Translational Research. April 2014, Volume 4, Issue 2, pp 159-170.

7. Ko, J., Mohtaram, N., Ahmed, F. Carlson, M., Willerth S.M. and Jun M. **Fabrication of multi-scale topographies using melt electrospinning for stem cell-based tissue engineering applications.** Journal of Biomedical Science Polymer Edition. 2014 Jan;25(1):1-17.

Review papers and Book Chapter:

1. Montgomery, A., Agbay, A., Edgar, J.M., Gabers, N., Gomez, J.C., Mohtaram, N., King, C., Mitchell, A., Rajwani, A., Rattray, D., Robinson, M., Shapka, A., Sun, L., Wong, A. and Willerth, S.M. **Combining protein-based biomaterials with stem cells for spinal cord injury repair.** OA Stem Cells. 2014 Jan 18;2(1):1
2. Mohtaram, N., Montgomery, A., and Willerth, S.M. **Biomaterial based drug delivery systems for controlled release of neurotrophic factors.** 2013 Apr;8(2):022001. doi: 10.1088/1748-6041/8/2/022001.
3. Mohtaram, N.K., Montgomery, A.L., Gomez, J.C., Agbay, A. and Willerth, S.M. **Neural tissue engineering applications.** Accepted for publication in the Encyclopedia of Biomedical Polymers and Polymeric Biomaterials. (2014). CRC Press.

Oral Presentations:

1. "Melt Electrospun Microfiber Scaffolds with Novel Architecture for Neuronal Differentiation of Human Induced Pluripotent Stem Cells ", ***31st Annual Meeting of The Canadian Biomaterials Society***, Halifax, NS, Canada, 2014. (This talk was awarded as the best talk in the tissue engineering session at the CBS meeting in Halifax)
2. "Encapsulated Polymeric Microspheres for Promoting Neural Differentiation of Pluripotent Stem Cells", ***31st Annual Meeting of The Canadian Biomaterials Society***, Halifax, NS, Canada, 2014.

3. "Development of Micro and Nanostructured Biomaterial Scaffolds for Neural Differentiation of Induced Pluripotent Stem Cells", ***3rd Student-based Biomaterials symposium***, Vancouver, BC, Canada, 2014. (Invited Speaker)
4. "Fabrication and Characterization of Hybrid Biomaterial Nerve Conduits for Neural Differentiation of Induced Pluripotent Stem Cells", ***30th Annual Meeting of The Canadian Biomaterials Society***, Ottawa, ON, Canada, 2013
5. "Multifunctional Electrospun Scaffolds for Promoting Neural Differentiation of Embryonic and Induced Pluripotent Stem Cells" ***BC Stem Cell and Regenerative Medicine Initiative***, Simon Fraser University (SFU), Vancouver, BC, Canada , 201
6. Nanofabrication of Electrospun Fibers for Controlled Release of Neural Bioactive Agents", ***8th International Conference on Micro Manufacturing***, Victoria, BC, Canada, 2013
7. Parametric Studies of Melt Electrospinning Poly(ε-caprolactone) Fibers for Tissue Engineering Applications'', ***8th International Conference on Micro Manufacturing***, Victoria, BC, Canada, 2013

Poster Presentations:

1. "Multifunctional Nanofiber Scaffolds for Induced Pluripotent Stem Cell Differentiation into Neural Phenotypes: A Strategy for Spinal Cord Injury Repair", ***Annaul Meeting of International Collaboration On Repair Discoveries (ICORD)***, UBC, Vancouver, Canada, 2014.

2. "Multifunctional Electrospun Scaffolds for Promoting Neural Differentiation of Induced Pluripotent Stem Cells". ***Biomedical Engineering Society (BMES) Annual Meeting***, Atlanta, Gerogia, USA, 2012
3. "Using electrospun poly(ε-caprolactone) nanofibers to promote the differentiation of induced pluripotent stem cells into neural phenotypes", ***The 3rd International Conference on Stem Cell Engineering (ICSCE),*** Seattle, WA, USA, 2012
4. Development of Micro and Nano-structured Neural Tissue Engineering Scaffolds", ***The 16th Annual Meeting of the Pacific Center for Advanced Materials (PCAMM)***, University of Victoria, Victoria, Canada, 2011

Future work

Future work could investigate the effects of immobilized aligned nanofiber scaffolds with signaling proteins to further enhance the neuronal differentiation of human iPSCs. It would be also an interesting idea to encapsulate growth factors inside conductive nanofibers while decreasing the fiber diameter to combine different physical cues such as topography and electrical conductivity and chemical cues to further enhance the neuronal differentiation of human iPSCs. Moreover, one may be also interested in surface modification of such nanofibers with immobilization of signaling proteins to further enhance the neuronal differentiation of neural progenitors derived from mouse iPSCs.

In this work, we used electrospinning technique to fabricate electrospun PCL fibrous scaffolds for PSC differentiation. However, there are many other techniques, including particulate leaching, gas foaming, fiber bonding, solvent casting and rapid prototyping, that can be used to design three dimensional scaffolds with varied physical and mechanical properties to further investigating the effect of physical cues on the neuronal differentiation of iPSCs.

Moreover, in addition to PCL polymer, it would be also interesting to use conjugated electro active polymers such Polypyrrole and Polyvinylidene difluoride in order to fabricate electroconductive scaffolds to test the electrical cues that could eventually regulate the neuronal differentiation of iPSCs.

For future work, the encapsulation of larger molecules such as growth factors, like GDNF, inside bimodal scaffolds to further enhance neuronal differentiation of human iPSCs will be also highly recommended. Additionally, using flow cytometry will yield to collect quantitative data for the neuronal differentiation of human iPSCS.

As future work, it will be interesting to investigate the effect of controlled release of GDNF from PCL nanofibers on the neuronal differentiation of human pluripotent stem cells using flow cytormetry to quantify the percentage of different neural phenotypes. A novel combination of the aligned encapsulated nanofibers with pluripotent stem cells would serve as a pioneering approach for neural tissue engineering and drug delivery applications. Since the scaffolds and cell culture methods are completely chemically defined, this will make this research to be a promising approach for clinical neural tissue engineering applications.

Bibliography

1. Evans, M.J. and M.H. Kaufman, *Establishment in culture of pluripotential cells from mouse embryos.* Nature, 1981. **292**(5819): p. 154-6.
2. Thomson, J.A., et al., *Embryonic stem cell lines derived from human blastocysts.* Science, 1998. **282**(5391): p. 1145-7.
3. Takahashi, K. and S. Yamanaka, *Induction of pluripotent stem cells from mouse embryonic and adult fibroblast cultures by defined factors.* Cell, 2006. **126**(4): p. 663-76.
4. Takahashi, K., et al., *Induction of pluripotent stem cells from adult human fibroblasts by defined factors.* Cell, 2007. **131**(5): p. 861-72.
5. Temple, S., *Division and differentiation of isolated CNS blast cells in microculture.* Nature, 1989. **340**(6233): p. 471-3.
6. Reynolds, B.A. and S. Weiss, *Generation of neurons and astrocytes from isolated cells of the adult mammalian central nervous system.* Science, 1992. **255**(5052): p. 1707-10.
7. Cao, Q., et al., *Functional recovery in traumatic spinal cord injury after transplantation of multineurotrophin-expressing glial-restricted precursor cells.* The Journal of neuroscience : the official journal of the Society for Neuroscience, 2005. **25**(30): p. 6947-57.
8. Nakamura, M., et al., *Cell transplantation for spinal cord injury focusing on iPSCs.* Expert opinion on biological therapy, 2012. **12**(7): p. 811-21.
9. Faulkner, J.R., et al., *Reactive astrocytes protect tissue and preserve function after spinal cord injury.* The Journal of neuroscience : the official journal of the Society for Neuroscience, 2004. **24**(9): p. 2143-55.
10. Turksen, K., *Human Embryonic Stem Cells Handbook.* Methods in Molecular Biology. **873**.
11. Marchetto, M.C.N., et al., *A Model for Neural Development and Treatment of Rett Syndrome Using Human Induced Pluripotent Stem Cells.* Cell, 2010. **143**(4): p. 527-539.
12. Nori, S., et al., *Grafted human-induced pluripotent stem-cell-derived neurospheres promote motor functional recovery after spinal cord injury in mice.* Proceedings of the National Academy of Sciences of the United States of America, 2011. **108**(40): p. 16825-16830.
13. Kobayashi, Y., et al., *Pre-Evaluated Safe Human iPSC-Derived Neural Stem Cells Promote Functional Recovery after Spinal Cord Injury in Common Marmoset without Tumorigenicity.* Plos One, 2012. **7**(12).
14. Oki, K., et al., *Human-induced pluripotent stem cells form functional neurons and improve recovery after grafting in stroke-damaged brain.* Stem Cells, 2012. **30**(6): p. 1120-33.
15. Nutt, S.E., et al., *Caudalized human iPSC-derived neural progenitor cells produce neurons and glia but fail to restore function in an early chronic spinal cord injury model.* Experimental Neurology, 2013. **248**: p. 491-503.
16. Qin, J., et al., *Transplantation of human neuro-epithelial-like stem cells derived from induced pluripotent stem cells improves neurological function in rats with experimental intracerebral hemorrhage.* Neuroscience Letters, 2013. **548**: p. 95-100.

17. Wang, A., et al., *Induced pluripotent stem cells for neural tissue engineering.* Biomaterials, 2011. **32**(22): p. 5023-32.
18. Saadai, P., et al., *Human induced pluripotent stem cell-derived neural crest stem cells integrate into the injured spinal cord in the fetal lamb model of myelomeningocele.* Journal of Pediatric Surgery, 2013. **48**(1): p. 158-163.
19. Willerth, S.M., *Neural tissue engineering using embryonic and induced pluripotent stem cells.* Stem Cell Research & Therapy, 2011. **2**(2): p. 17.
20. Dash, T.K. and V.B. Konkimalla, *Poly-epsilon-caprolactone based formulations for drug delivery and tissue engineering: A review.* Journal of Controlled Release, 2012. **158**(1): p. 15-33.
21. Xie, J.W., et al., *Electrospun nanofibers for neural tissue engineering.* Nanoscale, 2010. **2**(1): p. 35-44.
22. Ren, Y.J., et al., *Enhanced differentiation of human neural crest stem cells towards the Schwann cell lineage by aligned electrospun fiber matrix.* Acta Biomaterialia, 2013. **9**(8): p. 7727-36.
23. Ko, J., et al., *Fabrication of poly (-caprolactone) microfiber scaffolds with varying topography and mechanical properties for stem cell-based tissue engineering applications.* Journal of biomaterials science. Polymer edition, 2013.
24. Mohtaram, N.K., A. Montgomery, and S.M. Willerth, *Biomaterial-based drug delivery systems for the controlled release of neurotrophic factors.* Biomedical materials, 2013. **8**(2): p. 022001.
25. Xie, J.W., et al., *The differentiation of embryonic stem cells seeded on electrospun nanofibers into neural lineages.* Biomaterials, 2009. **30**(3): p. 354-362.
26. Park, S.H., et al., *Development of dual scale scaffolds via direct polymer melt deposition and electrospinning for applications in tissue regeneration.* Acta Biomaterialia, 2008. **4**(5): p. 1198-1207.
27. Lyons, J., C. Li, and F. Ko, *Melt-electrospinning part I: processing parameters and geometric properties.* Polymer, 2004. **45**(22): p. 7597-7603.
28. Lee, K.H., et al., *Mechanical behavior of electrospun fiber mats of poly(vinyl chloride)/polyurethane polyblends.* Journal of Polymer Science Part B-Polymer Physics, 2003. **41**(11): p. 1256-1262.
29. Larrondo, L. and R.S.J. Manley, *Electrostatic Fiber Spinning from Polymer Melts .2. Examination of the Flow Field in an Electrically Driven Jet.* Journal of Polymer Science Part B-Polymer Physics, 1981. **19**(6): p. 921-932.
30. Kim, S.E., et al., *Biodegradable porous PCL/HA scaffolds for bone tissue engineering.* Asbm7: Advanced Biomaterials Vii, 2007. **342-343**: p. 77-80.
31. Kim, J.S. and D.S. Lee, *Thermal properties of electrospun polyesters.* Polymer Journal, 2000. **32**(7): p. 616-618.
32. Dalton, P.D., et al., *Direct in vitro electrospinning with polymer melts.* Biomacromolecules, 2006. **7**(3): p. 686-690.
33. Dalton, P.D., et al., *Patterned melt electrospun substrates for tissue engineering.* Biomedical materials, 2008. **3**(3): p. 034109.
34. Dalton, P.D., et al., *Electrospinning of polymer melts: Phenomenological observations.* Polymer, 2007. **48**(23): p. 6823-6833.
35. Pedicini, A. and R.J. Farris, *Mechanical behavior of electrospun polyurethane.* Polymer, 2003. **44**(22): p. 6857-6862.

36. Willerth, S.M. and S.E. Sakiyama-Elbert, *Combining stem cells and biomaterial scaffolds for constructing tissues and cell delivery*, in *StemBook*2008: Cambridge (MA).
37. Willerth, S.M. and S.E. Sakiyama-Elbert, *Approaches to neural tissue engineering using scaffolds for drug delivery.* Adv Drug Deliv Rev, 2007. **59**(4-5): p. 325-38.
38. Willerth, S.M., et al., *The effects of soluble growth factors on embryonic stem cell differentiation inside of fibrin scaffolds.* Stem Cells, 2007. **25**(9): p. 2235-2244.
39. Lopez-Gonzalez, R. and I. Velasco, *Therapeutic Potential of Motor Neurons Differentiated from Embryonic Stem Cells and Induced Pluripotent Stem Cells.* Archives of Medical Research, 2012. **43**(1): p. 1-10.
40. Li, W.J., et al., *Electrospun nanofibrous structure: A novel scaffold for tissue engineering.* Journal of Biomedical Materials Research, 2002. **60**(4): p. 613-621.
41. Keung, A.J., et al., *Rho GTPases mediate the mechanosensitive lineage commitment of neural stem cells.* Stem Cells, 2011. **29**(11): p. 1886-97.
42. Engler, A.J., et al., *Matrix elasticity directs stem cell lineage specification.* Cell, 2006. **126**(4): p. 677-689.
43. Mahairaki, V., et al., *Nanofiber Matrices Promote the Neuronal Differentiation of Human Embryonic Stem Cell-Derived Neural Precursors In Vitro.* Tissue Engineering Part A, 2011. **17**(5-6): p. 855-863.
44. Ulery, B.D., L.S. Nair, and C.T. Laurencin, *Biomedical Applications of Biodegradable Polymers.* Journal of Polymer Science Part B-Polymer Physics, 2011. **49**(12): p. 832-864.
45. Bechara, S.L., A. Judson, and K.C. Popat, *Template synthesized poly(epsilon-caprolactone) nanowire surfaces for neural tissue engineering.* Biomaterials, 2010. **31**(13): p. 3492-3501.
46. da Silva, M.L.A., et al., *Cartilage Tissue Engineering Using Electrospun PCL Nanofiber Meshes and MSCs.* Biomacromolecules, 2010. **11**(12): p. 3228-3236.
47. Del Gaudio, C., A. Bianco, and M. Grigioni, *Electrospun bioresorbable trileaflet heart valve prosthesis for tissue engineering: in vitro functional assessment of a pulmonary cardiac valve design.* Annali Dell Istituto Superiore Di Sanita, 2008. **44**(2): p. 178-186.
48. Gupta, D., et al., *Aligned and random nanofibrous substrate for the in vitro culture of Schwann cells for neural tissue engineering.* Acta Biomaterialia, 2009. **5**(7): p. 2560-2569.
49. Horne, M.K., et al., *Three-Dimensional Nanofibrous Scaffolds Incorporating Immobilized BDNF Promote Proliferation and Differentiation of Cortical Neural Stem Cells.* Stem Cells and Development, 2010. **19**(6): p. 843-852.
50. Jiang, H., et al., *A facile technique to prepare biodegradable coaxial electrospun nanofibers for controlled release of bioactive agents.* Journal of controlled release : official journal of the Controlled Release Society, 2005. **108**(2-3): p. 237-43.
51. Ma, Q., et al., *[Preparation of novel bioactive PCL bone tissue engineering scaffold]*. Sheng wu yi xue gong cheng xue za zhi = Journal of biomedical engineering = Shengwu yixue gongchengxue zazhi, 2009. **26**(3): p. 550-4, 565.
52. Nisbet, D.R., et al., *Neurite infiltration and cellular response to electrospun polycaprolactone scaffolds implanted into the brain.* Biomaterials, 2009. **30**(27): p. 4573-4580.
53. Valmikinathan, C.M., S. Defroda, and X.J. Yu, *Polycaprolactone and Bovine Serum Albumin Based Nanofibers for Controlled Release of Nerve Growth Factor.* Biomacromolecules, 2009. **10**(5): p. 1084-1089.

54. Valmikinathan, C.M., et al., *Novel nanofibrous spiral scaffolds for neural tissue engineering.* Journal of Neural Engineering, 2008. **5**(4): p. 422-32.
55. Jin, G.Z., et al., *Neurite outgrowth of dorsal root ganglia neurons is enhanced on aligned nanofibrous biopolymer scaffold with carbon nanotube coating.* Neuroscience Letters, 2011. **501**(1): p. 10-14.
56. Jiang, X., et al., *Nanofiber topography and sustained biochemical signaling enhance human mesenchymal stem cell neural commitment.* Acta Biomaterialia, 2012. **8**(3): p. 1290-1302.
57. Wang, T.Y., et al., *Immobilization of neurotrophin GDNF on electrospun scaffolds promotes the survival and integration of transplanted neural stem cells.* Journal of tissue engineering and regenerative medicine, 2012. **6**: p. 205-205.
58. Tapan K. Dash, V.B.K., *Poly-ϵ-caprolactone based formulations for drug delivery and tissue engineering: A review.* Journal of Controlled Release, 2012. **158**: p. 19.
59. Kerkhoff, H. and F.G.I. Jennekens, *Peripheral-Nerve Lesions - the Neuropharmacological Outlook.* Clinical Neurology and Neurosurgery, 1993. **95**: p. S103-S108.
60. Moore, A.M., et al., *Controlled delivery of glial cell line-derived neurotrophic factor enhances motor nerve regeneration.* J Hand Surg Am, 2010. **35**(12): p. 2008-17.
61. Shimoke, K. and H. Chiba, *Nerve growth factor prevents 1-methyl-4-phenyl-1,2,3,6-tetrahydropyridine-induced cell death via the Akt pathway by suppressing caspase-3-like activity using PC12 cells: Relevance to therapeutical application for Parkinson's disease.* Journal of Neuroscience Research, 2001. **63**(5): p. 402-409.
62. Stroh, M., et al., *Diffusion of nerve growth factor in rat striatum as determined by multiphoton microscopy.* Biophysical Journal, 2003. **85**(1): p. 581-588.
63. Moore, A.M., et al., *Controlled Delivery of Glial Cell Line-Derived Neurotrophic Factor Enhances Motor Nerve Regeneration.* Journal of Hand Surgery-American Volume, 2010. **35A**(12): p. 2008-2017.
64. Hosseinkhani, H., *DNA nanoparticles for gene delivery to cells and tissue.* International Journal of Nanotechnology, 2006. **3**(4): p. 416-461.
65. Hosseinkhani, H. and M. Hosseinkhani, *Biodegradable polymer-metal complexes for gene and drug delivery.* Current drug safety, 2009. **4**(1): p. 79-83.
66. Yang, W.W. and E. Pierstorff, *Reservoir-based polymer drug delivery systems.* J Lab Autom, 2012. **17**(1): p. 50-8.
67. Chew, S.Y., et al., *Sustained release of proteins from electrospun biodegradable fibers.* Biomacromolecules, 2005. **6**(4): p. 2017-2024.
68. Han, D. and K.C. Cheung, *Biodegradable Cell-Seeded Nanofiber Scaffolds for Neural Repair.* Polymers, 2011. **3**(4): p. 1684-1733.
69. Maretschek, S., A. Greiner, and T. Kissel, *Electrospun biodegradable nanofiber nonwovens for controlled release of proteins.* Journal of controlled release : official journal of the Controlled Release Society, 2008. **127**(2): p. 180-7.
70. Kim, H.N., et al., *Nanotopography-guided tissue engineering and regenerative medicine.* Adv Drug Deliv Rev, 2013. **65**(4): p. 536-558.
71. Liao, I.C., S.Y. Chew, and K.W. Leong, *Aligned core-shell nanofibers delivering bioactive proteins.* Nanomedicine : nanotechnology, biology, and medicine, 2006. **1**(4): p. 465-471.

72. Meinel, A.J., et al., *Electrospun matrices for localized drug delivery: Current technologies and selected biomedical applications.* European Journal of Pharmaceutics and Biopharmaceutics, 2012.
73. Piras, A.M., et al., *New Multicomponent Bioerodible Electrospun Nanofibers for Dual-controlled Drug Release.* Journal of Bioactive and Compatible Polymers, 2008. **23**(5): p. 423-443.
74. Liao, I.C., S.Y. Chew, and K.W. Leong, *Aligned core-shell nanofibers delivering bioactive proteins.* Nanomedicine, 2006. **1**(4): p. 465-71.
75. Liao, S., S. Ramakrishna, and M. Ramalingam, *Development of Nanofiber Biomaterials and Stem Cells in Tissue Engineering.* Journal of Biomaterials and Tissue Engineering, 2011. **1**(2): p. 111-128.
76. Willerth, S.M. and S.E. Sakiyama-Elbert, *Cell therapy for spinal cord regeneration.* Adv Drug Deliv Rev, 2008. **60**(2): p. 263-76.
77. Martin, G.R., *Isolation of a Pluripotent Cell-Line from Early Mouse Embryos Cultured in Medium Conditioned by Teratocarcinoma Stem-Cells.* Proceedings of the National Academy of Sciences of the United States of America-Biological Sciences, 1981. **78**(12): p. 7634-7638.
78. Bain, G., et al., *Embryonic Stem-Cells Express Neuronal Properties in-Vitro.* Developmental Biology, 1995. **168**(2): p. 342-357.
79. Tetzlaff, W., et al., *A Systematic Review of Cellular Transplantation Therapies for Spinal Cord Injury.* Journal of Neurotrauma, 2011. **28**(8): p. 1611-1682.
80. Lam, H.J., et al., *In Vitro Regulation of Neural Differentiation and Axon Growth by Growth Factors and Bioactive Nanofibers.* Tissue Engineering Part A, 2010. **16**(8): p. 2641-2648.
81. Lee, M.R., et al., *Direct differentiation of human embryonic stem cells into selective neurons on nanoscale ridge/groove pattern arrays.* Biomaterials, 2010. **31**(15): p. 4360-4366.
82. Pellett, S., et al., *Sensitive and quantitative detection of botulinum neurotoxin in neurons derived from mouse embryonic stem cells.* Biochemical and biophysical research communications, 2011. **404**(1): p. 388-92.
83. Maden, M., *Retinoic acid in the development, regeneration and maintenance of the nervous system.* Nature reviews. Neuroscience, 2007. **8**(10): p. 755-65.
84. Oh, S., et al., *Stem cell fate dictated solely by altered nanotube dimension.* Proceedings of the National Academy of Sciences of the United States of America, 2009. **106**(7): p. 2130-2135.
85. Balu, R., et al., *Electrospun Polycaprolactone/Poly(1,4-butylene adipate-co-polycaprolactam) Blends: Potential Biodegradable Scaffold for Bone Tissue Regeneration.* Journal of Biomaterials and Tissue Engineering, 2011. **1**(1): p. 30-39.
86. Kim, D.H., et al., *Matrix nanotopography as a regulator of cell function.* Journal of Cell Biology, 2012. **197**(3): p. 351-360.
87. Sheets, K., et al., *Cell-Fiber Interactions on Aligned and Suspended Nanofiber Scaffolds.* Journal of Biomaterials and Tissue Engineering, 2013. **3**(4): p. 355-368.
88. Junka, R., et al., *Laminin Functionalized Biomimetic Nanofibers for Nerve Tissue Engineering.* Journal of Biomaterials and Tissue Engineering, 2013. **3**(4): p. 494-502.

89. Ghasemi-Mobarakeh, L., et al., *Electrospun poly(epsilon-caprolactone)/gelatin nanofibrous scaffolds for nerve tissue engineering.* Biomaterials, 2008. **29**(34): p. 4532-4539.
90. Lim, S.H., et al., *The effect of nanofiber-guided cell alignment on the preferential differentiation of neural stem cells.* Biomaterials, 2010. **31**(34): p. 9031-9.
91. Christopherson, G.T., H. Song, and H.Q. Mao, *The influence of fiber diameter of electrospun substrates on neural stem cell differentiation and proliferation.* Biomaterials, 2009. **30**(4): p. 556-564.
92. Cao, H., T. Liu, and S.Y. Chew, *The application of nanofibrous scaffolds in neural tissue engineering.* Adv Drug Deliv Rev, 2009. **61**(12): p. 1055-64.
93. Subramanian, A., U.M. Krishnan, and S. Sethuraman, *Development of biomaterial scaffold for nerve tissue engineering: Biomaterial mediated neural regeneration.* Journal of biomedical science, 2009. **16**: p. 108.
94. Ko, J., et al., *Fabrication of poly (epsilon-caprolactone) microfiber scaffolds with varying topography and mechanical properties for stem cell-based tissue engineering applications.* Journal of Biomaterials Science-Polymer Edition, 2014. **25**(1): p. 1-17.
95. Xie, J., et al., *Neurite Outgrowth on Electrospun Nanofibers with Uniaxial Alignment: The Effects of Fiber Density, Surface Coating, and Supporting Substrate.* ACS Nano, 2014.
96. Xie, J., et al., *Radially aligned, electrospun nanofibers as dural substitutes for wound closure and tissue regeneration applications.* ACS Nano, 2010. **4**(9): p. 5027-36.
97. Johnson, P.J., et al., *Tissue-engineered fibrin scaffolds containing neural progenitors enhance functional recovery in a subacute model of SCI.* Soft Matter, 2010. **6**(20): p. 5127-5137.
98. Sill, T.J. and H.A. von Recum, *Electrospinning: applications in drug delivery and tissue engineering.* Biomaterials, 2008. **29**(13): p. 1989-2006.
99. Shahbazi, E., et al., *Electrospun Nanofibrillar Surfaces Promote Neuronal Differentiation and Function from Human Embryonic Stem Cells.* Tissue Engineering Part A, 2011. **17**(23-24): p. 3021-3031.
100. Yoshimoto, H., et al., *A biodegradable nanofiber scaffold by electrospinning and its potential for bone tissue engineering.* Biomaterials, 2003. **24**(12): p. 2077-2082.
101. Yu, J., et al., *Induced pluripotent stem cell lines derived from human somatic cells.* Science, 2007. **318**(5858): p. 1917-20.
102. Ebert, A.D., et al., *Induced pluripotent stem cells from a spinal muscular atrophy patient.* Nature, 2009. **457**(7227): p. 277-U1.
103. Fu, J.P., et al., *Mechanical regulation of cell function with geometrically modulated elastomeric substrates (vol 7, pg 733, 2010).* Nature Methods, 2011. **8**(2): p. 184-184.
104. Downing, T.L., et al., *Biophysical regulation of epigenetic state and cell reprogramming.* Nature materials, 2013. **12**(12): p. 1154-62.
105. Pan, F., et al., *Topographic effect on human induced pluripotent stem cells differentiation towards neuronal lineage.* Biomaterials, 2013. **34**(33): p. 8131-9.
106. Sun, Y.B. and J.P. Fu, *Mechanobiology: a new frontier for human pluripotent stem cells.* Integrative Biology, 2013. **5**(3): p. 450-457.
107. Zoldan, J., et al., *The influence of scaffold elasticity on germ layer specification of human embryonic stem cells.* Biomaterials, 2011. **32**(36): p. 9612-9621.

108. Travis Cordie, T.H., Xin Jing, Jared Carlson-Stevermer, Hao-Yang Mi, Lih-Sheng Turng, Krishanu Saha *Nanofibrous Electrospun Polymers for Reprogramming Human Cells.* Cellular and Molecular Bioengineering, 2014. **7**(3): p. 379-393.
109. Madduri, S., M. Papaloizos, and B. Gander, *Trophically and topographically functionalized silk fibroin nerve conduits for guided peripheral nerve regeneration.* Biomaterials, 2010. **31**(8): p. 2323-2334.
110. Xu, H., et al., *Rapid prototyped PGA/PLA scaffolds in the reconstruction of mandibular condyle bone defects.* International Journal of Medical Robotics and Computer Assisted Surgery, 2010. **6**(1): p. 66-72.
111. Mohtaram, N., Ko, J., Montgomery, A., Carlson, M., Sun, L., Wong, A., Robinson, M., Jun, M., and Willerth, S.M. , *Multifunctional Electrospun Scaffolds for Promoting Neuronal Differentiation of Induced Pluripotent Stem Cells.* Journal of Biomaterials and Tissue Engineering, 2014. **In press**.
112. Dimos, J.T., et al., *Induced pluripotent stem cells generated from patients with ALS can be differentiated into motor neurons.* Science, 2008. **321**(5893): p. 1218-1221.
113. Brown, T.D., P.D. Dalton, and D.W. Hutmacher, *Direct Writing By Way of Melt Electrospinning.* Advanced Materials, 2011. **23**(47): p. 5651-+.
114. Baraam , Z., Litjens, Oostwaard,Brink, Laake, Lebrin, Kats, Hochstenbach, Passier, Sonnenberg and Mummery, *Recombinant vitronectin is a functionally defined substrate that supports human embryonic stem cell self-renewal via alphavbeta5 integrin.* Stem Cells, 2008. **26**(9): p. 2257-2265.
115. Ungrin, M.D., et al., *Reproducible, ultra high-throughput formation of multicellular organization from single cell suspension-derived human embryonic stem cell aggregates.* Plos One, 2008. **3**(2): p. e1565.
116. Chen, G.K., et al., *Chemically defined conditions for human iPSC derivation and culture.* Nature Methods, 2011. **8**(5): p. 424-U76.
117. Nakamura, M. and H. Okano, *Cell transplantation therapies for spinal cord injury focusing on induced pluripotent stem cells.* Cell research, 2013. **23**(1): p. 70-80.
118. Detta, N., et al., *Melt electrospinning of polycaprolactone and its blends with poly(ethylene glycol).* Polymer International, 2010. **59**(11): p. 1558-1562.
119. Nagy, Z.K., et al., *Solvent-free melt electrospinning for preparation of fast dissolving drug delivery system and comparison with solvent-based electrospun and melt extruded systems.* Journal of Pharmaceutical Sciences, 2013. **102**(2): p. 508-517.
120. Apostolides, C., et al., *Glial cell line-derived neurotrophic factor improves intrastriatal graft survival of stored dopaminergic cells.* Neuroscience, 1998. **83**(2): p. 363-372.
121. Barry J. Hoffer, A.H., Kate Bowenkamp, Peter Huettl, John Hudson, and L.-F.H.L. David Martin, Greg A. Gerhardt, *Glial cell line-derived neurotrophic factor reverses toxin-induced injury to midbrain dopaminergic neurons in vivo* Neuroscience Letters, 1994. **182**: p. 107-111.
122. Buj-Bello, A., et al., *GDNF is an age-specific survival factor for sensory and autonomic neurons.* Neuron, 1995. **15**(4): p. 821-828.
123. Chermenina, M., et al., *GDNF is important for striatal organization and maintenance of dopamine neurons grown in the presence of the striatum.* Neuroscience, 2014. **270**(0): p. 1-11.

124. Heller, A., S. Price, and L. Won, *Glial-derived neurotrophic factor (GDNF) induced morphological differentiation of an immortalized monoclonal hybrid dopaminergic cell line of mesencephalic neuronal origin.* Brain Research, 1996. **725**(1): p. 132-136.
125. Henderson, C., et al., *GDNF: a potent survival factor for motoneurons present in peripheral nerve and muscle.* Science, 1994. **266**(5187): p. 1062-1064.
126. Martin, D., et al., *Glial Cell Line-derived Neurotrophic Factor: the Lateral Cerebral Ventricle as a Site of Administration for Stimulation of the Substantia Nigra Dopamine System in Rats.* European Journal of Neuroscience, 1996. **8**(6): p. 1249-1255.
127. Tomac A, L.E., Lin LF, Ogren SO, Young D, Hoffer BJ, Olson L., *Protection and repair of the nigrostriatal dopaminergic system by GDNF in vivo.* Nature, 1995. **373**(6512): p. 335-9.
128. Chiocco, M.J., et al., *Neurotrophic factors for the treatment of Parkinson's disease.* Parkinsonism & Related Disorders, 2007. **13, Supplement 3**(0): p. S321-S328.
129. Duan, D., et al., *Long-term restoration of nigrostriatal system function by implanting GDNF genetically modified fibroblasts in a rat model of Parkinson's disease.* Experimental Brain Research, 2005. **161**(3): p. 316-324.
130. Patel, N.K., et al., *Intraputamenal infusion of glial cell line–derived neurotrophic factor in PD: A two-year outcome study.* Annals of Neurology, 2005. **57**(2): p. 298-302.
131. Wang, X., et al., *Intracerebral administration of ultrasound-induced dissolution of lipid-coated GDNF microbubbles provides neuroprotection in a rat model of Parkinson's disease.* Brain Research Bulletin, 2014. **103**(0): p. 60-65.
132. Xiao, C., et al., *Intrastriatal glial cell line-derived neurotrophic factors for protecting dopaminergic neurons in the substantia nigra of mice with Parkinson disease***. Neural Regeneration Research, 2007. **2**(4): p. 207-210.
133. Wang, F., et al., *GDNF-pretreatment enhances the survival of neural stem cells following transplantation in a rat model of Parkinson's disease.* Neuroscience Research, 2011. **71**(1): p. 92-98.
134. Lindvall, O. and L.U. Wahlberg, *Encapsulated cell biodelivery of GDNF: A novel clinical strategy for neuroprotection and neuroregeneration in Parkinson's disease?* Experimental Neurology, 2008. **209**(1): p. 82-88.
135. Binan, L., et al., *Differentiation of neuronal stem cells into motor neurons using electrospun poly-l-lactic acid/gelatin scaffold.* Biomaterials, 2014. **35**(2): p. 664-674.
136. Du, J., et al., *Comparative evaluation of chitosan, cellulose acetate, and polyethersulfone nanofiber scaffolds for neural differentiation.* Carbohydrate Polymers, 2014. **99**(0): p. 483-490.
137. Masaeli, E., et al., *Fabrication, Characterization and Cellular Compatibility of Poly(Hydroxy Alkanoate) Composite Nanofibrous Scaffolds for Nerve Tissue Engineering.* Plos One, 2013. **8**(2): p. e57157.
138. Min, S.K., et al., *Effect of topography of an electrospun nanofiber on modulation of activity of primary rat astrocytes.* Neuroscience Letters, 2013. **534**(0): p. 80-84.
139. Wang, T.-Y., et al., *Promoting engraftment of transplanted neural stem cells/progenitors using biofunctionalised electrospun scaffolds.* Biomaterials, 2012. **33**(36): p. 9188-9197.
140. Weightman, A., et al., *Alignment of multiple glial cell populations in 3D nanofiber scaffolds: Toward the development of multicellular implantable scaffolds for repair of neural injury.* Nanomedicine: Nanotechnology, Biology and Medicine, 2014. **10**(2): p. 291-295.

141. Zuidema, J.M., et al., *Enhanced GLT-1 mediated glutamate uptake and migration of primary astrocytes directed by fibronectin-coated electrospun poly-l-lactic acid fibers.* Biomaterials, 2014. **35**(5): p. 1439-1449.